

**The concealed Tamworth Belt (New England Orogen) - stratigraphic and
geophysical observations depicting a thrust-related geometry in southern
Queensland, Australia**

Dissertation

zur

Erlangung des Doktorgrades (Dr. rer. nat.)

der

Mathematisch-Naturwissenschaftlichen Fakultät

der

Rheinischen Friedrich-Wilhelms-Universität Bonn

vorgelegt von

Wolfram Wartenberg

aus

Dannenberg

Bonn 2005

Angefertigt mit Genehmigung der Mathematisch-Naturwissenschaftlichen Fakultät
der Rheinischen Friedrich-Wilhelms-Universität Bonn

1. Referent: *Prof. Dr. Andreas Schäfer*
2. Referent: *Prof. Dr. Tom McCann*

Tag der Promotion: 13. Mai 2005

Diese Dissertation ist auf dem Hochschulschriftenserver der ULB Bonn
http://hss.ulb.uni-bonn.de/diss_online *elektronisch publiziert. Erscheinungsjahr: 2005*

für meine Eltern, Frank und Rike

P R E F A C E

In March 1996, a joint venture project between the Geological Institute in Bonn (Rheinische Friedrich-Wilhelms-Universität), Germany, and the Australian Geological Survey Organisation (AGSO) in Canberra was initiated. Prof. Dr. A. Schäfer (Geological Institute, Rheinische Friedrich-Wilhelms-Universität Bonn) applied to the Deutsche Forschungsgemeinschaft (DFG) for financial assistance of the project „Sedimentologie und Provenanz von Konglomeraten als Schlüssel für die Tektonik des Bowen Basin im Vorland des New England Orogen, Ost-Australien” (*Sedimentology and provenance of conglomerates in the foreland of the New England Orogen as a key to the tectonic understanding of the Bowen Basin, Eastern Australia*). Within the proposal, the author was suggested as the research assistant working at AGSO and being supervised by Dr. Russell J. Korsch.

AGSO subsequently changed its name to Geoscience Australia (GA) and shall therefore be referenced in this thesis as GA.

The proposed project was followed the line of cooperative research in the past. Prof. Dr. Andreas Schäfer and Dr. Russell J. Korsch (GA) have been working on the tectonic interpretation of the Saar-Nahe Basin in western Germany (KORSCH & SCHÄFER 1991, 1995; SCHÄFER & KORSCH 1998). Their common interest in the sedimentation and tectonostratigraphic evolution of Permian-Triassic sedimentary basins in Eastern Australia set the cornerstone for this thesis. In September 1996, the author started working at GA. His research was integrated into the project '*Tectonic framework of Eastern Australia*', financed by the Australian Geodynamics Cooperative Research Centre (AGCRC) and led by Russell Korsch. In March 1997, the proposed joint venture project was approved by the DFG.

The main study area was chosen in an area of special tectonic interest, crossing the fault-dominated, eastern margin of the Early Permian-Middle Triassic Bowen Basin in the subsurface. Here, the Permian-Triassic rocks are covered by younger sediments. Cores and geophysical data provide the only information of the Bowen Basin sedimentary record. The initial aim was to produce a better understanding of the subduction-related processes that left the Bowen Basin in a foreland position, although it is generally interpreted as being initiated by back-arc extensional processes. The issue was to trace the accommodation record from the provenance area of the New England Orogen to the east, to the conglomerate horizons of the

Bowen Basin that crop out to the west, crossing the subsurface area of interest. Moreover, the tectonic events that created the unusual subsurface geometry: the Late Devonian to Late Carboniferous fore-arc sediments of the Tamworth Belt conformably overlain by the back-arc Bowen Basin succession, needed clarifying.

The Bowen Basin in Eastern Australia is contiguous with the Gunnedah Basin farther south. The two corresponding basins were examined in vicinity of the main study area; the Gunnedah Basin to the south-southwest (in northern New South Wales) and the Bowen Basin to the north (in southern Queensland). In both areas, Permian-Triassic conglomerates crop out and well control is available. Drill cores were analysed and, where possible, correlated with outcrop data. At least some of the conglomeratic horizons could clearly be linked to the New England Orogen as being the provenance area, although palynological control is sparse. However, the approach to trace the sedimentary record of the Gunnedah-Bowen Basin conglomerates from the depocentre across the subsurface Bowen Basin to a specific source area failed.

As a result, the field of interest gradually shifted. The key to understanding the history of the Bowen Basin was now searched for at the base of the Permian-Triassic basin. Focus was drawn to the apparently conformable stratigraphic relationship between the successions in the Bowen Basin and the underlying Tamworth Belt. The basin architecture and tectonic evolution of the Tamworth Belt was now also targeted. As the main tool to examine the subsurface geometry of the fore-arc basin along the eastern limit of the Bowen Basin, shallow seismic reflection profiles (on average 4 seconds two-way travel time) were interpreted. In order to provide more detailed information on the geometry of the area under investigation and to complement the seismic interpretation for the tectonic setting of the Tamworth Belt, aeromagnetic and gravity data were also reprocessed and interpreted.

During the author's time of research, one supporting paper was published in the proceedings of the NEO '99 Conference in Armidale, New South Wales, covering a talk on the subsurface geometry of the Tamworth Belt (WARTENBERG et al. 1999). Another paper has been published in a Special Publications volume of the Geological Society of London (WARTENBERG et al. 2003).

This thesis is based on the author's research in Australia.

TABLE OF CONTENTS

PREFACE	IV
TABLE OF CONTENTS	VI
ABSTRACT	IX
ACKNOWLEDGEMENTS	X
1. INTRODUCTION	1
2. GEOLOGY OF EASTERN AUSTRALIA	5
2.1. Introduction	5
2.2. New England Orogen	8
2.2.1. Tablelands Complex	8
2.2.2. Tamworth Belt	9
2.2.3. Magmatic Arc	11
2.2.4. Back-arc setting	12
2.3. Fault geometry	12
2.4. Deformation	13
3. STRATIGRAPHIC GEOMETRY OF THE TAMWORTH BELT	17
3.1. Documentation of stratigraphic units based on seismic reflection profiling	17
<i>Supplementary deep seismic data</i>	18
<i>Depth conversion of the seismic reflection profiles</i>	19
<i>Interpreted seismic reflections</i>	19
<i>Two distinct sequence boundaries above the Tamworth Belt</i>	21
3.1.1. Five Tamworth Belt reflections	21
3.1.2. Defined Tamworth Belt sequences	23
3.1.3. Representative seismic sections	25
<i>Composite profile A82-LT-24 – H82-T-109 – BMR86.MO1</i>	25
<i>A82-WR-21</i>	27
3.2. Comparison of defined units to existing stratigraphy	28
3.2.1. Palynology of previous studies	29
<i>Defined Supersequences</i>	30

3.2.2. Supporting borehole-stratigraphy	30
<i>Deep Crossing</i>	31
<i>Lithology and Wireline Logs</i>	31
<i>Comparing the borehole data to the seismic record</i>	33
3.2.3. Stratigraphic geometry – short discussion	34
4. MAGNETIC AND GRAVITY ANOMALIES	37
4.1. Introduction	37
4.2. Aeromagnetic data	37
4.2.1. Aeromagnetic data – presentation	39
4.2.2. Aeromagnetic data – interpretation	39
4.2.2.1. Aeromagnetic data – interpretation of the southern NEO	41
<i>Western Tamworth Belt</i>	42
<i>Eastern Tamworth Belt</i>	42
4.2.2.2. Aeromagnetic data – interpretation of the study area	43
4.3. Gravity data	48
4.3.1. Gravity data – presentation	49
4.3.2. Gravity data – interpretation	49
<i>Interpretation of the Southern New England Orogen</i>	49
<i>Interpretation of the study area</i>	50
4.4. Aeromagnetic and gravity data – discussion	51
5. STRUCTURAL GEOMETRY OF THE TAMWORTH BELT	57
5.1. Fault geometries from seismic sections	57
5.1.1. Additional information from deep seismic profiling	58
5.1.2. Composite seismic profiles across the subsurface Tamworth Belt	59
<i>Seismic sequences within the concealed Tamworth Belt</i>	59
5.2. Fault Maps	63
5.2.1. Moonie Fault plane	64
5.2.2. Introducing another thrust horizon	66

5.3. Discussion	67
5.3.1. The concealed Tamworth Belt – post-depositional deformation	68
5.3.2. Defining the eastern limit of the subsurface Tamworth Belt	69
5.3.3. Structure of the concealed Tamworth Belt	69
<i>The relationship between the Bowen Basin and the Tamworth Belt</i>	72
5.3.4. The concealed Tamworth Belt – fault history	73
5.3.5. The concealed Tamworth Belt – fault orientation	76
5.4. Subsurface geometries from reprocessed data – a different approach	77
5.4.1. Reprocessed seismic data – BMR86.MO1 (Millmerran profile)	77
5.4.2. Reprocessed seismic data – BMR84.14	78
5.5. Seismic data – Discussion	81
<i>Reactivation of faults</i>	81
<i>Faults of major importance</i>	82
<i>A second thrust sheet is identified</i>	83
<i>Subsidence history or tectonic evidence?</i>	83
<i>Configuration of the Tamworth Belt related to its evolution</i>	84
5.5.1. Structural Geometry – conclusion	85
6. SYNTHESIS	89
<i>Initiation of the fore-arc succession</i>	89
<i>Age control</i>	90
Comparison with previous studies	91
Final statement	100
7. CONCLUSIONS	103
APPENDIX:	
REFERENCES	
LIST OF FIGURES AND TABLES	
ABBREVIATIONS	
INTERPRETATION INDEX	
PERSONAL THANKS AND THOUGHTS	

ABSTRACT

The subsurface geometry and tectonic development of the Devonian-Carboniferous Tamworth Belt, a fore-arc basin in the New England Orogen, Eastern Australia, has been examined using seismic reflection, drill core data, aeromagnetic and gravity data. In the study area, in southern Queensland, the belt is covered discordantly by up to nearly 2000 metres of Jurassic-Cretaceous sediments.

The Tamworth Belt is affected in the west by the Moonie Fault, a short-cut thrust fault, which exhibits a fault-bend-fold geometry. An elongated positive magnetic anomaly is associated with the Moonie Fault, although the fault strikes beneath the thick Mesozoic cover. The western extent of the fore-arc basin lies far to the west of the study area, but probably is bounded by the Leichhardt Fault, a thrust fault that seems to root onto the same thrust flat at depth.

A major westward-dipping structure forms the main eastern boundary of the belt, with a series of eastward-dipping backthrusts located farther to the west. The eastern margin also coincides with a gravity and magnetic ridge, similar to the gravity and magnetic pattern of the Lower Devonian serpentinites and iron-enriched rocks that are exposed along the Peel Fault to the south.

In the study area, the Tamworth Belt is over 75 km wide and has been shortened by at least 35 km across strike. The sedimentary succession is moderately folded, and, due to thrust sheets sliding on top of each other, at least 12 km thick. Within the succession, six seismic sequences were identified, each of which is separated by a major sequence boundary.

Three major deformational events have been recognised – a Mid Permian period of compressional deformation, the Mid-Late Triassic Goondiwindi Event and the Late Cretaceous Moonie Event.

To the west of the Moonie Fault, Bowen-Gunnedah Basin rocks of Permian-Triassic age occur, comprising sediments that originate to the east of the Tamworth Belt succession and conformably overlie at least the uppermost sequences of the Tamworth Belt succession.

Within the Tamworth Belt succession, a hanging-wall syncline immediately to the east of the Moonie short-cut thrust fault may be correlated with the Rocky Creek Syncline in the northernmost exposed part of the fore-arc basin, approximately 170 km farther south.

The eastern boundary separates the forearc basin sediments from rocks of the Tablelands Complex, which is a subduction-related accretionary wedge assemblage. The overall geometry of the subsurface Tamworth Belt in the southern study area is similar to that seen on the deep seismic survey and on geological cross sections farther south, but is a wider belt to the north.

Keywords: Eastern Australia, New England Orogen, Tamworth Belt, Bowen Basin, Moonie Fault, Peel Fault, Gondwanaland, Tasman Orogenic Zone, Panthalassan Ocean, subduction-related geometry, foreland fold-thrust belt, thrust fault, fault-bend fold, fore-arc basin, Devonian-Carboniferous, Permian-Triassic sediments, seismic sequences, aeromagnetic data, gravity data.

ACKNOWLEDGEMENTS

The author is indebted to both his supervisors, *Prof. Dr. Andreas Schäfer* (Rheinische Friedrich-Wilhelms-Universität, Bonn) and *Dr. Russell J. Korsch* (Geoscience Australia, former Australian Geological Survey Organisation) for their initial encouragement and interest, and for their support, advice and constructive criticism throughout the time of research.

During my time spent at Geoscience Australia (GA), discussions with many colleagues have been extremely useful and provided valuable ideas to the final draft.

In particular, I deeply thank *Ms. Jennie Totterdell, Dr. Clinton Foster, Mr. Jeff Beckett, Mr. Winston Pratt, Dr. Chris Klootwijk, Mr. David W. Johnstone, Dr. Leonie E. A. Jones, Dr. Bruce Goleby, Mr. Peter Green, Ms. Kinta Hoffmann, Dr. Barry Drummond, Dr. Kevin Wake-Dyster, Mr. Christian Thun, Mr. Mike Mc Killop, Mrs. Natalie G. Sinclair, Mr. Andrew J. Cross, Mr. Ed Chudyk and Mr. Tim Barton.*

Technical assistance and valuable comments on software topics were given by *Dr. Chris Tarlowski, Mr. John Creasey and Mr. Malcolm G. Nicoll* (GA).

For drafting and reproducing some of the figures and maps I deeply thank *Mr. Joe Mifsud* (GA).

The author wishes to thank the *Deutsche Forschungsgemeinschaft* (DFG) and the *Australian Geodynamics Cooperative Research Centre* (AGCRC) for financial assistance and *Geoscience Australia* for office space and support. This work would not have been accomplished without the use of specific computer programs generously provided by GA.

Most of the seismic reflection data were acquired by petroleum exploration companies. Sections utilised in this study were collected as a contribution to the NGMA Sedimentary Basins of Eastern Australia project, which was a cooperative project between the *Geological Survey of Queensland* (GSQ), the *Geological Survey of New South Wales* (GSNSW) and Geoscience Australia. Additional seismic reflection lines were ordered as a contribution to the AGCRC project Tectonic Framework of Eastern Australia. The deep seismic reflection data as referred to in this thesis were acquired by the *GA Land Seismic Group*.

The gravity and aeromagnetic images used in this thesis have been compiled and reprocessed from data held in the Australia-wide GA magnetic and gravity databases. The author would like to thank the Geological Survey of Queensland, the Geological Survey of New South Wales and *Werrie Gold Ltd* for providing access to new aeromagnetic data.

Wenn irdische Kräfte an irdische Stoffe pochen, so gibt Bewegung Echo.

Hans Cloos (1936)

Whenever earthly power hits earthly matter, the echo will be movement.

1. INTRODUCTION

The New England Orogen is the easternmost tectonic unit of the Australian continent, consisting of arc, fore-arc and accretionary wedge rocks produced during the Neoproterozoic to Cretaceous within a plate convergent setting.

The various geological processes that formed the recent shape of the orogenic belt occurred during Devonian to Cretaceous times and are described in **Chapter 2** (*Geology of Eastern Australia*) in a regional overview of Eastern Australia. In the area of interest, in southern Queensland, most of the orogen is covered discordantly by a thick sedimentary package of Mesozoic sediments (*Fig. 1*). Here, the subsurface geometry of the underlying fore-arc basin, the Devonian-Carboniferous Tamworth Belt, was examined.

This thesis, using a database which is mainly restricted to industry shallow seismic profiles (and two additional deep seismic profiles), gravity and aeromagnetic potential field data and some isolated petroleum exploration wells, focuses on outlining the basin architecture and the tectonic evolution of the fore-arc basin and continues the outcome of earlier research (WARTENBERG *et al.*, 1999, 2003).

Seismic data within the study area suggest that the sequences of the Tamworth Belt and the Permian to Triassic Bowen Basin seem to be temporally and spatially related. This is dealt with in **Chapter 3** (*Stratigraphic geometry of the Tamworth Belt*), where distinctive Tamworth Belt seismic reflections are identified as stratigraphic units, and are then compared to units of existing sequence stratigraphy (e.g. Bowen Basin seismic reflections).

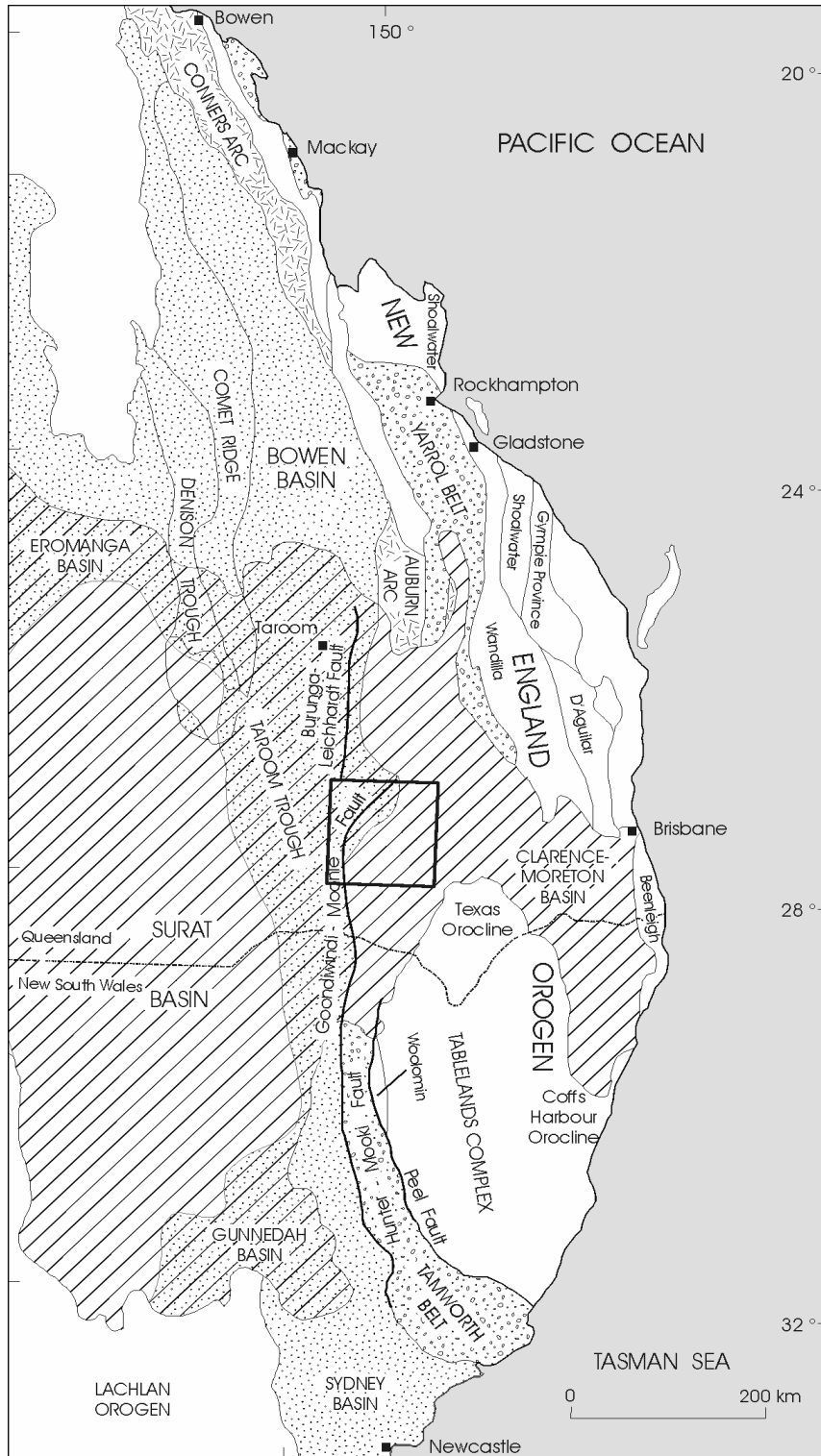


Fig. 1: Map of Eastern Australia, showing the relationship of the New England Orogen to the adjacent sedimentary basins. The Tamworth and Yarrol belts represent the Devonian-Carboniferous fore-arc basin that extends in the subsurface to the east of the Goondiwindi-Moonie and Burunga-Leichhardt faults.

The accretionary wedge assemblages displayed on the map consist of (from north to south) the Shoalwater and the Wandilla terranes, the D'Aguilar Block, the Beenleigh Terrane, the Woolomin and the Coffs Harbour associations.

The Conners and Auburn arcs represent the magmatic arc component.

The Sydney, Gunnedah and Bowen basins are part of the Permian-Triassic Bowen Basin system, with the Comet Ridge, the Denison and the Taroom troughs representing parts of major importance of the Bowen Basin (sensu stricto).

The Eromanga, Surat and Clarence-Moreton basins were formed during the Jurassic to Cretaceous.

The box at the northern end of the Goondiwindi-Moonie Fault identifies the study area.

See **Chapter 2** for



- Concealed margin of Permo-Triassic sediments
- ▨ Jurassic - Cretaceous sediments
- ▤ Permian - Triassic sediments
- ◻ Devonian - Carboniferous forearc basin
- ◻ Devonian - Carboniferous magmatic arc

Also, on in **Chapter 3**, attention is drawn to supporting borehole-stratigraphy that substantiates the seismic record. As the Bowen Basin - now situated in a foreland basin position - is generally interpreted as being back-arc initiated, the apparently conformable behaviour between the Tamworth Belt fore-arc basin and Bowen Basin sequences raises an interesting question: which tectonic processes left the Bowen Basin in a foreland position?

In an attempt to understand the tectonic processes, additional geophysical data were used to construct the recent boundary of the subsurface fore-arc basin. In **Chapter 4** (*Magnetic and gravity anomalies*) aeromagnetic and gravity anomalies are investigated and then correlated to the seismic record. Another question is raised here: does the Moonie Fault, a thrust fault of major displacement in the western part of the study area (*Fig. 1*), identify the westernmost boundary of the subsurface Tamworth Belt?

The conclusions drawn from the magnetic and gravity data lead to the discussion on the geometry and structural evolution of the Tamworth Belt. The arguments are summarised in **Chapter 5** (*Structural geometry of the Tamworth Belt*), which attempts to explain the present-day distribution of the Devonian-Triassic basin successions and thus attempts to answer the above questions. The structural geometry is described and the relative tectonic development of the fore-arc and back-arc basins to one another is examined. The resulting tectonic model is compared to the crustal architecture as interpreted on two deep seismic profiles (each of which was recorded to 20 seconds two-way travel time) to the north and to the south of the seismic study area (KORSCH et al. 1993, 1997; GLEN et al. 1993; WAKE-DYSTER et al. 1987) (*Fig. 5.2 & Fig. 5.3*).

The pre-deformation history of the study area and the pathways of later tectonic activity are finally discussed in **Chapter 6** (*Synthesis*) and are set in context with previous studies. **Chapter 7** (*Conclusions*) summarises the outcome of this study.

Das Auge hat sein Dasein dem Licht zu danken.
Aus gleichgültigen tierischen Hilfsorganen
ruft sich das Licht ein Organ hervor,
das seinesgleichen werde;
und so bildet sich das Auge am Lichte fürs Licht,
damit das innere Licht dem äußeren entgegentrete.

Johann Wolfgang Goethe

2. GEOLOGY OF EASTERN AUSTRALIA

The Australian continent is divided into several tectonic mega-elements, with the **Tasman Orogenic Zone** (Tasmanides, Tasman Orogenic System, Tasman Orogen) representing the youngest of these elements and forming the eastern margin of the continent. Australia's geological history, during the last billion years, is strongly influenced by two supercontinents, Neoproterozoic Rodinia and Palaeozoic Gondwanaland. **Gondwanaland** formed at the beginning of the Phanerozoic with the Tasman Orogenic Zone being located at the eastern edge of the palaeo-supercontinent. During the Early Cambrian, west-directed subduction of the Palaeo-Pacific Ocean along the eastern margin of the Tasmanides commenced (LI & POWELL, 2000).

2.1. Introduction

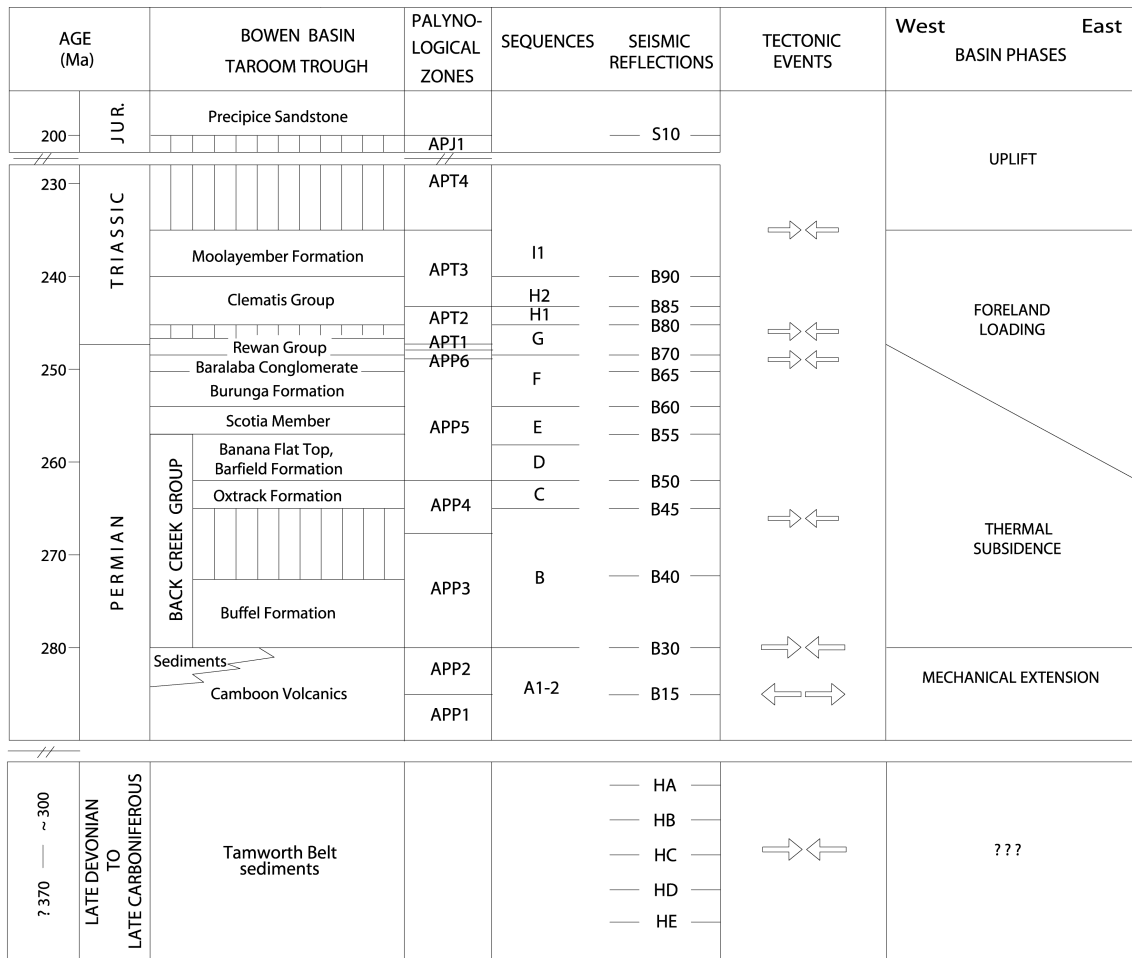
The easternmost and youngest accreted tectonic unit of the Tasman Orogenic Zone in Eastern Australia is the **New England Orogen** (Fig. 1). The tectonic evolution of the New England Orogen essentially started during the Devonian and Carboniferous at the eastern Gondwanaland margin where Gondwanaland faced the **Panthalassan Ocean**. Here, at low latitudes, west-directed subduction produced three parallel belts, representing a western Andean-style magmatic arc, a central fore-arc basin and an eastern accretionary wedge (KIRKEGAARD, 1974; MURRAY *et al.*, 1987; KORSCH *et al.*, 1993; SCHEIBNER & BASDEN, 1996). In the Early Carboniferous, Australian Gondwanaland drifted rapidly from lower latitudes to a near-south polar position (LI & POWELL, 2000), at the time, when the opposite edge of the supercontinent collided with Laurussia. In the Late Car-

boniferous, the tectonic regime of ancient Eastern Australia changed from compressional to extensional, possibly related to a change in the dynamics of the subduction system (KORSCH *et al.*, 1997, MURRAY *et al.*, 1987).

Subsequently, in the Early Permian (*c.*295 – 280 Ma), the initiation of the **Bowen-Gunnedah-Sydney basin system** occurred to the west of the continental margin magmatic arc in a back-arc tectonic setting (KORSCH *et al.*; 1993; TADROS, 1993). Also in the Early Permian, but probably later than the mechanical extension phase, oroclinal bending of the fore-arc basin and accretionary wedge (*c.*285 – 265 Ma) occurred to produce the **Texas and Coffs Harbour oroclines** (KORSCH & HARRINGTON, 1987; MURRAY *et al.*, 1987) (see *Fig. 1* for location).

The late Early to early Late Permian (*c.*265 – 262 Ma) saw another change in the dynamics of the subduction system, when the magmatic arc was re-established along the Palaeo-Pacific continental margin of Australia and the back-arc changed from an extensional to a contractional regime (KORSCH & TOTTERDELL, 1995c). This led to the formation of a retro-foreland fold-thrust belt west of the magmatic arc (*c.f.* CATUNEANU *et al.*, 1997) that was better developed in the Queensland sector of the New England Orogen than in New South Wales (KORSCH *et al.*, 1997). Moreover, the contractional regime resulted in the development of a significant retro-foreland basin phase in the Bowen-Gunnedah-Sydney basin system that extended until the Middle Triassic (KORSCH & TOTTERDELL, 1995b) (see *Table 2.1* for details of the stratigraphy). The large foreland basin accumulated major coal deposits mainly during the Late Permian.

From the Early Jurassic to Early Cretaceous, eastern Australia was still part of the eastern convergent margin of Gondwanaland, but almost all of it was situated in a back-arc setting, with only minor remnants of the magmatic arc being preserved near the Queensland coast (KORSCH & TOTTERDELL, 1996). The **Surat, Eromanga and Clarence-Moreton basins** (see *Fig. 1* for location) developed at this time within a back-arc setting, inboard of the continental margin volcanic arc. At times, this arc provided considerable amounts of detritus to the basins. Therefore, these basins contain a relatively thick, sometimes volcanoclastic, succession which blanketed much of the Devonian-Carboniferous subduction-related units, including the fore-arc basin component (Tamworth Belt), part of which, in



Tab. 2.1: Chart showing the lithostratigraphy, seismic reflections and basin phases of the Bowen Basin and Tamworth Belt successions. Note, that the top of the Bowen Basin successions are defined by an unconformity (APT4) overlain by Surat Basin sediments. For the location of the Taroom Trough, see Fig. 1.

southern Queensland and northern New South Wales, is still covered by up to nearly 2000 metres of sediments (see Fig. 1 for location and Figs 3.4 & 3.7 for the Surat sediments).

The basin genesis and tectonic development of the Tamworth Belt was accompanied by major climate changes in ancient Australia. During the Devonian to Carboniferous, Australia was located at low latitudes with a warm climate. Glacial conditions dominated Australia’s climate during the Late Carboniferous to Earliest Permian. At the end of the Permian, the palaeo-environment again was suspect to drastic climate changes, leading to red-bed deposition in Early Triassic times (LI & POWELL, 2000).

In order to provide a better understanding of the geological setting of the Tamworth Belt,

the relevant components of the New England Orogen and adjacent basins (e.g. back-arc Bowen Basin), together with some background information on geometry and tectonic deformation, are introduced in the following subsections.

2.2. New England Orogen

The New England Orogen (NEO) is the easternmost and youngest accreted tectonic unit of the Tasman Orogenic Zone, extending over approximately 1500 kilometres from Bowen in Queensland (22° S) to Newcastle in New South Wales (32° S) (Fig. 1). It consists of magmatic arc, fore-arc and accretionary wedge rocks produced during Late Devonian to Cretaceous plate convergence at the interface of eastern Gondwanaland and the Panthalassan Ocean (LEITCH, 1975; MURRAY *et al.*, 1987; KORSCH *et al.* 1990). The New England Orogen may be subdivided into a southern and a northern unit, due to the presence of the Mesozoic Surat and Clarence-Moreton basins that conceal much of the central part of the orogen (SCHEIBNER *et al.*, 1996; C. G. MURRAY *et al.*, 1997a). Thus, it is difficult to correlate the southern and the northern fore-arc basin successions (**Tamworth** and **Yarrol belts**, respectively, in *Fig. 1*). The accretionary wedge assemblages occur in outcrop across the whole eastern part of the New England Orogen (e.g. in New South Wales the **Tablelands Complex** assemblage - consisting of the Woolomin, Sandon and Coffs Harbour associations and in Queensland the Beenleigh, D'Aguilar, Wandilla and Shoalwater terranes) (see *Fig. 1*), whereas the magmatic arc component is only exposed in the northern NEO (**Conners** and **Auburn arcs** in *Fig. 1*).

Another tectonostratigraphic unit, the Early Permian-Early Triassic **Gympie Province** to the very east of the previously mentioned belts (see *Fig. 1* for location), has been proposed as being an exotic terrane (C.G. MURRAY, 1997b). It probably accreted during the Middle Triassic Hunter-Bowen Orogeny (HARRINGTON & KORSCH, 1985).

2.2.1. Tablelands Complex

The convergent plate margin model for Eastern Australia in the Late Devonian-Carboniferous interprets the accretionary wedge assemblages as a once-continuous accreted trench-fill that grew eastwards towards the Panthalassan Ocean (KORSCH *et al.*, 1990). Its clastic sedimentary components are mainly represented by volcanoclastic deep-

water turbidites derived from the magmatic arc to the west. There are also infaulted slices of basalt, chert and pelagic mudstone which are considered to be fragments of the oceanic crust (KORSCH, 1977). The provenance of the turbidites in the accretionary wedge, however, can be linked to the fore-arc basin compositions, because the detritus was derived from the same volcanic arc (CAWOOD, 1983; KORSCH, 1984). Within the study area, the accretionary wedge rocks are represented by components of the Tablelands Complex that are covered by the Early Jurassic to Early Cretaceous Clarence-Moreton and Surat basins (see Fig. 1).

2.2.2. Tamworth Belt

The fore-arc basin succession of the New England Orogen is represented by the Late Devonian to Late Carboniferous Tamworth and Yarrol belts, located between the arc to the west and the accretionary wedge to the east. The Tamworth Belt succession is the preserved fore-arc unit of the southern New England Orogen (including the Hastings Block; see Fig. 2.2). It is dominated by volcanoclastic sedimentary rocks deposited predominantly in a shallow-marine shelf environment (MCKELVEY & MCPHIE, 1995; SCHEIBNER, 1998). Volcanic material (e.g. volcanic flows and tuff) is more abundant in the western part of the region, closer to the active magmatic arc (MCPHIE, 1987). A more detailed description of the Tamworth Belt sediments is given by CAWOOD (1983) and KORSCH (1984). Sandstone compositions described by MURRAY (1997c) and plotted within the QFL-triangle of DICKINSON & SUSZEK (1979) and DICKINSON *et al.* (1983), form a coherent group that contains mainly lithic fragments, defining the provenance field of the fore-arc basin sediments as an undissected arc tectonic environment (Fig. 2.1).

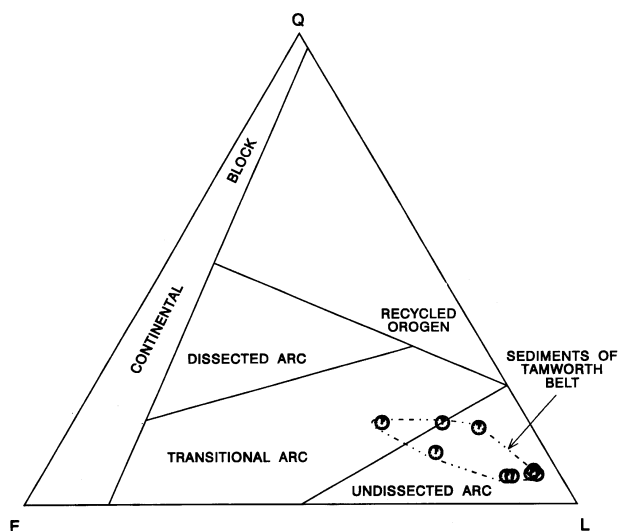
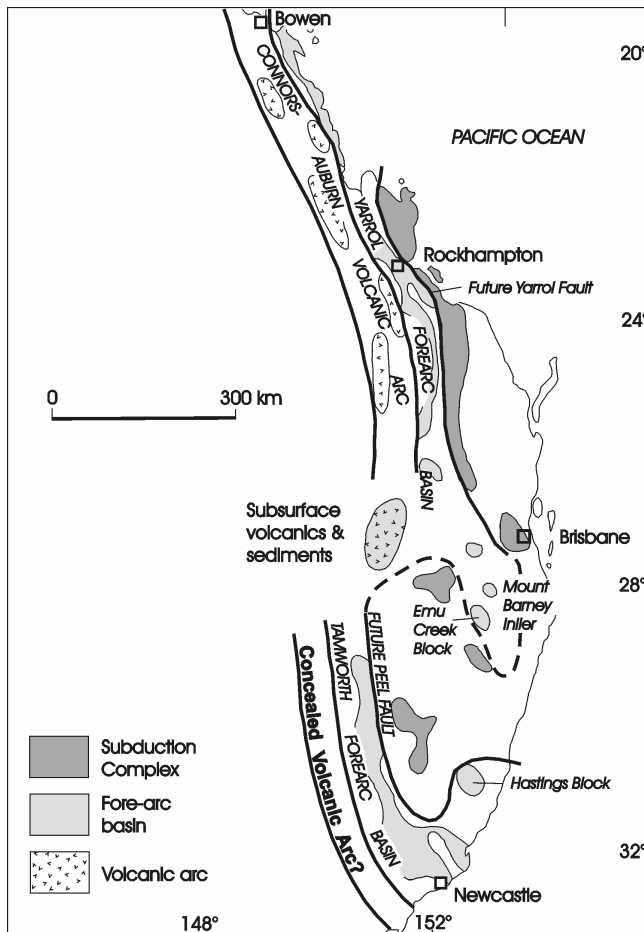


Fig. 2.1: QFL plot of sandstones from the Tamworth Belt in relation to provenance fields of DICKINSON & SUSZEK (1979) and DICKINSON *et al.* (1983) after MURRAY (1997c). The uniform tectonic setting of the sandstones is considered to be evidence for a common origin (note, however, that only about eight samples were used from a restricted area).

part of the region, closer to the active magmatic arc (MCPHIE, 1987). A more detailed description of the Tamworth Belt sediments is given by CAWOOD (1983) and KORSCH (1984). Sandstone compositions described by MURRAY (1997c) and plotted within the QFL-triangle of DICKINSON & SUSZEK (1979) and DICKINSON *et al.* (1983), form a coherent group that contains mainly lithic fragments, defining the provenance field of the fore-arc basin sediments as an undissected arc tectonic environment (Fig. 2.1).

The Tamworth Belt is exposed in northern New South Wales but continues northwards in the subsurface into southern Queensland, covered by the Mesozoic sediments of the Surat and Clarence-Moreton basins (*Fig. 1*). The exposed part of the fore-arc unit has been subdivided into several blocks (see overlying terrane map in *Fig. 4.1* of **Chapter 4.2.1**), of which the Tamworth North and Tamworth South blocks identify a NNW-SSE-trending synclinal zone to the east of the Permian-Triassic Gunnedah Basin. Both fore-arc basin blocks contain with long linear thrust faults along strike, mimicking the geometry of a major fold-thrust system (WOODWARD, 1995). Moreover, the outcropping Tamworth Belt may be divided into two units running sub-parallel to the overall basin trend, with the Carboniferous fore-arc deposits to the west and the Devonian sedimentary succession to the east.

In the area of interest, in southern Queensland, the eastern boundary of the Tamworth Belt succession curves to the northeast. It is here, where the Devonian-Carboniferous juxtaposition of the fore-arc and accretionary wedge belts, that can still be seen in the northern and southern part of the orogen, is complicated by the above noted Early Permian oroclinal bending (see **Chapter 2.1**).



The eastern boundary of the Tamworth Belt forms part of the Texas and Coffs Harbour oroclines in the subsurface. Components of the oroclines that are considered to be part of the fore-arc basin succession include rocks of the **Emu Creek Block** and Carboniferous outcrops

Fig. 2.2: Cartoon of the Late Devonian- Early Carboniferous palaeogeography (not palin-spastically restored), showing present-day distribution of the arc, fore-arc basin and accretionary wedge subduction complex (after MURRAY *et al.*, 1987). The dashed heavy line represents the presumed limit of the fore-arc basin boundary in the subsurface after Early Permian oroclinal bending (see **Chapter 2.1**).

at **Mount Barney** (MURRAY *et al.*, 1987) (*Fig. 2.2*), some 200 kilometres to the east of the northernmost outcropping and near-longitudinal oriented Tamworth Belt rocks.

South of Mount Barney, the fore-arc basin occurs to the east of the northern Coffs Harbour Block, beneath the Clarence-Moreton Basin (*cf. Fig. 1*). Here the Baryulgil Serpentine is located to the east of the Emu Creek Block and forms the boundary between the fore-arc basin sediments and the accretionary wedge assemblage (*Fig. 2.2*). North of Mount Barney, the fore-arc basin succession surfaces and eventually links with the exposed Yarrol Belt farther north (*see Fig. 2.2*), representing the fore-arc unit of the subduction-related system of the northern New England Orogen.

The Yarrol Belt has been described by DAY *et al.* (1983) and recently its geology has been updated by the Queensland Department of Mines and Energy (MURRAY *et al.*, 1997a). As its fore-arc basin equivalent to the south (Tamworth Belt), the Yarrol Belt basin fill is dominated by volcanoclastic sedimentary rocks, deposited within a shallow-marine environment.

2.2.3. *Magmatic Arc*

There are apparently no arc-related rocks south of the Mesozoic cover (*Fig. 1*) and thus, no arc components are identified within the study area in southernmost Queensland. The BMR deep seismic survey across southern Queensland (BMR84.14, BMR86.16, BMR86.17) suggested a possible position of the volcanic arc beneath younger Permian extensional volcanics (WAKE-DYSTER *et al.* 1987) (*see Fig. 5.3 of Chapter 5.1.1.*).

In describing the original tectonic setting along the eastern margin of Gondwanaland for the Silurian to Early-Middle Devonian, two scenarios have been proposed to justify the absence of the arc in the southern New England Orogen.

AITCHISON & FLOOD (1995) interpret the absence of the arc as related to a change in subduction direction over time. They envisage a western continental margin and an eastern island arc with the intervening oceanic crust being subducted to the east. After subduction ceased, there was a polarity change in the direction of subduction, with oceanic crust subducting to the west from Late Devonian to Late Carboniferous.

KORSCH *et al.* (1997), however, argue against this flip in subduction sense. They have suggested that the subduction system always dipped westward and that the arc could now be buried beneath the younger Permian-Triassic sedimentary rocks of the Bowen-Gunnedah Basin (see *Fig. 1* for location). This study follows the latter interpretation, implying a constant western-directed subduction polarity with the Silurian island arc possibly getting accreted and converted to a continental margin arc by Middle Devonian times.

It shall be pointed out, however, that dating of rocks that were classified by DAY *et al.* (1978) as arc components of the above mentioned Connors and Auburn arcs identifies their age as Late Carboniferous and Early Permian. Moreover, none of the rock-samples represent a Late Devonian age, questioning the position of the arc even in the northern New England Orogen. Recent work on rock specimen dated a few samples within the Earliest Carboniferous (*c.* 360-350 ma), being overprinted by younger volcanics and hence proving at least some evidence for the arc (HUTTON *et al.*, 1999).

2.2.4. *Back-arc setting*

The back-arc **Bowen Basin**, located to the west of the Tamworth Belt, consists of terrestrial to shallow marine successions (for definition of the relevant successions in southern Queensland, see DERRINGTON *et al.*, 1959; cf. *Tab. 2.1*). It was initiated by Early Permian lithospheric extension and, from the middle Permian, subsidence was driven by foreland loading (KORSCH & TOTTERDELL, 1996). In the northern New England Orogen, where the arc is present, the Bowen Basin is bounded to the east by volcanic rocks which are remnants of the intermittently active volcanic arc. To the south, it also continues in the subsurface beneath the younger Surat Basin sediments. The Bowen Basin is part of an elongate Early Permian-Middle Triassic basin system that includes, from south to north, the Sydney, Gunnedah and Bowen basins (see *Fig. 1* for location).

2.3. **Fault geometry**

Petroleum exploration industry seismic lines across the eastern part of the Bowen Basin system show that the approximate eastern limit of this basin system is defined by a major system of discrete Middle Triassic thrust faults and displacement transfer zones (KORSCH & TOTTERDELL, 1995a). These faults are, from south to north, the **Hunter, Mooki, Kel-**

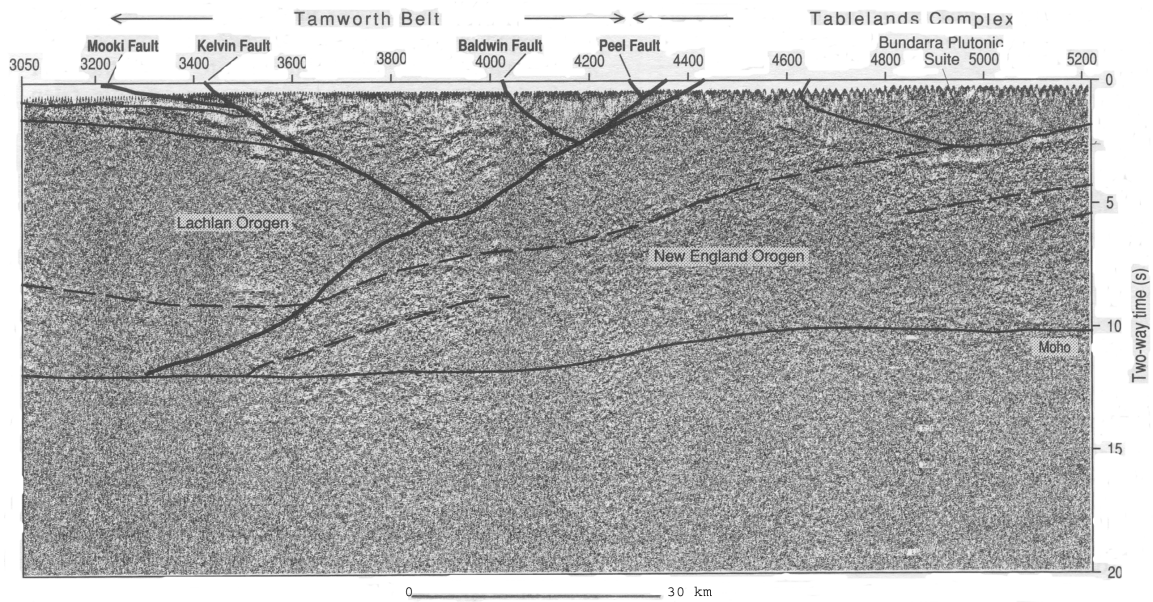


Fig. 2.3: Unmigrated deep seismic profile BMR91.G01 across the Tamworth Belt and Tablelands Complex of the New England Orogen from KORSCH *et al.* 1997 (see Fig. 3.1 for location). Vertical scale approximately equals horizontal scale assuming an average crustal velocity of 6000 ms^{-1} .

vin, Moonie, Goondiwindi, Leichhardt and Burunga faults (see Fig. 1 for location). Movement on all of these faults is west-directed, apart from the northernmost Burunga Fault, which is directed towards the east.

To the south of the study area, in northern New South Wales, the Tamworth Belt has been thrust over the eastern margin of the Gunnedah Basin. Farther north, in southern Queensland, the thrust front overrides the eastern margin of the Bowen Basin. The eastern limit of the exposed part of the Tamworth Belt is defined by the **Peel Fault**, to the east of which occur accretionary wedge rocks of the Tablelands Complex (Fig. 1). In outcrop, in northern New South Wales, the Peel Fault dips steeply to the east, and is interpreted on the deep seismic line BMR91.G01 to be a splay off of a major westward-dipping structure that cuts to the base of the crust (Fig. 2.3) (see also Fig. 5 in KORSCH *et al.*, 1993, 1997).

2.4. Deformation

Deformation in the Tamworth and Yarrol belts was mainly controlled by west to west-northwest-directed thrusting, forming part of a **foreland thrust belt** (WOODWARD, 1995; HOLCOMBE *et al.*, 1997). In the Bowen and Surat basins, KORSCH & TOTTERDELL

(1995b) and KORSCH *et al.* (1998) have defined several deformational events, most of which were contractional in nature. At least *two* of the *deformational events* seen in the subsurface Tamworth Belt can be related to events in the Bowen and Surat basins. These are the Middle-Late Triassic **Goondiwindi Event** and the early Late Cretaceous **Moonie Event**.

In the study area, the Devonian-Carboniferous Tamworth Belt, therefore, is a fore-arc basin which is conformably overlain and concealed by the Early Permian to Middle Triassic back-arc Bowen Basin and, subsequently, unconformably overlain by the Early Jurassic to Early Cretaceous Surat Basin (FIELDING *et al.*, 1990; O'BRIEN *et al.*, 1990; KORSCH *et al.*, 1992a, 1992b) (see *Fig. 1*). Much of the hydrocarbon-driven research in this area has been concentrated in the Surat Basin. Thus, the precise geometry and evolutionary history of the underlying Tamworth Belt has been relatively ignored, but is addressed in this thesis.

Alles Geologische liegt zwischen einem ältesten und einem jüngsten

Johann Wolfgang Goethe

3. STRATIGRAPHIC GEOMETRY OF THE TAMWORTH BELT

Data used for identifying the stratigraphic geometry of the Tamworth Belt consist mainly of seismic reflection profiles and information from petroleum exploration wells. These data were used to subdivide the sequences within the Tamworth Belt succession, and continues the documentation of overlying data that has been developed by KORSCH & TOTTERDELL (1995) and BRAKEL *et al.* (in press). The study area is located at the southern limit of the industry seismic data east of the Moonie Fault. Here, the highest concentration of seismic profiles across the subsurface fore-arc basin allows for seismic interpretation.

3.1. Documentation of stratigraphic units based on seismic reflection profiling

A regional network of shallow seismic reflection profiles was used to form a grid covering much of the subsurface Tamworth Belt in southernmost Queensland. Data used in the seismic study area consist of a series of 109 good quality seismic profiles (for distribution pattern and cover area, see *Fig. 3.1*), acquired to an average of 3 to 4 seconds two-way travel time (TWT). These seismic profiles were originally acquired by the petroleum exploration industry as part of their exploration of the overlying Surat Basin. The majority of the seismic lines are unmigrated (usually final stacks) and are displayed with a datum of 244 metres above sea level.

In comparison to the Queensland part of the fore-arc basin, the seismic coverage of the subsurface part of the belt in northernmost New South Wales is very sparse and limited

to a few lines across its western margin. Here, the quality of the seismic data for the subsurface Tamworth Belt in general decreases from the west to the east.

Supplementary deep seismic data

Two deep seismic profiles (acquired to 20 s TWT; approximately 60 km depth) supplement the seismic coverage of the study area. The reflection pattern seen across the exposed part of the Tamworth Belt on deep seismic line BMR91.G01 (see figures 3, 4 and 5 in KORSCH *et al.*, 1993, 1997; see also Figs 2.3 & 5.2 this thesis; for location see Fig. 3.1) in the vicinity of Boggabri to Manilla is of similar quality to the industry seismic lines in northern New South Wales. The second deep seismic profile, line BMR84.14 (Fig. 5.3; for location see Fig. 3.1), crosses the subsurface Tamworth Belt towards the northern limit of the industry seismic data in the study area, and is

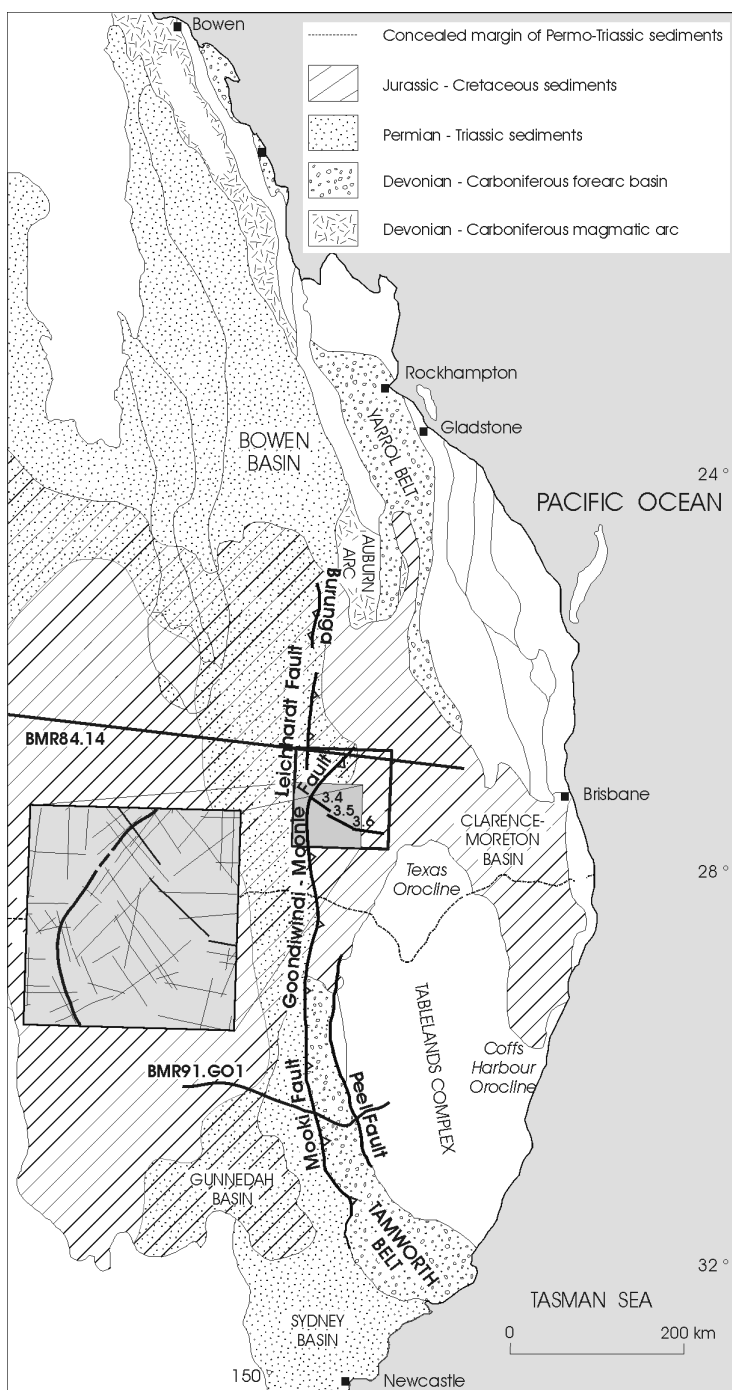


Fig. 3.1: Map of Eastern Australia showing the locations of the seismic profiles within the study area (box to the left shows in detail the region marked in light grey at the northern end of the Goondiwindi-Moonie Fault, representing the area with the highest concentration of seismic profiles and thus the area of seismic interpretation and 3D imaging). The black heavy solid lines marked as 3.4, 3.5 and 3.6 depict the location of the longest composite seismic profile in the study area (see Figs 3.4, 3.5 & 3.6). The east-west black heavy solid lines are the deep seismic profiles BMR84.14 and BMR91.G01 respectively. For further details, see Fig. 1.

in an anomalous region where the belt is extremely wide due to repetition by the oroclinal bending (KORSCH *et al.*, 1997).

Depth conversion of the seismic reflection profiles

On the shallow seismic reflection profiles, the depth conversion was done using a program that picks the stacking velocities and converts them to depth. In general, the conversion from time [s] to depth [km] can be simplified by taking the two-way travel time values times three. The deep seismic data were acquired at a different vertical scale and have an average velocity of 6000 m/s.

Interpreted seismic reflections

Beneath the base of the Bowen Basin (*Fig. 3.2*), within the Tamworth Belt succession, five reflections (**HA**, **HB**, **HC**, **HD**, **HE**) were interpreted throughout the area, although **HE** is restricted to the very eastern part of the region (see **Chapter 3.1.1** for details). In general, the Tamworth Belt reflectors span a Late Devonian to Late Carboniferous age (*Tab. 2.1*). Of the interpreted reflections within the subsurface Tamworth Belt, **HE** represents the **oldest** identified seismic reflection and **HA** the **youngest** respectively. After interpretation of the individual seismic profiles, maps were produced using UNIX-based PETROSYS software.

In this study, the author initially intended to introduce the seismic reflections in geological order with the fore-arc basin reflections designated HA (oldest) to HE (youngest). However, during the early stage of the research, the naming of the seismic sequences was the result of a more informal identification process. Difficulty was experienced in tracing the older seismic reflections throughout the study area and thus only the two youngest Tamworth Belt reflections, HA and HB, were introduced in the author's first published abstract (WARTENBERG *et al.*, 1998). As research progressed and some additional seismic profiles were interpreted, the author identified three older reflections and named them HC, HD and HE. In order to ensure the continuity of the initial nomenclature, the author decided against superseding the preliminary scheme. Hence, within the Tamworth Belt sedimentary package HA represents the youngest and uppermost mapped seismic sequence boundary.

The precise ages of the individual reflectors, however, could not be determined, since it was not possible to correlate them with units in the wells (see **Chapter 3.2.2** for details). Therefore, in order to ensure that the contour maps of the region were representative, the original database (heavy line box shown at the northern end of the Moonie Fault in *Fig.*

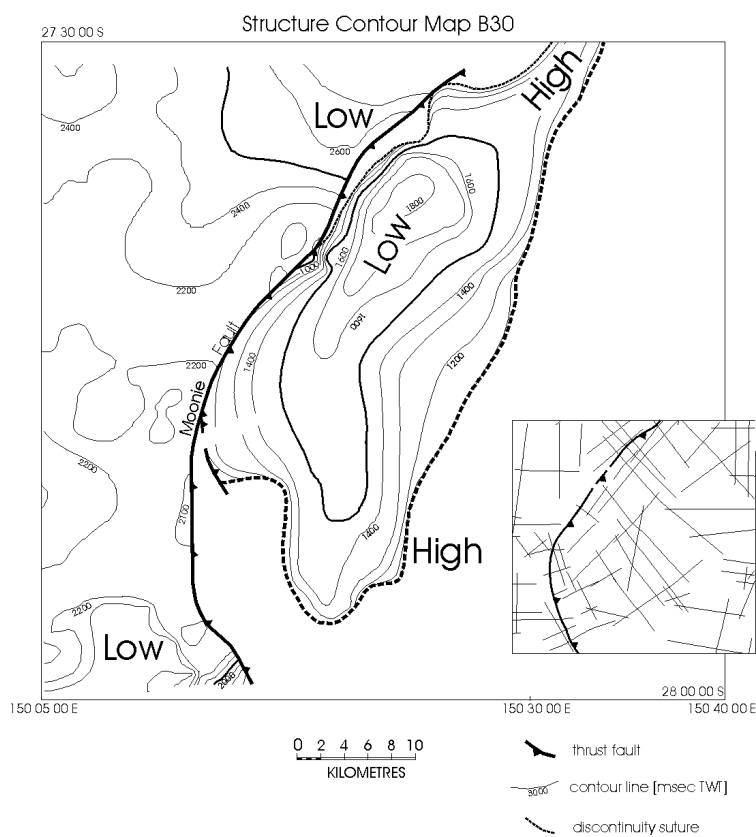


Fig. 3.2: Structure Contour Map of the *B30* seismic reflector, representing the base of the Bowen Basin. The heavy solid lines represents the Moonie Fault and a fault of minor displacement, which is interpreted to be a splay-off fault of the Moonie Fault. The heavy dotted line depicts the position where *B30* is cut by the Mesozoic horizon *S10*.

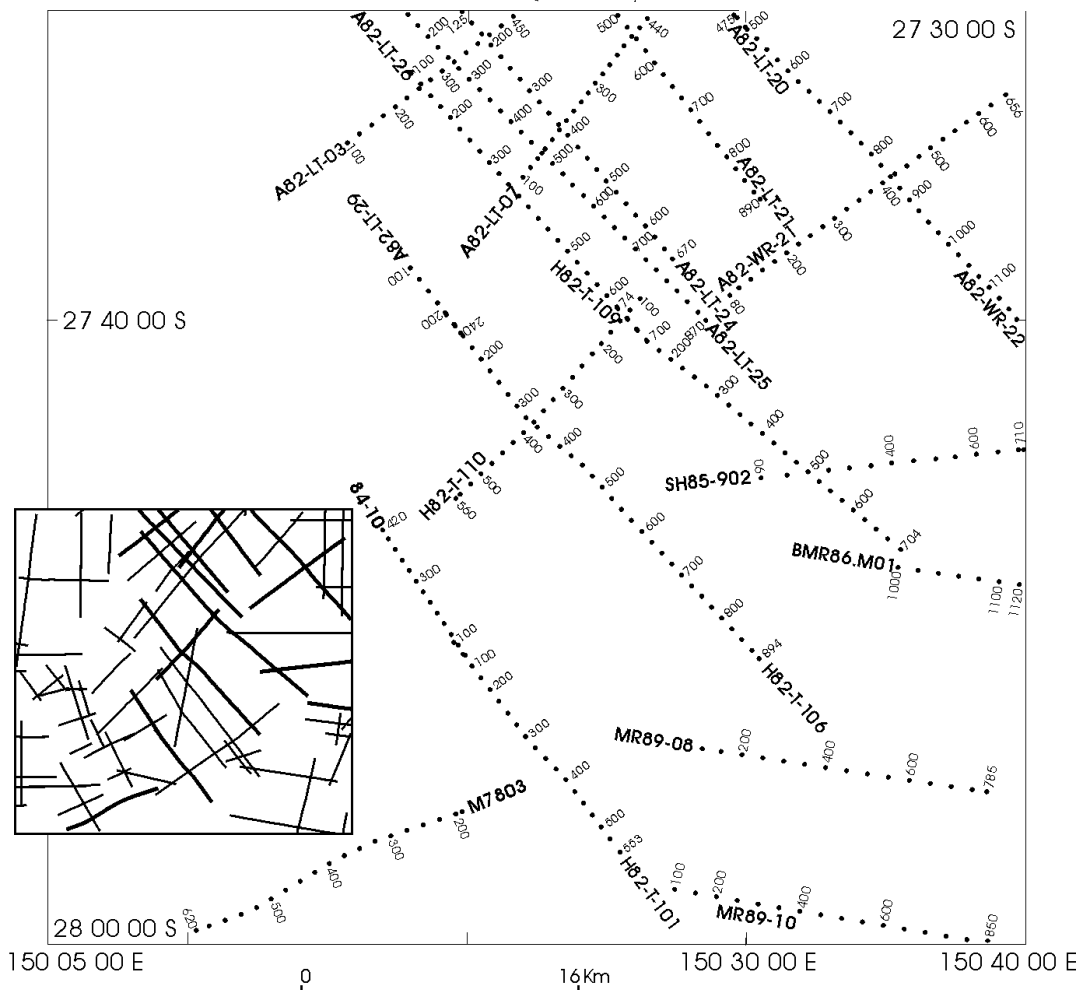


Fig. 3.3 (bottom): Map identifying the shotpoints of the seismic reflection profiles of key interest within the seismic study area. The alpha-numeric code at the end of each seismic line identifies the seismic survey and line number. The box at the bottom left shows the overall seismic coverage (cf. *Fig. 3.1*).

3.1) was restricted to the area containing the highest concentration of seismic profiles to allow for seismic interpretation and three-dimensional imaging (shaded box shown in *Fig. 3.1*, compare with the bigger heavy line box; cf. *Fig. 3.3*).

Two distinct sequence boundaries above the Tamworth Belt succession

On the seismic profiles, the overlying Surat Basin can be clearly identified and is represented by a series of strong, subhorizontal reflections, the strongest of which, in the middle of the succession, correspond to the coals in the Middle Jurassic Walloon Coal Measures (see *Figs 3.4 & 3.5*). The base of the Surat Basin is a sequence boundary defined by a pronounced angular unconformity between it and older units of the Bowen Basin and the Tamworth Belt (*Fig. 3.4, Tab. 2.1*). This basal surface is termed **S10**, following the terminology of TOTTERDELL *et al.* (1992).

Another reflection, termed **B30** identifies a second sequence boundary above the Tamworth Belt reflections and defines the base of the Bowen Basin (*Fig. 3.2*). It represents the base of Early Permian marine rocks and is marked by a high acoustic signal (TOTTERDELL *et al.*, 1992, 1995; BRAKEL *et al.*, in press) (*Fig. 3.4, Tab. 2.1*). To the west of the study area, however, in the Taroom Trough (see *Fig. 3.1*), the basal Bowen Basin is identified on seismic reflection profiles as the **B15** horizon, representing the initial period of lithospheric extension and thus being of pre-**B30**-age (TOTTERDELL *et al.*, 1995; BRAKEL *et al.*, in press).

3.1.1. Five Tamworth Belt reflections

The best quality seismic data to identify and to characterise the five distinctive Tamworth Belt reflections (HA, HB, HC, HD, HE) within the structurally deformed tectonic environment is found on profiles that occur in the broad and flat-bottomed eastern part of the hanging-wall asymmetrical syncline to the east of the Moonie Fault (*Fig. 3.4*). Closed loops of continued seismic reflection correlation with intersecting profiles verify the ties for each reflection.

HE, the oldest identified Tamworth Belt seismic reflection, may be traced within the study area only at great depths (<2500 ms TWT) and is restricted to the easternmost part of the region. It can be identified only on a few profiles to the southeast that were

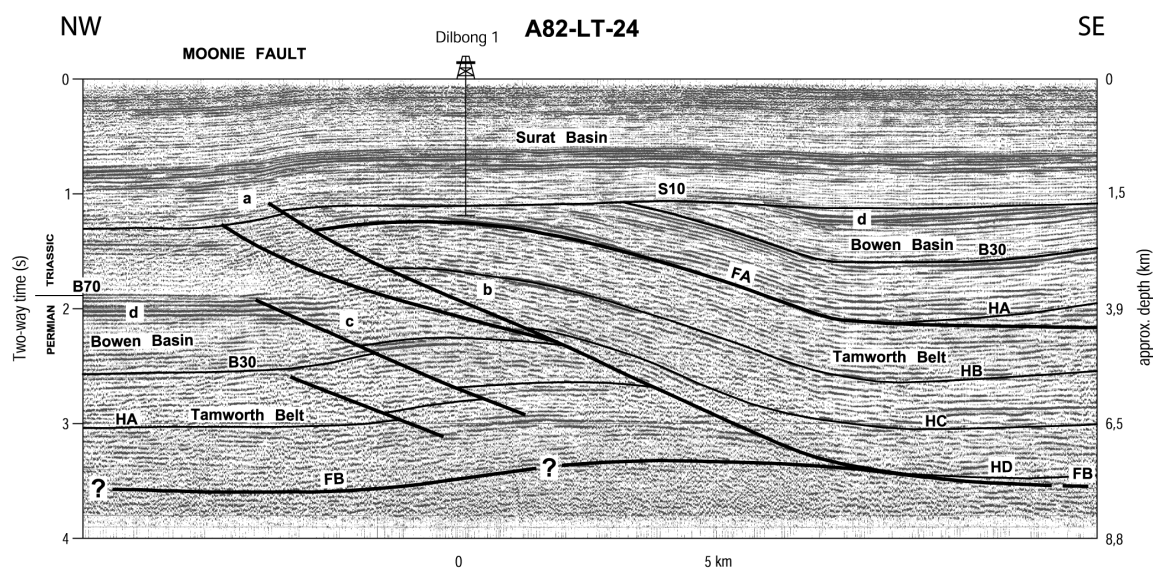


Fig. 3.4: Interpretation of seismic reflection profile A82-LT-24 (final stack) located at the eastern margin of the Bowen Basin. Heavy solid lines represent faults, such as the Moonie Fault as it cuts up section during NW-directed movement (marked as “b”). Its fault tip line cuts the Mesozoic platform cover (marked as “a”, see text for details). Two synthetic faults are recognised (highlighted as “c”).

The light solid lines represent interpreted seismic horizons. *HA*, *HB*, *HC* and *HD* are within the Tamworth Belt succession. *B30* and *S10* represent the sequence boundaries at the base of the Bowen and Surat basins, respectively, and *B70* represents the approximate position of the Permian-Triassic boundary. The strong seismic reflections marked as “d” identify Latest Permian coal measures within the Bowen Basin.

processed down to 4 s TWT, such as MR89-08, MR89-10 and BMR86.MO1 (for location, see *Fig. 3.3*). Elsewhere, on 3 s TWT seismic data, it rarely can be identified within the hanging-wall syncline, where Tamworth Belt sequences of older age can be observed along its flatly west-dipping east limb. However, as the quality of the eastern seismic lines is poor (see above), the western end of the Millmerran profile displays the *HE* reflection best (*Fig. 3.6*), identifying a clearly imaged discontinuity surface below baselapping reflections. However, *HE* is within a strongly deformed zone, located between two westward-dipping, basin bounding faults to the east and is therefore hard to pick on the seismic record close to the eastern margin of the Tamworth Belt (*Fig 3.6*).

Reflector *HD* represents a seismic discontinuity surface within the lower Tamworth Belt sequence, and can best be traced within the westward-dipping sedimentary succession in the eastern part of the study area. On line *H82-T-109* (*Fig. 3.5*) *HD* is interpreted as a truncating seismic horizon below toplapping reflections.

The seismic horizon *HC*, perhaps, is the strongest of all identified Tamworth Belt reflections in the study area. It is characterised by seismic reflections baselapping on to it

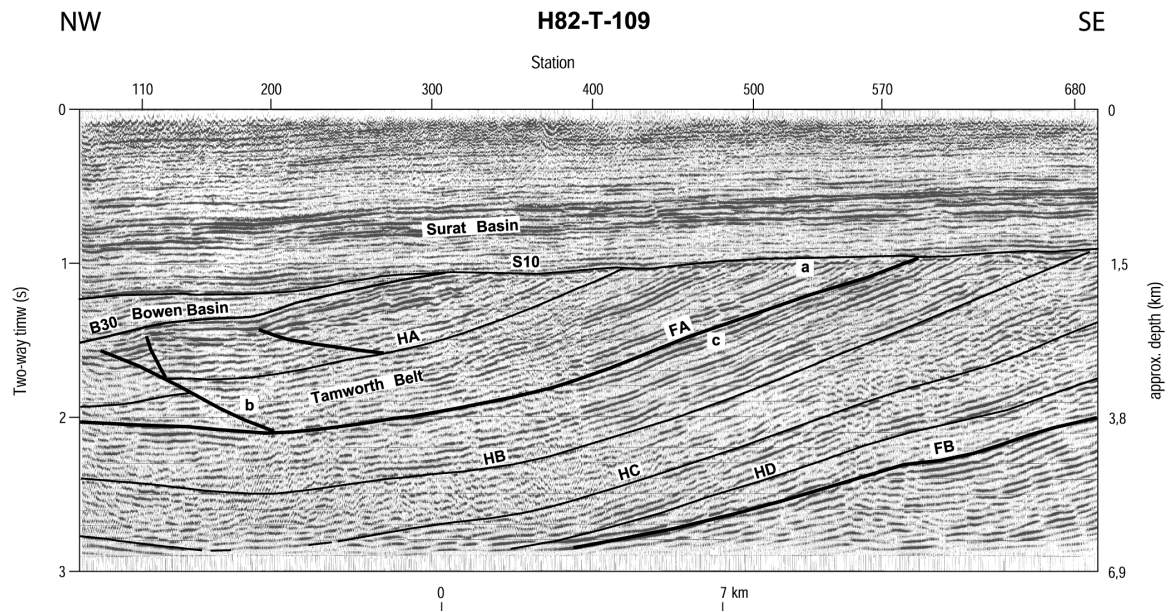


Fig. 3.5: Interpretation of the migrated seismic reflection profile H82-T-109 located south-east of line A82-LT-24, perpendicular to strike of the subsurface Tamworth Belt (cf. Fig. 3.4; see text for details). The light solid lines represent interpreted seismic horizons. *HA*, *HB*, *HC* and *HD* are within the Tamworth Belt succession. *B30* and *S10* represent the sequence boundaries at the base of the Bowen and Surat basins, respectively. Beneath the *S10* discontinuity a weathering surface may be identified (marked as “a”).

Heavy solid lines represent interpreted faults. The fault marked as “b” depicts a back-thrust off a fault plane “c” that runs subparallel to the fore-arc basin sequences (see Chapter 5 for details).

(Fig. 3.5). On some seismic profiles in the study area, *HC* may be traced to depict the structure of an older ramp.

HB defines a distinct change of the reflection pattern on the seismic images and can be identified to truncate baselapping reflections (Figs 3.4 & 3.5). The *HB* reflection can often be traced to be a base of a package of reflections above a non-reflective zone within the seismic record.

The uppermost Tamworth Belt seismic reflection, *HA*, identifies a baselap horizon (Figs 3.4 & 3.7), that, at the western end of the hanging-wall succession, quite often is cut by a sub-horizontal running fault (see “*FA*” on Fig. 3.4). Also, the *HA* reflection can be recognised by truncation of reflections.

3.1.2. Defined Tamworth Belt sequences

In the subsurface, within the Tamworth Belt, six seismic sequences are recognised on the basis of reflection truncation geometries, separated by the above mentioned five seismic

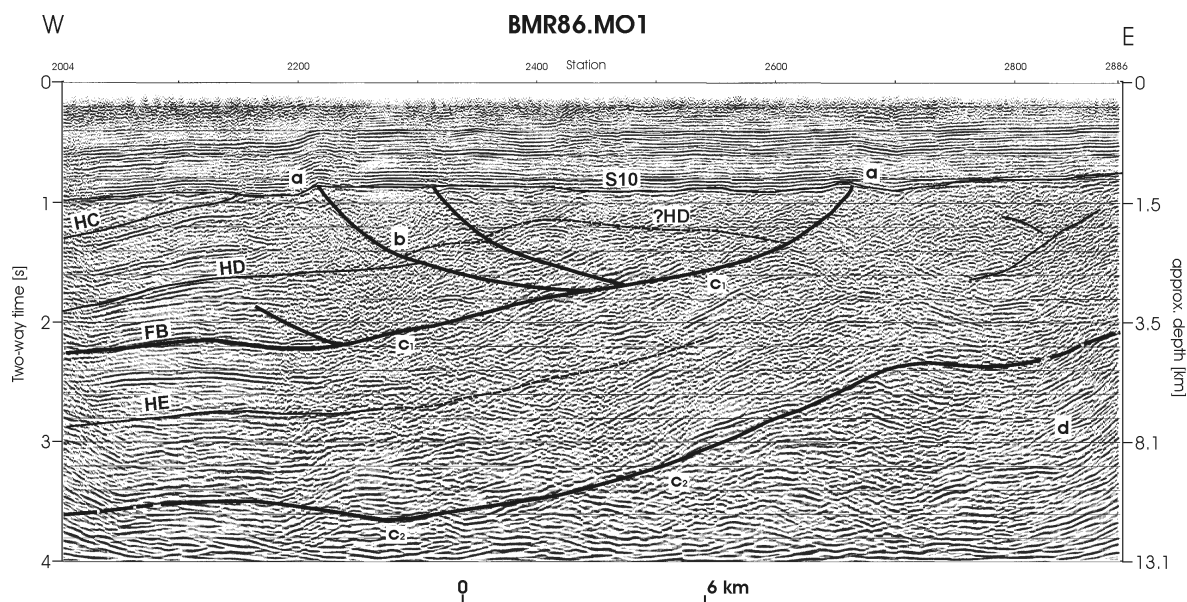


Fig. 3.6: Interpretation of the migrated seismic reflection profile BMR86.MO1 (“Millmerran profile”) located to the east of line H82-T-109 at the eastern end of the Tamworth Belt (see text for details). Heavy solid lines represent interpreted faults. Two faults of major importance are marked as “c₁” and “c₂”, respectively. “b” is interpreted as a back-thrust off the westward-dipping fault marked as “c₁”. “a” indicates the reactivation of faults influencing the lowermost sequences of the Mesozoic Surat Basin cover (S10 represents the base of the Surat Basin).

Light solid lines represent Tamworth Belt seismic reflections. HE, HD and HC are within the fore-arc basin succession. The ratio of vertical to horizontal scale approximately equals 1.

horizons and showing more or less parallel reflections. Occasionally, the horizons become conformable but can be traced across the seismic line by reflection correlation. Internally, the seismic sequences appear to be very similar in terms of individual reflection properties (e.g. amplitude, continuity, etc.), although there are variations both in terms of these particular properties and also the relationship with either the underlying or overlying horizons. The within-sequence variation of these zones is, therefore, indicative of the changing pattern of facies distribution over time. The Tamworth Belt sequences appear to slightly thicken towards the east, reaching their maximum thickness - at least within the southern part of the study area - close to the eastern margin of the belt (to the west of the zone including “c₁” and “c₂” on Fig. 3.6). Especially the sequence that is defined between the HA and the HB seismic reflection is more often imaged to thicken towards the east. The uppermost succession of the youngest Tamworth Belt sequence, that is, the sedimentary section beneath the B30 base of the Bowen Basin, often is seen to be defined by relatively high amplitude and more or less continuous reflections of subparallel behaviour.

3.1.3. Representative seismic sections

“Excellent seismic images represent a real opportunity for quantitative insight into both regional structural development and fundamental deformational mechanisms” (GONZALEZ-MIERES & SUPPE, 2004) - the same holds for the stratigraphic relationships displayed on seismic profiles. Within the investigated area, seismic imaging of the subsurface fore-arc basin is proof of this statement - at least at first site. The overall structural geometry seems to be relatively simple: a foreland fold thrust belt contains the fore-arc basin sedimentary record within its hanging-wall. In order to discuss the sedimentary record and the subsurface geometry of the Tamworth Belt, several representative seismic sections shall be discussed. Seismic reflections within the hanging-wall unit were identified and help to improve the tectono-stratigraphic understanding of the Devonian-Carboniferous sequences. The location of the seismic profiles of key interest within the study area are shown in *Figure 3.3*. The analysis of the seismic data, however, invokes a complex tectonic architecture. This required the author to separate the stratigraphic geometry (this chapter) from the structural development of the Tamworth Belt sequence (**Chapter 5**).

Composite profile A82-LT-24 – H82-T-109 – BMR86.M01

Within the seismic study area, the longest composite seismic cross section across the subsurface Tamworth Belt runs for approximately 66 kilometres and provides good quality seismic data (for location, see *Fig. 3.3*). It starts in the northwest with line A82-LT-24 (*Fig. 3.4*), which imaged the Moonie thrust fault at its western end (*Fig. 3.1*). It proceeds along line H82-T-109 (*Fig. 3.5*) and ends in the east with line BMR86.M01 (“*Millmerran*” profile, *Fig. 3.6*). The Millmerran line does not cross the eastern boundary but depicts the belt’s geometry in close vicinity to it (see *Fig. 3.6*). A82-LT-24 and H82-T-109 are industry lines that were acquired in 1982 by Alliance Minerals and Hartogen Exploration, respectively. The former was recorded to four seconds (~ 8.8 km depth) and the latter to three seconds two-way travel time (TWT) (~ 6.9 km depth). Both profiles were processed as final stacks. Line H82-T-109 was reprocessed as a migrated profile (*Fig. 3.5*). The third line to the east, BMR86.M01 (*Fig. 3.6*), was originally acquired by the Bureau of Mineral Resources (now Geoscience Australia - GA). The Millmerran profile was the only seismic line within the study area that was recorded to six seconds TWT (~ 18 km depth). The original quality of this profile, however, was poor, and therefore in

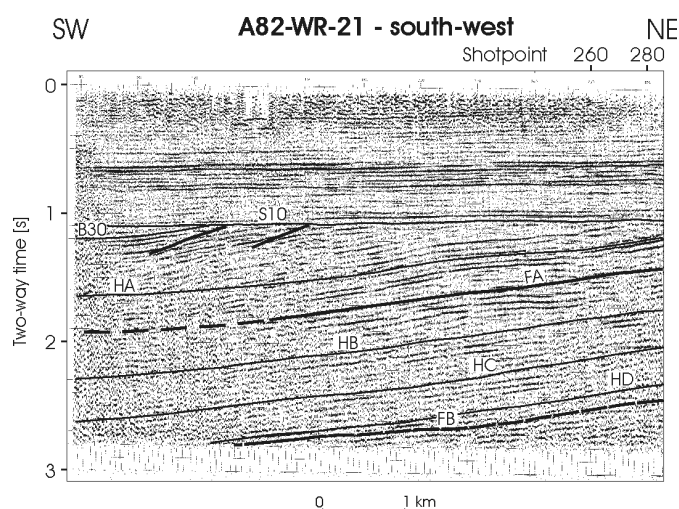
1998 GA undertook additional processing of the profile to improve the display in order to better integrate the data into the existing database. The reprocessed Millmerran profile was subsequently redisplayed at the same vertical scale as the two industrial lines.

Unfortunately, the three sections do not tie to one another, but the basin geometry has allowed correlation between the profiles (gaps between the lines are approximately 1100 m and 3000 m wide) and neighbouring seismic profiles (e.g. A82-LT-25, see *Fig. 5.16* and SH85-902, see *Fig. 3.3* for location) underline the belt's geometry that is shown on the composite cross-section. The only sections across the entire subsurface Tamworth Belt, depicting the Moonie Fault to the west and the Peel Fault to the east, are the two deep seismic profiles BMR84.14 to the north and BMR91.G01 to the south (both recorded to 20 s TWT), both of which are located at some distance from the seismic study area (*Fig. 3.1*) (see **Chapter 5.1.1.**). Three other shallow seismic (3 s TWT) composite sections across the subsurface Tamworth Belt also depict the Moonie Fault at the western end with the broad and moderately folded hanging-wall to the east of it, but do not picture the eastern end of the fore-arc basin succession. As for the seismic lines A82-LT-24 and H82-T-109, each of the seismic profiles was acquired in 1982 by Alliance Minerals and Hartogen Exploration, respectively. From north to south, the seismic traverses are A82-LT-20/A82-WR-22, A82-LT-29/H82-T-106 and 8410/H82-T-101 (see *Fig. 3.3* for location).

The seismic profile A82-LT-24 is situated in the western part of the investigated area (*Fig. 3.3*) and was acquired perpendicular to the strike of the fore-arc basin. Here, the

Fig. 3.7 (previous page and beneath): Interpretation of the seismic reflection profile A82-WR-21 (final stack) located to the north-east of the study area. Heavy solid lines represent fault reflections. The light solid lines represent interpreted seismic horizons. HA to HD are within the Tamworth Belt succession. S10 represents the sequence boundary at the base of the Surat Basin. See text for details.

The profile on the previous page displays the seismic expression of the south-western part of the seismic line. Note onlap of the upper beds of the Tamworth Belt onto HA.



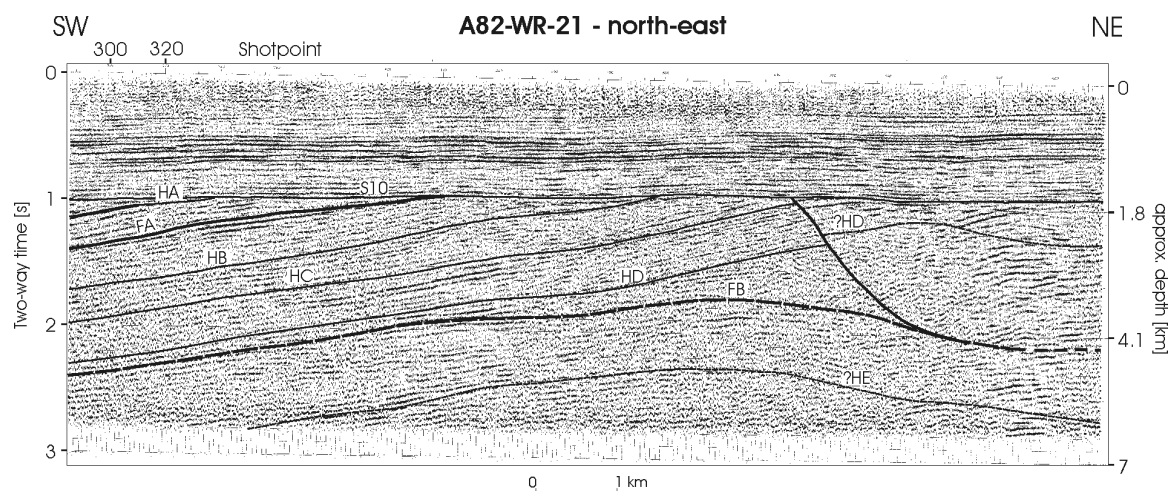
seismic reflections *HD* to *HA* may be tracked on to the east limb of the asymmetric syncline that identifies the eastern part of a thrust-related fault-bend fold (see **Chapter 5.1.**).

Within the study area, the subsurface Tamworth Belt succession is bounded across strike by two major fault structures. The Moonie Fault to the west is identified as a thrust fault at the north-western end of line A82-LT-24, with north-west-directed movement beneath the Surat Basin sedimentary cover (*Fig. 3.4*). On the seismic profile BMR86.MO1 two major westward-dipping faults (“*c*₁” and “*c*₂” on *Fig. 3.6*) are identified, that form a zone representing the easternmost margin of the Tamworth Belt and are covered by the Surat Basin succession (*S10* in *Fig. 3.6*). The main focus concerning the stratigraphic geometry of the Tamworth Belt sequence shall therefore be drawn on the area between the Moonie Fault to the west and the west-dipping faults to the east.

A82-WR-21

Towards the north-eastern end of the study area, the seismic profile A82-WR-21 (*Fig. 3.7*) images the reflection pattern of the eastern flank of the pre-Jurassic syncline (see *Fig. 3.3* for location; cf. *Fig. 3.5*). Here, in the hanging-wall of the Moonie Fault, the Tamworth Belt succession has an apparent dip to the south-west (*Fig. 3.7*), displaying the youngest identified fore-arc basin reflections *HD* to *HA* (except *HE*) above a sub-parallel fault plane which can be linked to the Moonie Fault to the west.

The *HA* reflection is cut by the base of the Surat Basin at the Shotpoint (SP) 320,



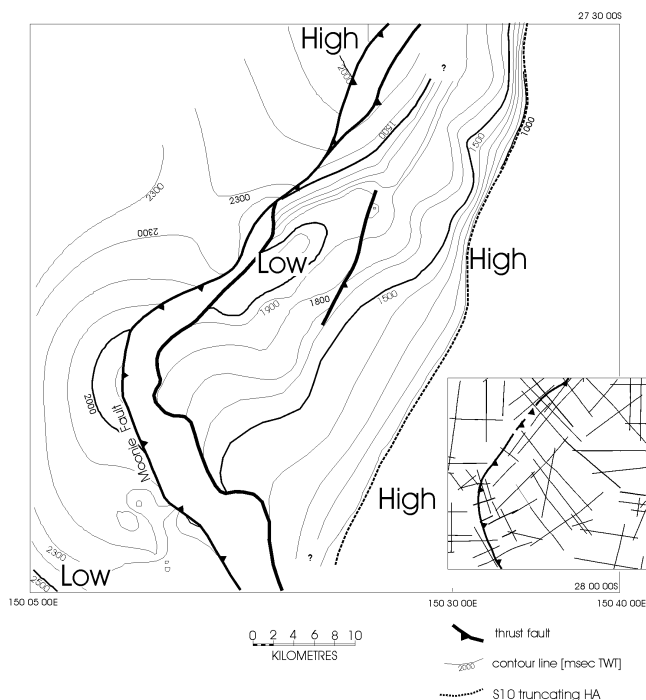


Fig. 3.8: Structure Contour Map showing the distribution of the seismic horizon *HA* (uppermost Tamworth Belt reflection) within the study area. The heavy solid lines represent faults cutting the fore-arc basin reflection. The light dotted line represents the line where *HA* is truncated by *S10* (base Surat Basin).

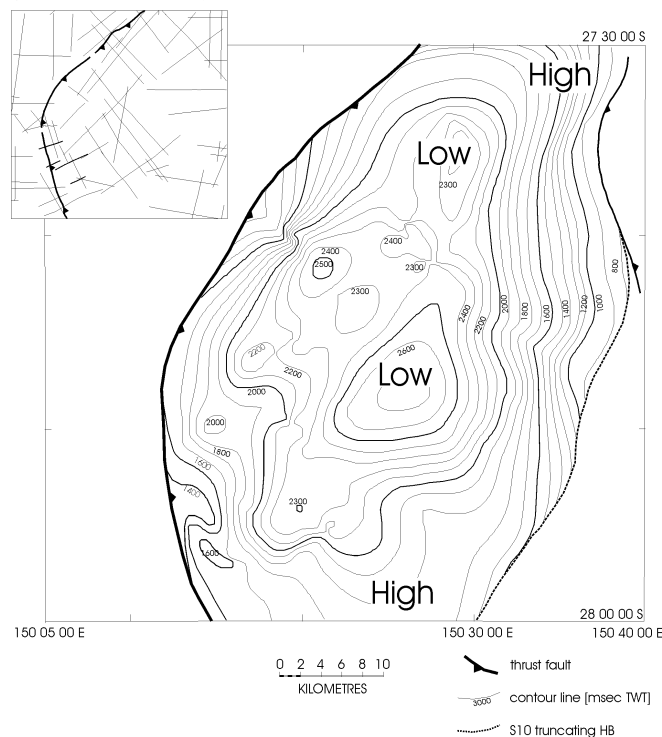


Fig. 3.9: Structure Contour Map showing the distribution of the seismic horizon *HB* within the study area. The heavy solid lines represent faults cutting the fore-arc basin reflector. The light dotted line represents the line where *HB* is truncated by *S10* (base Surat Basin).

at a depth of *c.*950 ms TWT and dips south-westwards, identifying a baselap horizon (at SP 280 - 300) above two strong seismic reflectors (see south-western part of *Fig. 3.7*). At the north-eastern end of the profile, beneath the Surat Basin cover (beneath *S10*), the seismic reflection pattern is clearly of a different character than the seismic record at the south-western end of the profile (*Fig. 3.7*). Strong and more disrupted reflections mimic the seismic record of the hanging-wall sequence and are interpreted to be set off the south-western fore-arc basin succession by a north-east dipping fault that may be interpreted as another back-thrust of a major fault plane (*FB* in *Fig. 3.7*).

3.2. Comparison of defined units to existing stratigraphy

The uppermost Tamworth Belt seismic reflection *HA* is of most interest, when comparing the seismic sequences identified here to those seismic sequences

interpreted by earlier research. TOTTERDELL *et al.* (1995) and BRAKEL *et al.* (in press) identified another seismic reflection beneath the base of the Bowen Basin (*B30*), termed *B15*, and correlated *B15* to the initial period of lithospheric extension (see Chapter 3.1).

3.2.1. Palynology of previous studies

The uppermost Tamworth Belt reflections are of Late Carboniferous age (*Tab. 2.1*), implying for *B15* (the base of the Bowen Basin in the Taroom Trough to the west of the study area) not to be of Early to Mid Permian age but older. In general, the defined seismic sequences in the Tamworth Belt are difficult to date because palynological control is sparse, provided by only a few samples from drill core across the entire region.

The oldest palynoflora, from the Durabilla 1 well, is *Visean* (Early Carboniferous) (DE JERSEY in MURRAY, 1994), confirming the correlation with the exposed Tamworth and

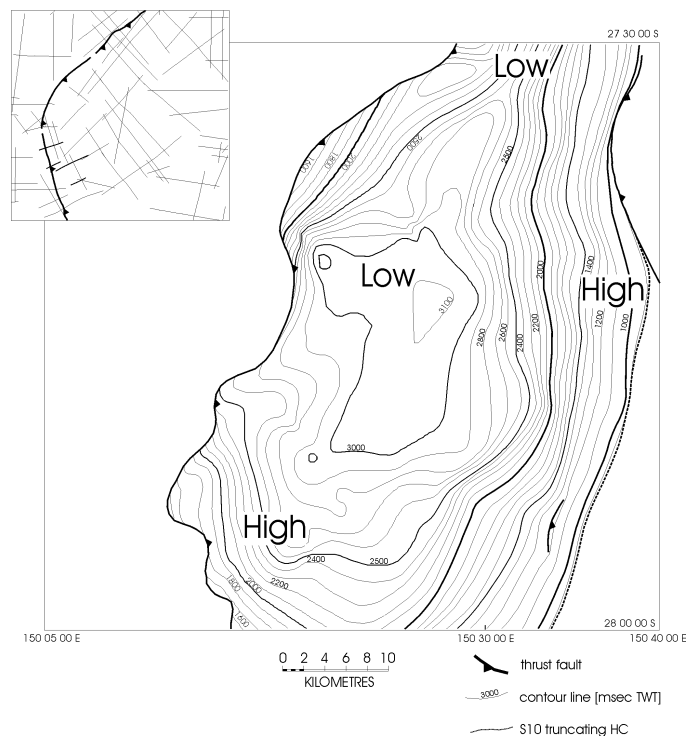


Fig. 3.10: Structure Contour Map showing the distribution of the seismic horizon *HC* within the study area. The heavy solid lines represent faults cutting the fore-arc basin reflection. The light dotted line represents the line where *HC* is truncated by *S10* (base Surat Basin).

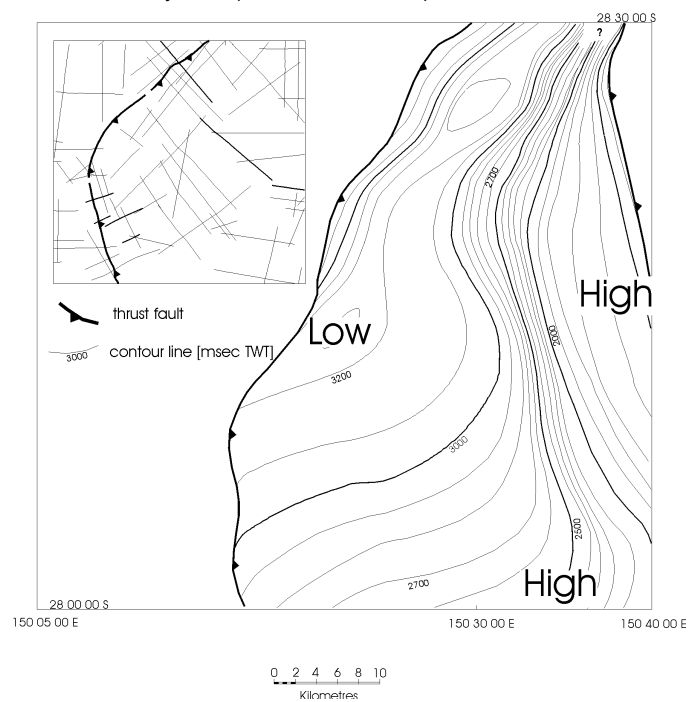


Fig. 3.11: Structure Contour Map showing the distribution of the seismic horizon *HD* within the study area. The heavy solid lines represent faults cutting the fore-arc basin reflection.

Yarrol belts. Palynological samples from five other wells have been dated as Late Carboniferous to earliest Permian (see MURRAY, 1994), equivalent to the uppermost parts of the exposed belts. In three other wells, including Gilgai 1 (see *Fig. 6.1* for location), the palynoflora was dated as Early Permian (J. L. MCKELLAR, pers. comm., 1994) (*APP 2.1* stage of PRICE, 1997), which provides a correlation with the sequence at the base of the Bowen Basin (*Supersequence A* of BRAKEL *et al.*, in press).

Defined Supersequences

In the Bowen Basin, Supersequence A (BRAKEL *et al.*, in press) occurs immediately below the *B30* sequence boundary, implying that the seismic sequence in the subsurface Tamworth Belt between *B30* and the seismic reflection *HA* is its equivalent. However, the interpretation of the grid of seismic lines in the study area does not provide more refined estimates of the ages of the sequences.

3.2.2. Supporting borehole-stratigraphy

Eight exploration wells support the seismic coverage of the subsurface fore-arc basin geometry in the area of interest, five of which penetrate the Tamworth Belt (see **Chapter 6 – age control**). Moreover, the borehole data of another ninety-one wells, piercing pre-Jurassic rocks, has been examined by the author. However, out of the total of ninety-nine wells, it was only the data of well *Deep Crossing* that shows evidence for upper Tamworth Belt sequences close to the seismic study area (*Fig. 3.12*, see *Fig. 6.1* for location). As the primary target of most of the drilling within the study area was for hydrocarbons expected to be in the Early Jurassic *Precipice Sandstone*, the majority of the boreholes terminated soon after having penetrated the *Hutton-Evergreen-Precipice sequence* immediately above the base of the Surat Basin (*S10*; see *Fig. 3.12*). Hence, in most of the wells, the unconformably underlying Permo-Carboniferous rocks have been penetrated only at the metre scale and therefore can not be correlated with the reflection pattern seen on the seismic profiles. The basement rocks beneath the *Precipice Sandstone* in wells that intersect the seismic reflection profiles imaged in this thesis, were listed as *Carboniferous basement* (187.1 m thick) for the well **Durabilla**, *Kuttung Formation* (10.1 m thick) for the well **Dilbong**, and were not listed at all in the well **Gilgai**.

Note: *Kuttung Formation* as referred to in most of the drilling reports is not a proper geological term. The rocks identified as *Kuttung Formation* are meant to be pre-Permian Volcanics and/or volcanic derived sediments.

In the wells studied, the Gunnedah-Bowen Basin system is represented by the *Maules Creek Formation* (Early Permian), the *Back Creek Formation* (Late Permian) and the *Cabawin Formation* (Early Triassic). The Early Jurassic *Precipice Sandstone* and *Evergreen Shale* are members of the disconformably overlying Surat Basin (*Fig. 3.12*).

Deep Crossing (Lat.: 27.468971S Long.: 150.486693E)

A minor aim during the drilling of the Deep Crossing well was to develop a better understanding of the sand units in the Permian Back Creek Formation (*Tab. 2.1*). The well Deep Crossing terminated at a total depth of 2912 m, and, although it penetrated 1284.5 metres of pre-Jurassic rocks, there were no sediments of the Blackwater and Back Creek groups found. Initially, these sediments were suspected to occur in Block I as shown on the lithology profile of *Figure 3.12*. The location of the well does not occur on any of the seismic traverses within the study area, but it is in close vicinity to the seismic profiles A82-LT-07 (approx. 800 m), A82-LT-08 (approx. 1930 m), A82-LT-19 (approx. 300 m), A82-LT-20 (approx. 1845 m) and A82-WR-22 (approx. 3240 m). Owing to the extremely sparse coverage of pre-Jurassic borehole data along the seismic lines in the study area, the information gained from the Deep Crossing logs was used to trace at least the uppermost seismic reflection of the subsurface Tamworth Belt.

Lithology and Wireline Logs

The base of the Surat Basin (*S10* on the seismic profiles) is marked in Deep Crossing by a boundary between the Jurassic Precipice Sandstone and undifferentiated volcanogenic rocks of unknown age beneath it at a depth of 1627.5 m (see *Fig. 3.12*). The Gamma Ray, Sonic and Resistivity logs identify this boundary as a transitional sequence that may be interpreted as a weathering zone (see “a” in *Fig. 3.12*). ADAMSON & DORSCH (1988) interpreted the well information by defining several segments in the

borehole record beneath the Surat Basin succession (see *Fig. 3.12*). The pre-Jurassic well data correspond to four blocks, subdivided using the wireline logs (from older to younger **Block IV, III, II** and **I** of *Fig. 3.12*). Moreover, ADAMSON & DORSCH (1988) defined six lithological units, designated **Unit A** (youngest) to **Unit F** (oldest).

The upper sequence is predominantly characterised by volcanogenic rocks with a shaly intersection of *c.*65 m in thickness at the top of **Block I** and **Unit A**, respectively. On the lithology log, this sequence is identified at a more shallow depth than the corresponding signal of the relevant wireline data – leaving the signal of the Gamma Ray, Sonic and Resistivity more to be trusted when depth-correlating the borehole data with the seismic record (compare *b*₁, *b*₂, *b*₃ and *b*₄ of *Fig. 3.12*). **Block I** is characterised by a very irregular profile (“kinky graph”) of the Sonic log (better observed on the larger scaled original log) and the Gamma Ray log and a frequently changing, high amplitude signal of the Resistivity log, identifying a frequent change in lithology. **Block II** depicts

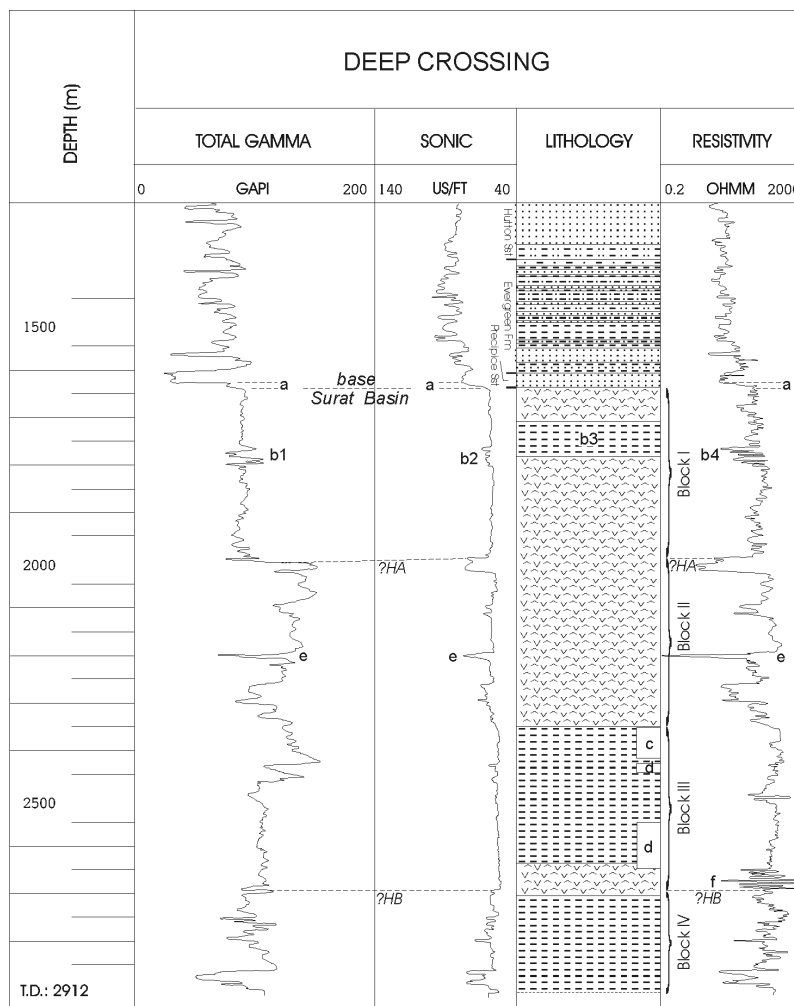
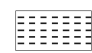





Fig. 3.12: Borehole data from the well Deep Crossing (*Lat.*: 27.46 89 71S; *Long.*: 150.48 66 93E) drilled by the petroleum exploration industry.

Precipice Sst, Evergreen Fm and Hutton Sst represent the lowermost sedimentary succession of the Jurassic-Cretaceous Surat Basin. **Block IV** to **Block I** and **Unit F** to **Unit A** were identified by ADAMSON & DORSCH (1988).

The correlations between the well-data and the interpreted seismic reflection profiles are marked “a” to “f” and are referred to in **Chapter 3.2.2**.

-  Shale
-  Siltstone
-  Sandstone
-  Volcanogenic rocks

a distinctive strong shift in the interval transit time of the Sonic log and clearly identifies a change in the lithology within the volcanic rock sequence (see “e” in *Fig. 3.12*). ADAMSON & DORSCH (1988) here defined the lithological boundary *Unit C/Unit B* at a depth of *c.*2200 m. The uppermost part of ADAMSON & DORSCHS’ *Unit D* is represented by hard and highly silicified sandstone with angular break (highlighted as “c” in *Fig. 3.12*). Within *Block III*, at a depth of *c.*2450 m and, respectively between *c.*2540 m and *c.*2645 m, ADAMSON & DORSCH observed a strong flow in the lithological groundmass (Marked “d” in *Fig. 3.12*). The top of *Unit E* and *Block IV*, respectively, is coincident with a slight shift in the interval transit time of the Sonic log and a higher amplitudinal signal of the Gamma Ray and the Resistivity respectively (“f” in *Fig. 3.12*). The bottom 50 metres of well Deep Crossing identify the sixth lithological unit, *Unit F*, and depict a clear change in all wireline logs displayed.

Comparing the borehole data to the seismic record

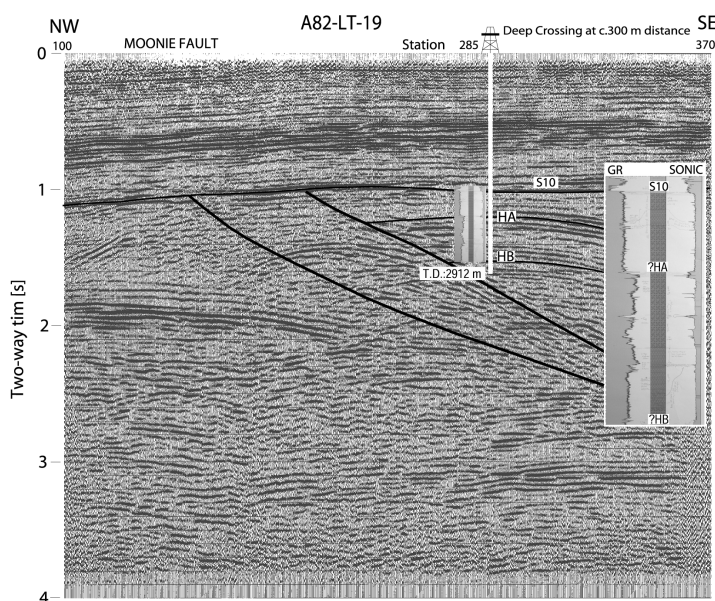


Fig. 3.13: Seismic profile A82-LT-19 (final stack), located immediately to the north of the study area (for location see *Fig. 6.1*), showing the position of the well Deep Crossing jump-tied on top of the seismic image (cf. *Fig. 3.12*) (the distance between the borehole location and the seismic survey approximately is 300 m). Black solid lines represent faults. Light solid lines represent seismic reflections.

The transitional sequence at the base of the Jurassic succession (*Precipice Sandstone*) marked as “a” in the Gamma Ray, Sonic and Resistivity logs substantiates the interpretation of various seismic profiles where a disruptive seismic signal was observed and was interpreted to depict a weathering zone along the basal Surat Basin reflection *S10* (cf. “a” in *Fig. 3.12* and “a” in *Fig. 3.5*).

The shaly intersection at the top of *Block I* (*Fig. 3.12*) can be compared to a zone of a diffractive seismic pattern of *c.*40 ms TWT on the seismic profiles which may correspond to a zone of tectonic weakness within the uppermost Tamworth Belt succession (see fault structures in *Fig 3.5*).

HA being the uppermost Tamworth Belt seismic reflection, may be identified by the borehole data in the volcanogenic rocks at a depth of *c.*2000 m in Deep Crossing Well (*Fig. 3.12*), depicting the Block I/BlockII boundary (ADAMSON & DORSCH, 1988). Here, the seismic horizon is coincident with a strong shift in the interval transit time of the Sonic log and a higher amplitudinal signal of the Gamma Ray (see “?HA” in *Fig. 3.12*).

The Tamworth Belt seismic reflection *HB* is interpreted to occur within the lower sequence of a volcanic intersection at *c.*2690 m. On the Sonic log a slight shift in the interval transit time is observed, corresponding to a higher amplitudinal signal of the Gamma Ray and the Resistivity respectively (see “f” in *Fig. 3.12*). Moreover, the *HB* reflection corresponds with the top of the lithological Unit E as defined by ADAMSON & DORSCH (1988).

The bottom 50 metres of the borehole data depict a clear change in the wireline log record. Although the Sonic log of Deep Crossing shows a sharp and strong change in the interval transit time, the seismic data that are located nearby do not show any distinct changes in the reflection pattern. However, the location of the well Deep Crossing does not directly intersect any of the seismic profiles and thus the cause of the lithological and wireline signals of the bottom 50 metres of the well may not be displayed as a distinctive feature on the seismic reflection record.

3.2.3. Stratigraphic geometry – short discussion

The individual Tamworth Belt seismic reflections designated *HE* (older) to *HA* (younger) identify five intra-fore-arc basin boundaries and can be recognised in the subsurface sedimentary record to lie more or less conform to each other. The oldest seismic reflection *HE* is within a strongly deformed zone, located between the two ba-

sin bounding faults and is therefore hard to pick on the eastern side of the seismic record, close to the eastern margin of the fore-arc basin. The Tamworth Belt sedimentary succession thickens towards the basin bounding fault zone to the east. Six defined seismic sequences appear to be internally very similar in terms of individual reflection properties such as amplitude and continuity. In the foot-wall, on the western side of the Moonie Fault, the Tamworth Belt reflections are less continuous. In the hanging-wall, to the east of the Moonie Fault, the stratigraphical record of the fore-arc basin succession is seen best. However, as the subsurface Tamworth Belt has been subject to major thrusting, sequence repetition within the interpreted fore-arc basin succession is likely to occur.

Es gab Steine links und Steine rechts
Und niedriges dürres Gestrüpp dazwischen,
und dreimal vernahm er ein tiefes knappes
Knacken,
obwohl niemals jemand zu sehen war.

Rudyard Kipling

4. MAGNETIC AND GRAVITY ANOMALIES

4.1. Introduction

Gravity and aeromagnetic data from eastern Australia are held by Geoscience Australia. The digital information has been modified using ER Mapper 5.5a software, based on a geodetic Map Projection with a Geodetic Datum of AGD 66 (Australian Grid Data). Total Magnetic Intensity (**TMI**) and gravity datasets (**Bouguer Gravity**) were produced in pseudocolour mode and are here displayed in either RGB-colour (*Red-Green-Blue*) or shades of grey. The original datasets for both aeromagnetic and gravity information were initially generated to provide an overview of these parameters for the entire Australian continent. As part of this study, however, both the aeromagnetic and gravity data were reprocessed in order to provide more detailed information on the geometry of the area under investigation. The New England Orogen region was mapped from 19° S to 34° S and from 147° E to 154° E, the study area, in larger scale, from 27° 15' S to 28° S and from 150° 05' E to 150° 40' E.

4.2. Aeromagnetic data

The aeromagnetic images (gradient-enhanced residuals of total magnetic intensity) are based on the 1996 Geoscience Australia 1:5 000 000 scale Magnetic Anomaly Map of Australia (TARLOWSKI *et al.*, 1996) and on the 1976 Geoscience Australia 1:2 500 000 scale Magnetic Anomaly Map of Australia (BMR, 1976). The data from surveys in the Tamworth Belt are reasonable closely spaced, with an average line spacing of about 400 metres, with some surveys having a

line spacing of 200 metres (flown by the state geological surveys). As part of this study, the generated images were modified by using a Gaussian Equalise with transform limits from 4430 nT to 5560 nT. This was based on a contrast maximise using a 3 x 3 North-South Kernel Sunangle Filter. A 3 x 3 West-East Kernel Sunangle Filter was used in the algorithm's Intensity Layer. An Average 5 x 5 Kernel Lowpass Filter was added to the Pseudo Layer (e.g. Fig. 4.1). Additional techniques (e.g. smoothing and draping colours) were used in order to enhance the anomaly contrast in such a way as to make it possible to view it as a grey-scale image (e.g. Fig. 4.2).

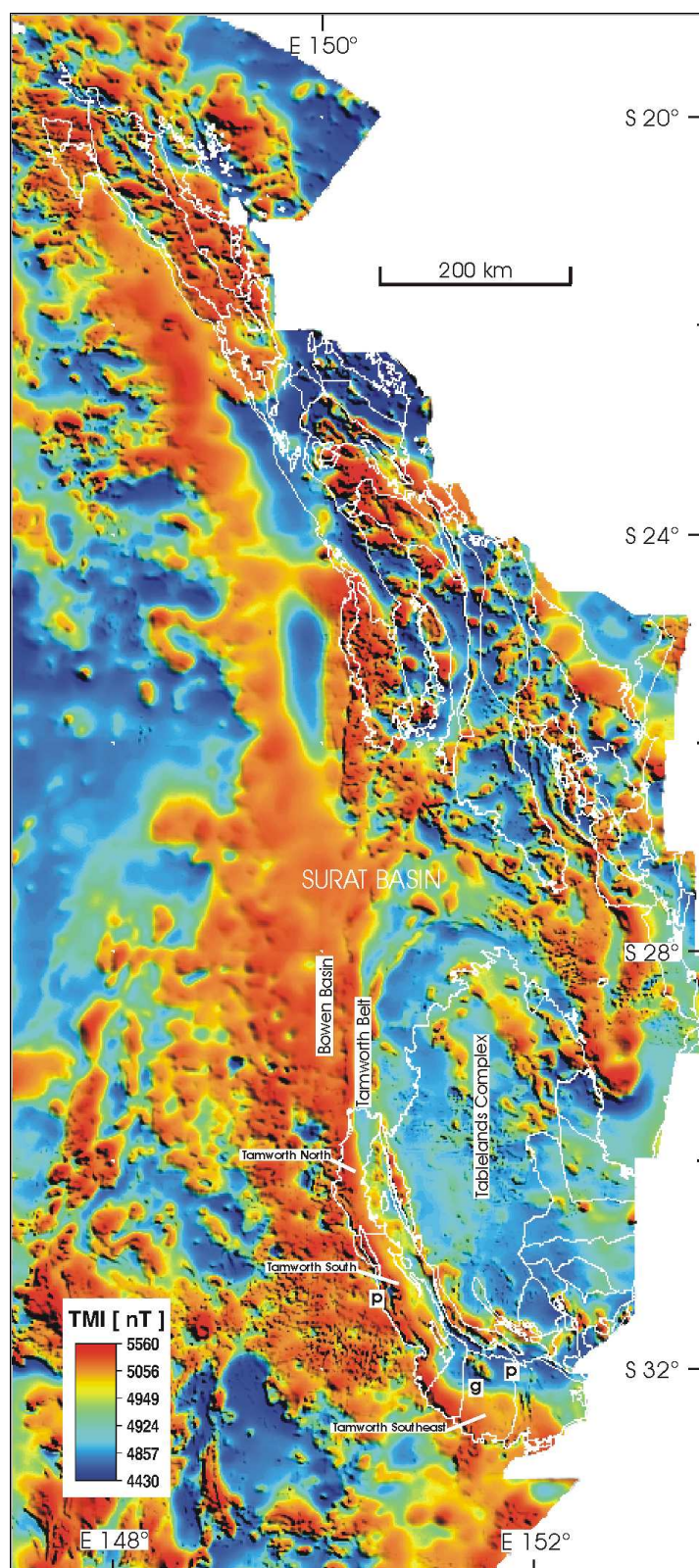


Fig. 4.1: Aeromagnetic anomaly image, using Total Magnetic Intensity [nT], overlain by a terrane map of the New England Orogen (white solid lines). The pseudocolour image is based on aeromagnetic data collected by Geoscience Australia and the Geological Surveys of New South Wales and Queensland. The aeromagnetic features marked as *p* and *g* refer to surface geology, depicting the location of Permian sediments and granite, respectively (see text for details).

4.2.1. Aeromagnetic data – presentation

Aeromagnetic images of the New England Orogen and the surrounding region indicate that the Bowen Basin has a higher Total Magnetic Intensity than most of the New England Orogen. The Tamworth Belt to the east is generally identified through lower magnetic anomaly values (*Figs 4.1, 4.2, 4.6 & 4.7*). The aeromagnetic response of the subsurface Tamworth Belt is characterised by a moderate decrease in magnetic intensity from west to east (*Figs 4.1, 4.6 & 4.7*). A slightly right-curved, N-S-trending disrupted magnetic ridge (*c.* 5010 – 5060 nT on *Fig. 4.1*) identifies the easternmost limit of the Tamworth Belt in the southern New England Orogen, extending over approximately 400 kilometres from S32° to S28° (*Figs 4.1 & 4.2a*).

In the study area, the close line spacing of maximum 400 m allowed the author to construct several magnetic traverses along key seismic lines using the ER Mapper software, in order to complete the seismic interpretation of the subsurface Tamworth Belt succession across strike (*Figs 4.3, 4.4, 4.5; cf. 4.7*).

4.2.2. Aeromagnetic data – interpretation

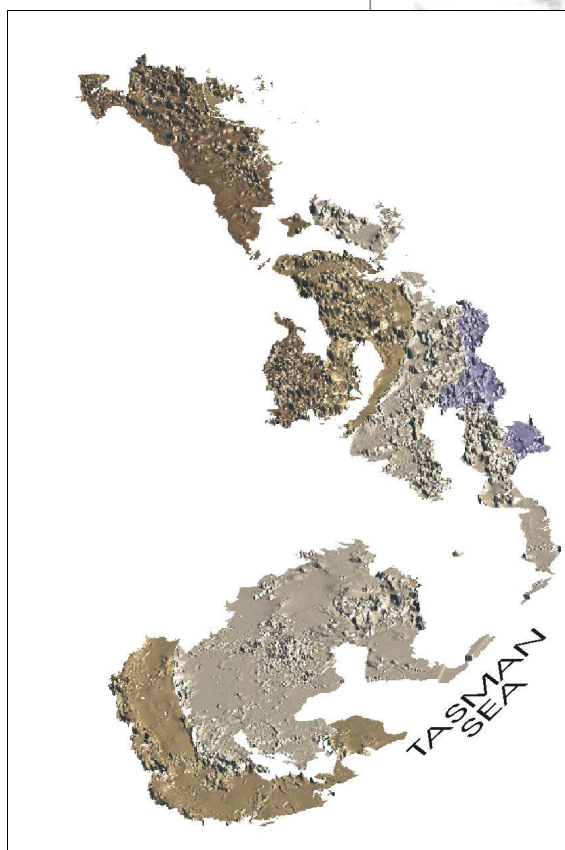
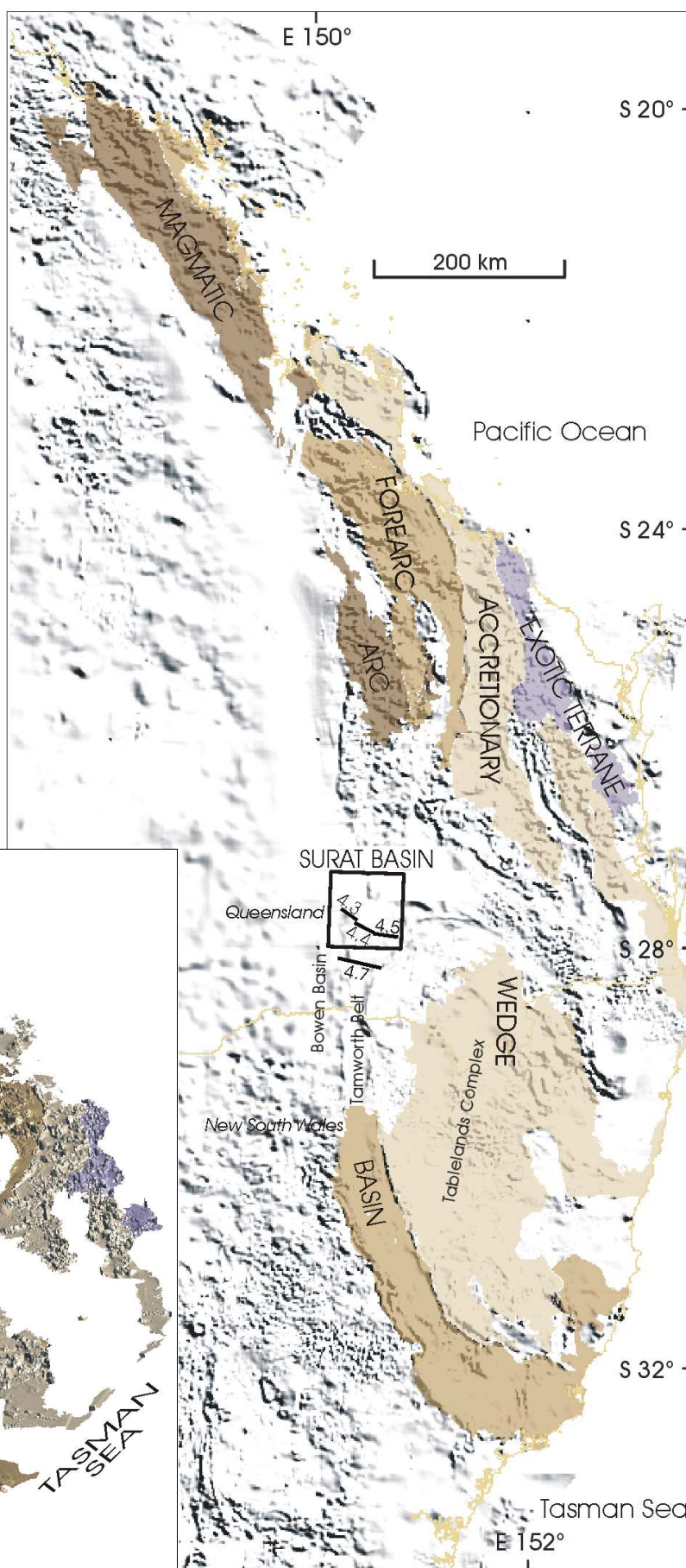
By interpreting TMI images based on a line spacing of maximum 400 metres, one can expect to obtain valuable information on any major geological feature near the surface. The techniques described in **Chapter 4.2**. (e.g. draping colours) are used to emphasise the expression of anomalies attributable to near-surface geology.

As discussed above, the seismic reflection profiles indicate that the Mesozoic platform cover (Surat Basin) is subhorizontal (*Figs 3.4, 3.5 & 3.6*). This is supplemented by borehole data from wells across the entire study area, drilled into sediments of the Surat Basin (*cf. Chapter 3.2.2.*). On the aeromagnetic images, some distinct features are seen (*see Fig. 4.1*) although the Mesozoic cover of the Surat Basin is at least up to 2000 metres thick and intermediate or mafic rocks do not occur within the sedimentary succession. It is assumed that the rock types of the Surat Basin are very similar throughout the entire study area and are therefore of a constant magnetic intensity. The Surat Basin sits directly and disconformably on a basement of Bowen Basin and Tamworth Belt, and the geometry of this basement could well explain at least some of the magnetic responses.

Although it is not possible to state categorically that the magnetic anomalies relate to the basement's observed fault and fold geometry, it is possible that the stronger mag-

Fig. 4.2a (right): Grey-scale Aeromagnetic anomaly image overlain by a simplified terrane map of the New England Orogen, identifying outcropping magmatic arc, fore-arc and accretionary complex rocks using different shades of brown. The box represents the study area and shows the location of the three magnetic profiles (marked as 4.3, 4.4 and 4.5) as to be seen in Figs 4.3, 4.4 & 4.5, respectively (cf. Fig. 1). The profile numbered 4.7, located directly south of the study area, refers to the position of the aeromagnetic traverse shown in Fig. 4.7.

Fig. 4.2b (beneath): Three dimensional terrane map of the New England Orogen. Note the zone of magnetic highs along the boundary between the fore-arc basin and accretionary wedge (brown coloured and light-brown coloured, cf. Fig. 4.2a).



netic features in the images are due to Middle and Late Palaeozoic rocks. Thus, it is probable that the Mesozoic Surat Basin cover functions as a kind of “dilution filter”, affecting the overall Total Magnetic Intensity. The relatively deep sourced magnetic signals would penetrate, but be diluted by the Mesozoic sedimentary cover. This would explain two large linear magnetic anomalies along the western and the eastern end of the Tamworth Belt (*Figs 4.1 & 4.2*) that are associated with faults of major displacement beneath the Mesozoic platform cover, namely the Moonie Fault to the west and the Peel Fault to the east (*Figs 3.4, 3.5 & 3.6*).

4.2.2.1. Aeromagnetic data – interpretation of the Southern NEO

The aeromagnetic anomaly image of Eastern Australia shows that the Bowen Basin system has an overall higher Total Magnetic Intensity than the subduction-related structural units of the New England Orogen to the east of it (cf. labelled Tamworth Belt, Tablelands Complex and Bowen Basin in *Fig. 4.1*).

However, in the southern New England Orogen, within the northernmost blocks of the outcropping Tamworth Belt succession (namely the *Tamworth North* and the *Tamworth South*, see *Fig. 4.1*, cf. **Chapter 2.2.2.**), the aeromagnetic anomaly image identifies two different levels of intensity, running sub-parallel to the overall basin trend (*Fig. 4.1*). Here, adjacent to the Bowen Basin in the west, the Total Magnetic Intensity seems to mimic the occurrence of the outcropping Tamworth Belt succession. To the west, higher magnetic intensities showing orange to dark red TMI values on the pseudocolour images characterise Carboniferous sediments that are more abundant in volcanic flows and tuffs (*c.5050 – 5560 nT in Fig. 4.1*). To the east, ranging from light blue to yellow on the pseudocolour aeromagnetic images, lower intensities are considered to identify Devonian sediments that were predominantly deposited in a shallow marine environment (*c.4850 – 5000 nT in Fig. 4.1*).

Some remnant aeromagnetic lows, however, can be identified by blue to dark blue values on the pseudocolour anomaly images, ranging from *c.4430 – 4850 nT (Fig. 4.1)*. Based on the surficial geology, these lower magnetic values characterise Permian sediments at the western margin of the Tamworth Belt or even within the fore-arc basin unit (see “*p*” in *Fig. 4.1*). Within the south eastern part of the belt, some isolated aeromagnetic highs

are observed where plutonic bodies can be identified in outcrop (e.g. Barrington Tops Granite in the *Tamworth Southeast* block; see “g” in *Fig. 4.1*).

Western Tamworth Belt

In the northern part of the exposed Tamworth Belt in New South Wales, to the south of the study area, a NNW-SSE-trending magnetic ridge occurs along the fore-arc basin’s western margin (*Fig. 4.1 & 4.2*). Here, the *Mooki Fault* (see *Fig. 2.3*) can be traced in outcrop to strike NNW-SSE (cf. **Chapter 2.3.**) and can be connected to the subsurface *Moonie Fault* farther north (*Fig. 3.1*; see *Fig. 5.13*). Associated with these faults, that thrust Devonian to Triassic sediments against flat-lying Permian strata, are TMI values that are slightly higher than the overall high values of the Total Magnetic Intensity seen in the Bowen Basin to the west of the thrust faults (*Fig. 4.3*).

In northernmost New South Wales, along the western end of the Tamworth North Block (*Fig. 4.1*), RAMSAY & STANLEY (1976) postulate that Permian to Triassic intermediate to mafic intrusive rocks of high susceptibility have been emplaced at depth on the Mooki thrust and that these rocks are the cause of the anomaly. A second type of the causative body, however, has been associated with the Mooki Fault farther north, extending for more than 20 kilometres. Here, RAMSAY & STANLEY (1976) defined “a linear anomaly, which has a profile characteristic of a structure laminated parallel with its strike”. They describe the anomaly causing intrusive rock as hawaiite of conjectural age, but imply a Miocene age.

Eastern Tamworth Belt

In northern New South Wales, where the rocks of the southern New England Orogen are exposed at the surface (cf. simplified terrane map in *Fig. 4.2* with overlain Terrane map in *Fig. 4.1*), the eastern margin of the Tamworth Belt is identified by the previously mentioned slightly right-curved, N-S-trending, disrupted magnetic ridge, identified by red values on the pseudocolour images (c.5010 – 5060 nT in *Fig. 4.1*). Along this magnetic anomaly, serpentinites and related mafic igneous rocks that intruded along the Peel Fault can be traced in outcrop (cf. *Fig. 1 & Fig. 4.1*) and are responsible for higher TMI-values (RAMSAY & STANLEY, 1976). The age of the causative mafic to ultramafic rocks is de-

scribed to be Lower Devonian or pre-Devonian (RAMSAY & STANLEY, 1976).

Within the region that is covered by Surat Basin sediments, that is, between the northern and the southern New England Orogen terranes (cf. terrane map overlain in *Figs 4.1 & 4.2*), a NE-SW trending ridge – which appears to change to a N-S orientated feature farther south – defines the easternmost boundary of the Tamworth Belt in southern Queensland. Off this aeromagnetic ridge, a second, smaller and more disrupted ridge of unknown cause can be seen bifurcating immediately to the west, trending NE-SW (*Figs 4.1 & 4.8*).

If traced farther southwards, the eastern aeromagnetic feature may be connected to the magnetic ridge of the exposed part of the elongate masses of serpentinites in northern New South Wales. Thus, the easternmost magnetic anomaly ridge may be interpreted as a distinctive feature defining the boundary between the Tamworth Belt and the Tablelands Complex, or, in other words, the boundary between the fore-arc basin and the accretionary wedge, respectively (*Figs 4.1, 4.2 & 4.7*).

4.2.2.2. Aeromagnetic data – interpretation of the study area

On the south-eastern side of the **A82-LT-24** seismic profile, beneath the disconformably overlying Surat Basin succession, a thrust with a ramp-flat geometry has been interpreted, ramping up north-west directed and identifying the Moonie Fault (*Fig. 3.4*). On the A82-LT-24 magnetic traverse, the Tamworth Belt succession and some overlaying remnants of the Bowen Basin succession to the south-east are identified by relatively low TMI values of *c.*4950 nT, whereas to the north-west, where oldest Bowen Basin sediments overlay the fore-arc basin succession, the Total Magnetic Intensity is observed to be higher, with values of *c.*5050 nT (*Fig. 4.3*). An asymmetrical high in the magnetic data in the centre of the traverse can be correlated with the thrust ramp on the seismic profile (cf. *Figs 4.3 & 3.4*; see **Chapter 3.1.2.** for details). The asymmetry of this magnetic high is typical for magnetic anomaly graphs of dipoles as seen at medium latitudes (*Fig. 4.3a*). The magnetic peak, which is higher than the values in the Bowen Basin to the north-west (*c.*5145 nT in *Fig. 4.3*), indicates that a magnetically source rock for the anomaly has been emplaced along the fault.

On the images showing the Total Magnetic Intensity of the southern New England Orogen (*Figs 5.1, 5.2 & 5.2a*), the asymmetrical high identifies a linear anomaly that is

parallel to the strike of the Moonie-Goondiwindi fault system. To the north-west of the Texas Orocline, where the Moonie Fault strikes NE-SW and the Tamworth Belt succession is influenced by oroclinal bending, the linear anomaly becomes more disrupted (*Fig. 4.8*), but still is parallel to orientation of the Moonie Fault. As this Moonie anomaly extends for over 200 kilometres (*Fig. 4.1*), from the study area to the north to northern New South Wales to the south, its cause is unlikely to be explained by intermediate to ultramafic intrusive rocks. Moreover, the age of the causative body is uncertain.

On a hypothetically basis, this may confirm the structural geometry of the Moonie Fault ramping up north-west directed beneath the Surat Basin succession and, due to the faulting, bringing up more magnetic rocks of the Tamworth Belt closer to the surface (i.e. volcanogenic compared with more quartz-rich in the Surat and Bowen basins; cf. *Figs 4.3 & 4.3a*). However, as no sharp lineation but more a zone of elongated, stronger magnetic signals defines the Moonie Fault, fluids that occur along the thrust containing ferro-oxides

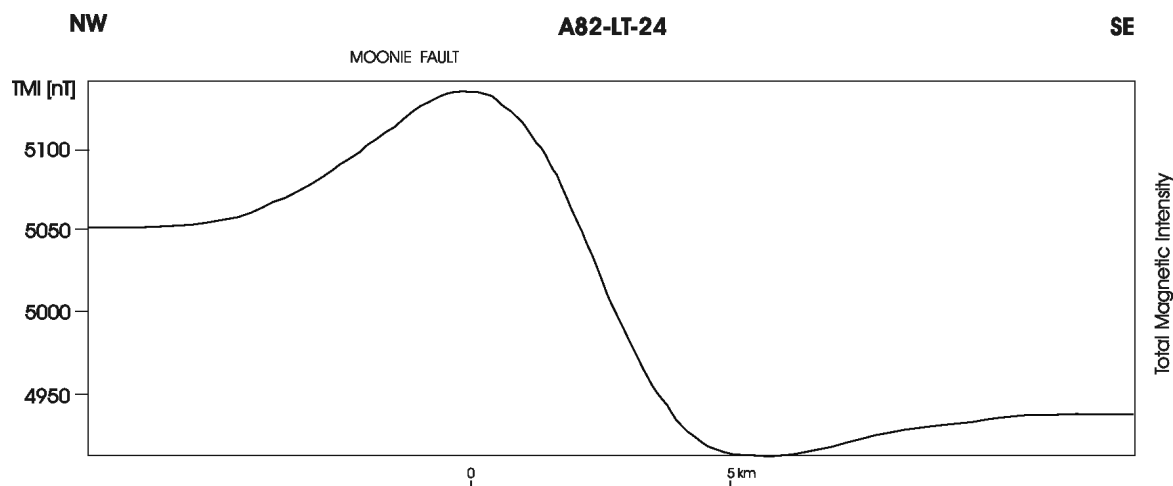


Fig. 4.3a (right): Magnetic anomaly graph of a dipole formed on a thin vertical sheet at medium latitudes; here: 27° N (from MUSSETT & KHAN, 2000). The earth's field inclination is marked as the arrow.

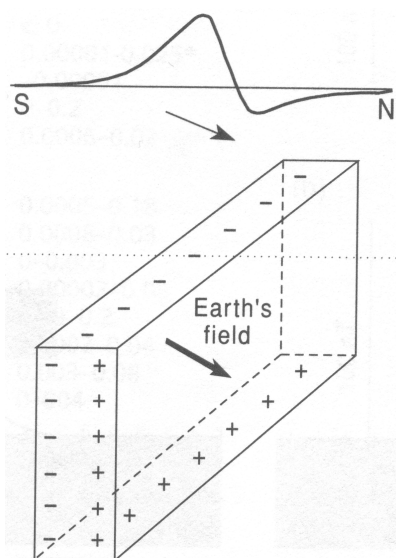


Fig. 4.3 (top): Magnetic traverse (Total Magnetic Intensity) along the seismic reflection profile A82-LT-24 (cf. *Fig. 3.3*). The magnetic high occurs at the Moonie thrust ramping to the NW. The precise location of the Moonie Fault is displayed in **Chapter 5.1.2** on *Fig 5.4*. For details see text.

and ferro-hydroxides may also be the cause for the diffusive anomaly on the corresponding image.

In general, field studies on fluid migration suggest, that, within the middle crustal layer that shows more of a brittle reaction to deformational movements, the fluids take more drastic measures, not only along the fault-plane, but also angular to it. Thus, the resulting ferromagnetic signature would create a more diffusive anomaly on the corresponding image as seen in the study area.

The approximate depth of the top of the causative body was calculated using Peter's half-slope method (MUSSETT & KHAN, 2000). It varies from *c.*4800 metres (traverse A82-LT-24) to *c.*6250 metres (traverse A82-LT-20, see **chapter 5.1.2.**, *Fig. 5.7*). This, when applied to the depth converted seismic reflection data, indicates that part of the hanging-wall strata close to the thrust ramp is reasonable for the magnetic high. This is possibly in the vicinity of the anticlinal part of the seismic reflection HC (cf. *Figs 3.4, 3.5 & 3.6*). However, as (i) the sediment facies of the fore-arc basin succession varies to much to be precisely depth-correlated with the seismic reflection data and (ii) the magnetic anomalies in general vary dependant on the strike of the causative body (MUSSETT & KHAN, 2000), the source of the magnetic anomaly is speculative.

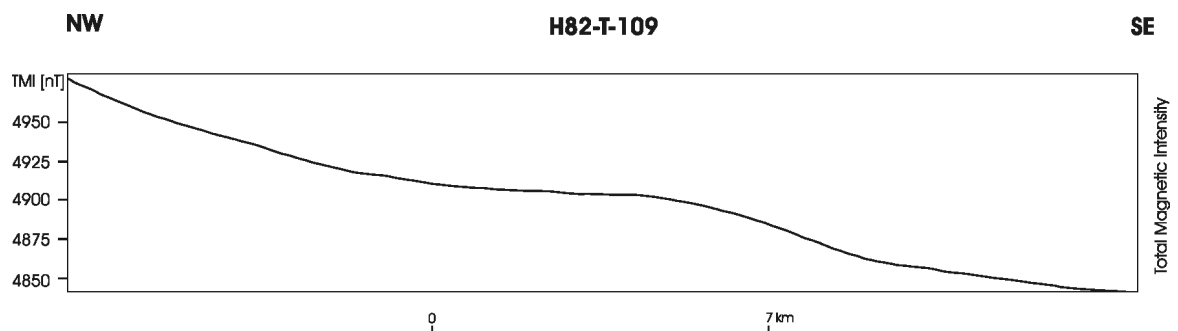
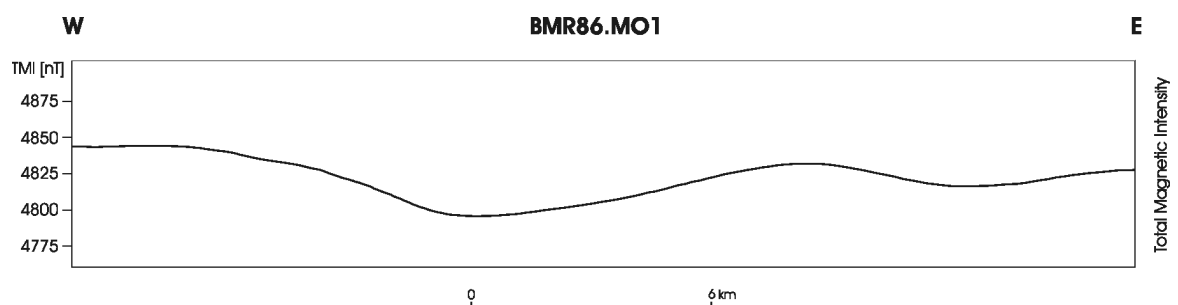


Fig. 4.4: Magnetic traverse (Total Magnetic Intensity) along the seismic reflection profile H82-T-109 (cf. *Fig. 3.4*), located between A82-LT-24 to the west and BMR86.MO1 to the east. For details, see text.

Fig. 4.5: Magnetic traverse (Total Magnetic Intensity) along the seismic reflection profile BMR86.MO1 (cf. *Fig. 3.5*), located to the east of H82-T-109. For details, see text.



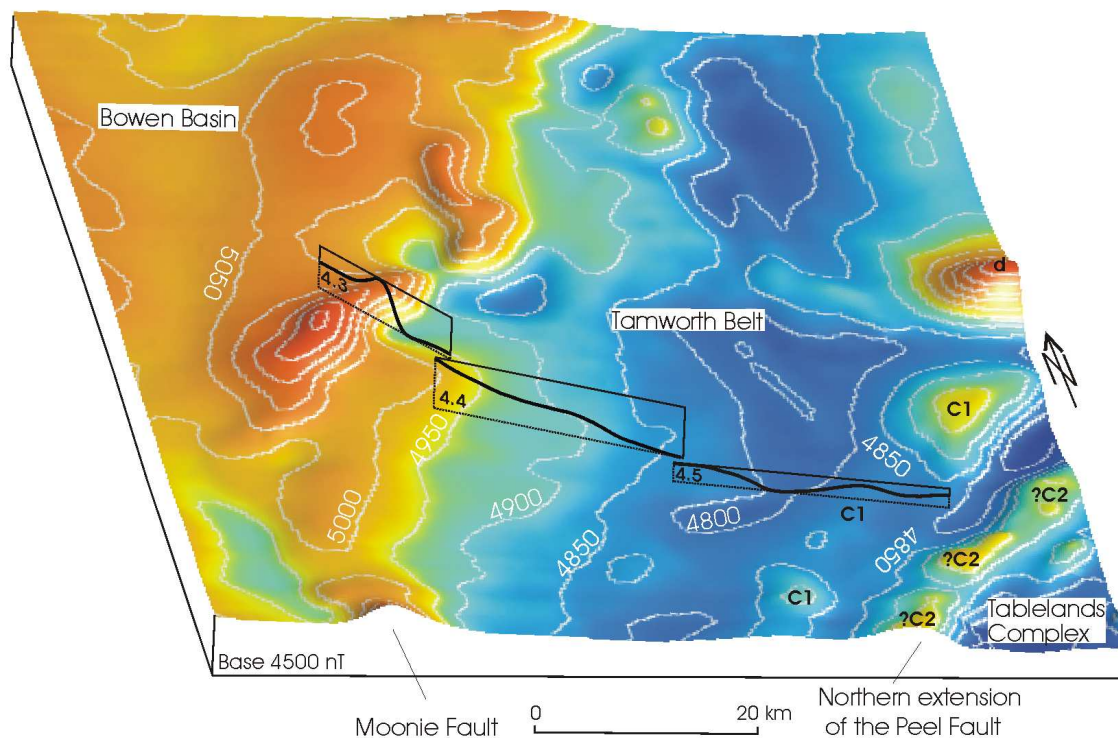


Fig. 4.6: Three dimensional aeromagnetic image of the study area, displayed in contours with a line spacing of 50 nT. The base of the block diagram is the 4500 nT contour line. The black solid lines highlighted 4.3, 4.4 and 4.5 refer to the locations of the aeromagnetic traverses shown in *Figs 4.3, 4.4 & 4.5* and to the locations of the corresponding seismic profiles seen in *Figs 3.4, 3.5 & 3.6*, respectively. The aeromagnetic high marked as c_1 can be correlated with the westward-dipping fault c_1 on the corresponding seismic profile of *Fig. 3.6*. The aeromagnetic ridge marked as $?c_2$ can be correlated with the northern extension of the Peel Fault (cf. c_2 in *Fig. 3.6*). The magnetic high marked as d may be correlated with a duplex structure referred to in the text (cf. *Fig. 4.8*).

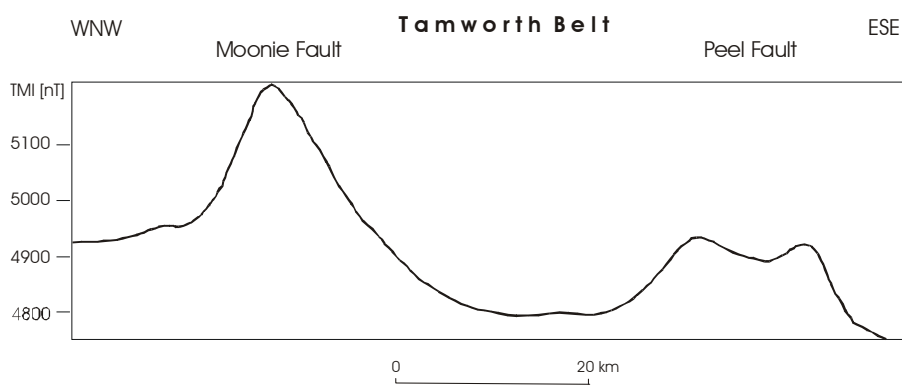


Fig. 4.7: Aeromagnetic anomaly traverse across the Tamworth Belt showing the Total Magnetic Intensity [nT]. See "4.7" in *Fig. 4.2a* for location (directly south of the study area).

Southeast of traverse A82-LT-24, on **H82-T-109** (*Fig. 4.4*), the total magnetic intensity gently decreases south-eastwards for another 130 nT, starting at 4975 nT in the north-west and reaching its minimum at the south-eastern end of the profile at approximately 4845 nT. Although the fore-arc succession dips moderately to the north-west (*Fig. 3.5*), it does not coincide with the Total Magnetic Intensity direction of incidence (*Fig. 4.4*). However, the decrease in magnetic intensity - as one goes down the section - implies that the upper sequences in the Tamworth Belt are more magnetic than the lower ones. Moreover, it substantiates the correlation between the Moonie Fault and the higher magnetic anomaly associated with it; in other words, more the structural processes in the subsurface seem to cause the magnetic highs rather than the strata themselves.

On the Millmerran profile (**BMR86.MO1**, *Fig. 4.5*) located farther to the east, two small highs are noted on the eastern end of the magnetic intensity section. These highs can be correlated with two major west-dipping faults (see “c₁” and “c₂” on *Fig. 3.6*) that are covered by the base of the Surat Basin on the corresponding seismic profile, with the eastern fault indicating the northern extension of the exposed Peel Fault in New South Wales (cf.

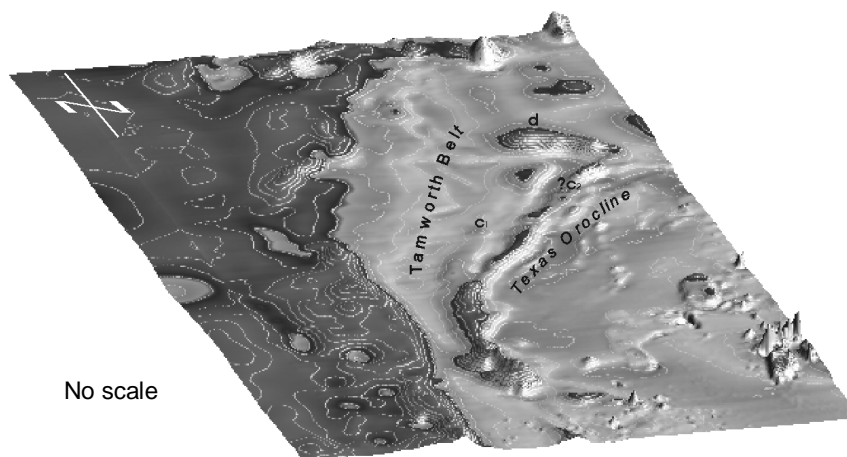


Fig. 4.8: Three-dimensional aeromagnetic image of that part of the NEO, that was influenced by oroclinal bending, forming the Texas Orocline, and subsequently was covered by Surat Basin sediments. (cf. *Fig. 4.6* for terminology).

Figs 3.6, 4.5, 4.6 & 4.7). The Total Magnetic Intensity graph on the western end of the traverse directly correlates to the values seen in traverse H82-T-109 (cf. *Figs 4.6 & 4.7*). The magnetic low in the middle of the Millmerran traverse coincides with the end of continuous seismic reflections of the Tamworth Belt sequences (*Fig. 3.6*).

Immediately south of the study area, a WNW-ESE-oriented aeromagnetic anomaly profile (see *Fig. 4.2* for location, *Fig. 4.7* for details) was constructed in the region where the Tamworth Belt narrows significantly. As a consequence, the structural geometry of the belt is similar to that observed in the exposed part of the fore-arc basin farther to the south. This profile confirms the above described magnetic anomalies and supports the fault-related asymmetries in the subsurface Tamworth Belt (such as the asymmetry of the magnetic signal for the Moonie Fault in *Fig. 4.3* and the westward-dipping faults in *Fig. 4.5*, respectively) (cf. *Figs 4.6 & 4.7*).

4.3. Gravity data

The gravity anomaly map of the New England Orogen region (*Fig. 4.9*) is based both on onshore residual Bouguer gravity anomalies (A. S. MURRAY *et al.*, 1997) and on offshore free air gravity anomalies (SANDWELL & SMITH, 1997). The transform limits displaying the New England Orogen

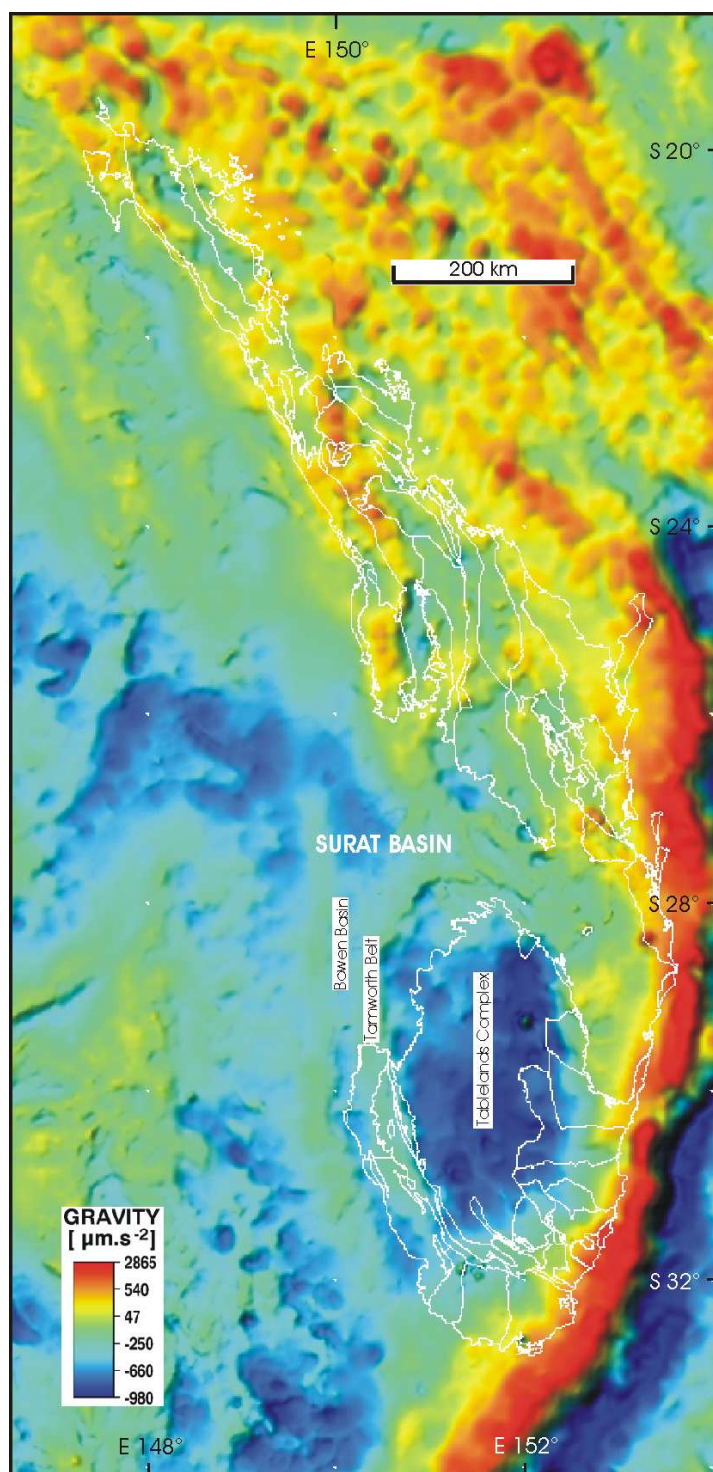


Fig. 4.9: Gravity anomaly image of the New England Orogen based on onshore residual Bouguer gravity anomalies and offshore free air gravity anomalies ($\mu\text{m s}^{-2}$). The pseudocolour image is overlain by the terrane map of the exposed part of the New England Orogen (white solid lines).

area range from $-976.12 \mu\text{m s}^{-2}$ to $2886.64 \mu\text{m s}^{-2}$, the values in the image displaying the study area range from $-579.05 \mu\text{m s}^{-2}$ to $488.96 \mu\text{m s}^{-2}$. The image contrast was enhanced by sun shading with an azimuth of 315° and an elevation of 75° and therefore can also be expressed as grey-scale anomaly maps (cf. *Fig. 4.9 & Fig. 4.10*).

4.3.1. Gravity data – presentation

On the Bouguer anomaly map (*Fig. 4.9*), a number of features substantiate the gradient-enhanced residuals of the Total Magnetic Intensity. Because of the small scale grid coverage (a maximum of 11 km between the gravity stations), however, no gravity traverses along the key seismic lines were constructed as part of this study.

4.3.2. Gravity data – interpretation

Gravity data are of great importance to characterise the structural signature of pre-Jurassic rocks, especially in the northernmost part of the Southern New England Orogen, where the gravity signals seem to correlate to the tectonic setting. Although the gravity signals are more diffusive because of the long distances between the gravity stations, the cause of the anomaly can be picked easily on the contrast enhanced images (*Figs 4.9 & 4.10*). Its location, however, can not be identified precisely (at least less precise than the location of the magnetic anomaly causing bodies).

Interpretation of the Southern New England Orogen

In northern New South Wales, to the west of the Tablelands Complex accretionary wedge assemblage, two gravity ridges may be identified along the strike of the Tamworth Belt succession. Following these gravity lineaments into southern Queensland, they may be interpreted as a major tectonic structure, ranging from $c.32^\circ \text{ S}$ to $c.28^\circ \text{ S}$ and $c.27^\circ \text{ S}$ respectively (*Figs 4.9 & 4.10*). In the eastern Gunnedah-Bowen Basin - to the west of the study area - a more diffuse and disrupted ridge extends in a near longitudinal direction (*Figs 4.9 & 4.10*). This gravity lineament ($c.-100$ to $50 \mu\text{m s}^{-2}$), where documented in the seismic data, occurs to the west of the Mooki-Moonie faults in the Gunnedah an Bowen basins, but may be correlated to the western border of the fore-arc basin succession (see **Chapter 6**, *Comparison with previous studies - western boundary*).

Interpretation of the study area

In the region east of the Moonie Fault system, the most noticeable feature is that of a strong gravity signal along the exposed part of the Peel Fault in northern New South Wales (Figs 1, 4.9, 4.10 & 4.12). This is due to the higher Bouguer Gravity values of the serpentinites and related mafic-ultramafic rocks that occur along the fault (cf. Figs 4.9, 4.10 & 4.12). The gravity signal is part of a distinctive curvilinear gravity ridge (c.10 to 50 $\mu\text{m s}^{-2}$) at the eastern end of the investigated area, identifying the boundary between the Tamworth Belt and the Tablelands Complex and, moreover, the Texas Orocline in southern Queensland (cf. Figs 1 & 4.9).

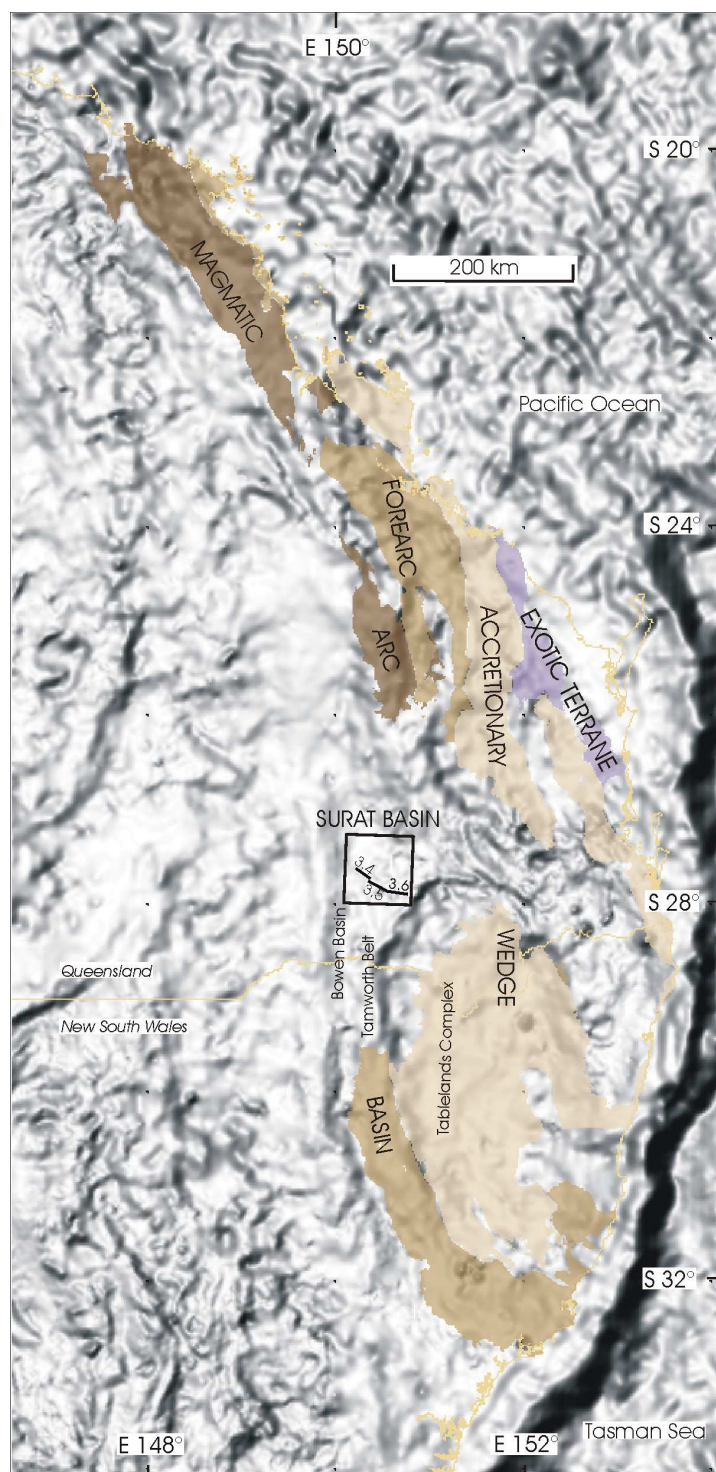


Fig. 4.10: Grey-scale Gravity anomaly image overlain by a simplified terrane map of the New England Orogen, identifying magmatic arc, fore-arc and accretionary complex rocks using different shades of brown. The box represents the study area, showing the location of the three seismic and magnetic profiles (marked as a, b and c) as seen in Figs 3.4, 3.5, 3.6 and 4.3, 4.4 & 4.5 respectively.

4.4. Aeromagnetic and gravity data – discussion

Higher magnetic signals in the Tamworth Belt may be correlated with structural differences in the subsurface fore-arc basin geometry (cf. *Figs 4.3, 4.5 & 4.6*).

In northern New South Wales, to the south of the study area, the Tamworth Belt is exposed on the surface. Here, two distinctive magnetic ridges were identified by RAMSAY & STANLEY (1976), located along the Mooki Thrust to the west (the fault equivalent in northern NSW to the Moonie Thrust in southern Queensland) and along the Peel Fault to the east (*Fig. 4.11*). The Peel anomaly is regarded to be caused by ultramafic and related rocks of a serpentinite belt, whereas the Mooki anomaly is suggested to be a composite anomaly caused by pluglike intermediate intrusives and a c.20 kilometres-long dike of hawaiite, respectively RAMSAY & STANLEY (1976).

Tracing the Mooki anomaly to the north, it continues along the Moonie Fault in southern Queensland, identifying a more or less continuing aeromagnetic lineament for at least 200 kilometres (*Fig. 4.1*). In the study area, where the structural geometry is influenced by the Texas Orocline to the south-east, the magnetic signal becomes more disrupted. The overall Mooki-Moonie magnetic anomaly, however, is stronger and less disrupted than the Peel anomaly to the east.

Because of the fact, that

- (1) the overall nature of the aeromagnetic anomaly ridge associated with the Moonie Fault is strong and ongoing,
- (2) the calculated depth of the causative body using Peter's half slope method (see **Chapter 4.2.2.2.**) picks the location of the cause of the anomaly close to the Moonie thrust ramp and /or within the hanging-wall strata,
- (3) no seismic body due to potential intrusive rocks was interpreted at the base of the Moonie Fault on the seismic reflection profiles,

the author questions, that the aeromagnetic anomaly can only be caused by intrusive rocks that were emplaced at the base of the thrust fault. If intrusive rocks would have been emplaced at the base of the Moonie Fault, the resulting magnetic anomaly ridge would be more disrupted, that is, the causative intrusive rocks would be expected to be more plug-like in form.

Ferromagnetic minerals present within the fore-arc basin succession and brought up closer to the surface by contractional (thin-skinned) tectonic forces are reasonable for

the large linear magnetic anomaly along the western part of the Tamworth Belt (see above). No sharp lineation but more a zone of stronger magnetic signals defines the Moonie Fault. Therefore, ferro-oxides/ferro-hydroxides within the hanging-wall sequence may also be responsible for the higher aeromagnetic response above the thrust fault, ramping north-westwards.

However, cause and age of the Moonie aeromagnetic anomaly is speculative.

In the study area, in southern Queensland, two aeromagnetic ridges were identified within the incidence of the subsurface Tamworth Belt (Figs 4.1, 4.2b, 4.6 & 4.8). To the east, the easternmost magnetic lineament of a northwards bifurcating ridge was linked to the Peel Fault farther south (c_2 in Figs 4.6 & 4.8). It defines the border between the accretionary wedge and the fore-arc basin units, following the indication of the Texas Orocline (cf. Fig. 4.8). Another aeromagnetic ridge is associated with the Moonie Fault, to the west of the study area, and occurs along strike of the thrust fault (Figs 3.3, 4.1 & 4.6). Between the two aeromagnetic ridges there is a gravity ridge, also following the curvilinear trend that can be observed in the aeromagnetic data (cf. Figs 4.1, 4.8, 4.9 & 4.12).

The three-dimensional images of the New England Orogen were created using ER-Mapper software and show the aeromagnetic data (“a” in Fig. 4.12a), the gravity data (“b” in Fig. 4.12a) and the gravity data overlain by the aeromagnetic data (“c” in Fig. 4.12a). The interrelation between the aeromagnetic and the gravity features are displayed

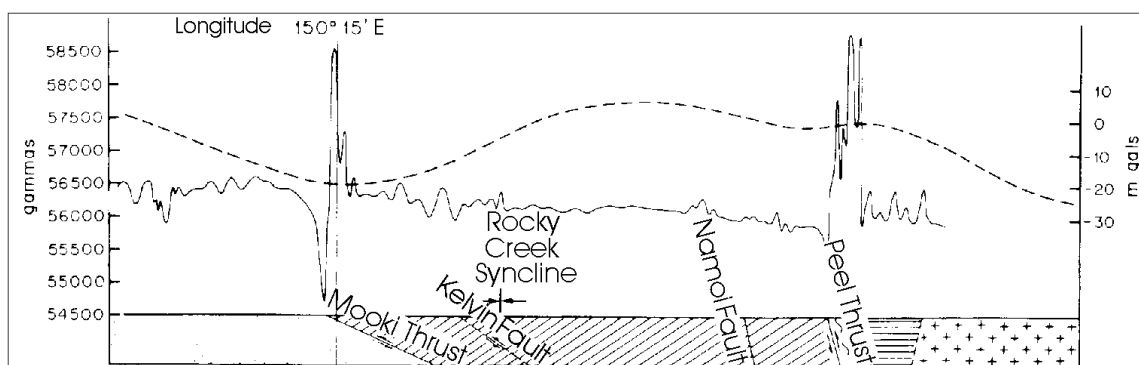
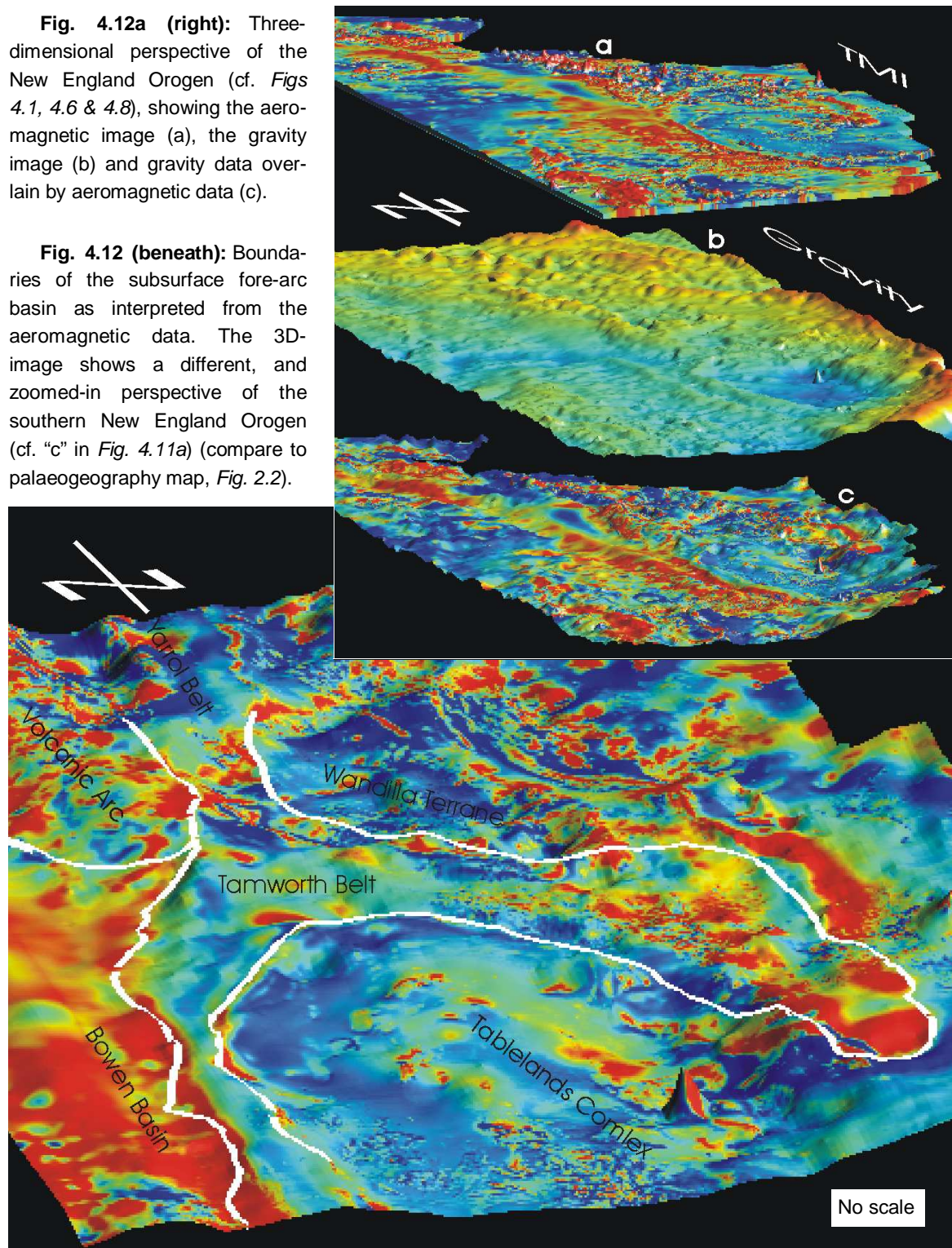


Fig. 4.11: Magnetic traverse across the exposed part of the Tamworth Belt in northern New South Wales plotted with Bouguer Gravity (dashed line) (from RAMSAY & STANLEY, 1976). The profile runs WSW-ENE and is located to the east of the Gunnedah Basin, approximately 200 km to the south of the study area (see Fig. 1). Two strong anomalies can be recognised, located at the Mooki Thrust to the west (which is the fault equivalent to the Moonie Fault in southern Queensland) and at the Peel Fault to the east. The simplified geological cross section is shown at the bottom part of the profile.

Fig. 4.12a (right): Three-dimensional perspective of the New England Orogen (cf. *Figs 4.1, 4.6 & 4.8*), showing the aeromagnetic image (a), the gravity image (b) and gravity data overlain by aeromagnetic data (c).

Fig. 4.12 (beneath): Boundaries of the subsurface fore-arc basin as interpreted from the aeromagnetic data. The 3D-image shows a different, and zoomed-in perspective of the southern New England Orogen (cf. "c" in *Fig. 4.11a*) (compare to palaeogeography map, *Fig. 2.2*).



and correspond best in the southern New England Orogen (*Fig. 4.12*). In order to identify the extent of the subsurface Tamworth Belt lying within the transition zone between the southern and the northern New England Orogen, both the magnetic and the gravity data were used to map the boundaries of the fore-arc basin in the subsurface thus defining the

Tamworth Belt boundary where it is covered by younger sediments in southern Queensland (*Fig. 4.12*, white solid line).

The image was constructed by putting two different anomaly layers on top of each other. The colour code illustrates the aeromagnetic anomaly and is referenced to the same values as on *figure 4.1* (red represent relatively high and blue relatively low TMI values). The relief mimics the gravity data (cf. *Fig. 4.10*). Thus, morphological highs represent relatively high values of the gravity field, while morphological lows represent lower values, respectively (cf. map “c” of *Fig. 4.12*). Hence, the morphological gravity ridge substantiates the information gained from the elongated magnetic pseudocolour highs, assuming, that thrust-related processes can cause an overall higher magnetic and gravity anomaly. Within the southern New England Orogen, two subduction-related structural units can be clearly separated from each other on both, the aeromagnetic anomaly image and the gravity anomaly image. Here, where the fore-arc basin Tamworth Belt is highly deformed due to subsequent tectonic deformation, the belt can be interpreted to consist of more anomaly causing mafic rocks - especially along its fault-dominated boundaries - than the accretionary wedge assemblage Tablelands Complex to the east.

The proposed terrane boundaries as interpreted from the aeromagnetic data, the gravity data and the seismic reflection data (of which the latter is predominantly restricted to the western part of the visualised area) are the first attempt to outline the New England Orogen terranes in the subsurface and will be refined when new data become available (cf. *Figs 4.1, 4.9 & 4.12*).

Allein die Sphäre der ausgebildeten Natur ist unaufhörlich beschäftigt, sich auszubreiten.

Immanuel Kant

5. STRUCTURAL GEOMETRY OF THE TAMWORTH BELT

Relevant geophysical data in the study area consist of seismic reflection profiles and gravity and aeromagnetic data. Together with petroleum exploration well information, these data were used to provide a complete view of the fore-arc Tamworth Belt buried underneath the Bowen and Surat basins. The boundaries and subsurface geometry of the Tamworth Belt will be defined below.

5.1. Fault geometries from seismic sections

In the study area, a series of major NW- and W-directed thrusts can be recognised on the basis of seismic data (e.g. *Figs 3.4 & 3.6*). The most significant of these structures, the Moonie Fault (*Fig. 3.4*), is part of a larger Middle Triassic fault system (see **Chapter 2.3** for details). The complexity of this thrust event is indicated by the presence of synthetic thrusts (*Fig. 3.4*) and backthrusts (“b” in *Fig. 3.6*). Two major westward-dipping faults (“c₁” and “c₂” in *Fig. 3.6*) may form the eastern boundary of the Tamworth Belt. The western Tamworth Belt boundary could not be defined using the present data because it continues beneath the Bowen Basin to the west of the study area. Moreover, the base of the subsurface Tamworth Belt succession could not be defined due to the shallow character of the seismic profiles (the majority of the seismic lines of the investigated area has a recording time of 3 seconds TWT). Thus the base of the Tamworth Belt is below the lower limit of the seismic sections. However, the hanging-wall geometry is characterised by the Moonie Fault to the west (“b” in *Fig. 3.4*) and the two W-dipping faults to the east (“c₁” and “c₂” in *Fig. 3.6*) and thus

images the structure of the subsurface Tamworth Belt succession (*Fig. 3.5*).

5.1.1. Additional information from deep seismic profiling

Two deep seismic profiles (BMR84.14 to the north and BMR91.G01 to the south, recorded to 20 seconds TWT), both of which are located some distance from the seismic study area, provide supplementary east-west cross-sections across the Tamworth Belt, (for location, see *Fig. 3.1*). They were acquired by the Bureau of Mineral Resources (now Geoscience Australia) and show the overall geometry of the Tamworth Belt and the adja-

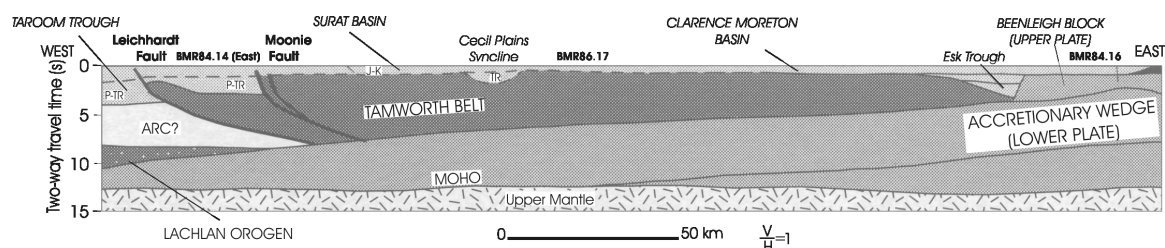


Fig. 5.1: Cartoon of the crustal architecture in the vicinity of the eastern part of the deep seismic survey BMR84.14 immediately to the north of the study area (from KORSCH *et al.*, 1997) (for location see *Fig. 3.1*).

cent tectonic successions (GLEN *et al.*, 1993; KORSCH *et al.*, 1993, 1997; FINLAYSON, 1990; Wake-Dyster *et al.*, 1987).

The fore-arc basin succession to the north of study area, as displayed on the deep seismic survey, line BMR84.14, identifies a shallow westward-dipping base of the Tamworth Belt (*Fig. 5.1*). Here, the Tamworth Belt is in an anomalous region and its sedimentary succession is extremely wide due to repetition by the oroclinal bending (cf. **Chapters 2.2.2.** and **3.1.**, respectively).

The Tamworth Belt, as seen on the southern deep seismic profile BMR91.G01 (*Fig. 5.2*), has a doubly vergent structural geometry with a steep westward-dipping eastern margin.

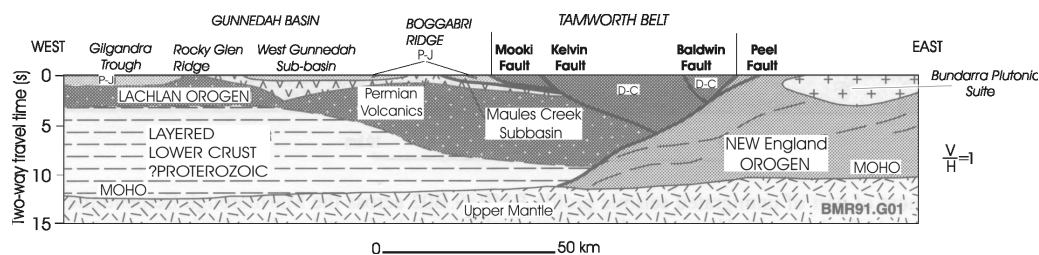


Fig. 5.2: Cartoon of the crustal architecture in the vicinity of the deep seismic survey BMR91.G01 to the south of the study area in the Southern New England Orogen (from KORSCH *et al.*, 1997) (for location see

This change in structural geometry of the fore-arc basin unit, from broad and flat bottomed in the north to narrow and bounded by steep faults in the south, represents the overall variation in the basin geometry that can be seen in the study area (*Fig. 4.8*, chapter 4.2.2.2.). The uppermost part (6 seconds TWT) of the northern BMR84.14 profile, was reprocessed by Geoscience Australia (GA) in 1999 to better integrate the data into the existing dataset. The interpretation will be discussed in **Chapter 5.5.2.**

5.1.2. Composite seismic profiles across the subsurface Tamworth Belt

The tectono-stratigraphic geometry of the successions in the Tamworth Belt will be discussed by presenting three NW-SE-directed composite shallow seismic profiles across the subsurface fore-arc basin. From north to south these traverses are (see *Fig. 3.3* for location) A82-LT-20 and A82-WR-22, A82-LT-24, H82-T-109 and BMR86.M01 and A82-LT-29 and H82-T-106.

Seismic sequences within the concealed Tamworth Belt

In the fore-arc basin, five reflections, defining six seismic sequences, could be recognised. Variations in reflection amplitude and continuity within individual sequences, however, is interpreted in terms of lateral changes in the depositional environment. The identified seismic sequences appear to thicken slightly towards the eastern part of the region (*Fig. 3.5*), reaching their maximum thickness close to the eastern faulted margin (adjacent to the Peel Fault). The succession between the *B30* and *HD* reflections on the H82-T-109 seismic line (*Fig. 3.5*) is about 5000 metres thick (*c.*1800 ms TWT). Farther east, on the Millmerran profile (*Fig. 3.6*), the fore-arc succession below the *HD* reflector is about 7000 metres thick (*c.*2000 ms TWT). The entire thickness of the Tamworth Belt succession is, therefore, at least 12 kilometres. This is similar to the values obtained by LIANG (1991) and WOODWARD (1995) in the exposed part of the Tamworth Belt in New South Wales. However, reprocessing of the uppermost 5000 ms TWT of the Millmerran and the BMR 84.14 profiles has led to a different approach in understanding the fore-arc basin geometry with the identification of two thrust sheets stapled upon each other that are responsible for the entire thickness of the Tamworth Belt succession in the study area (see **Chapter 5.4.**).

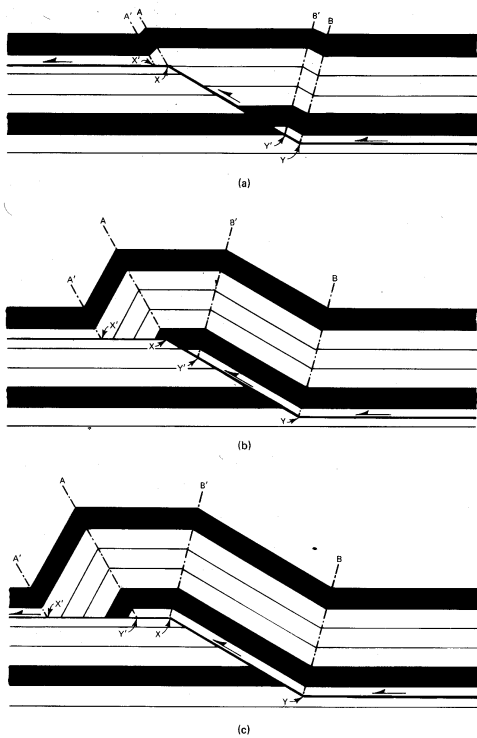
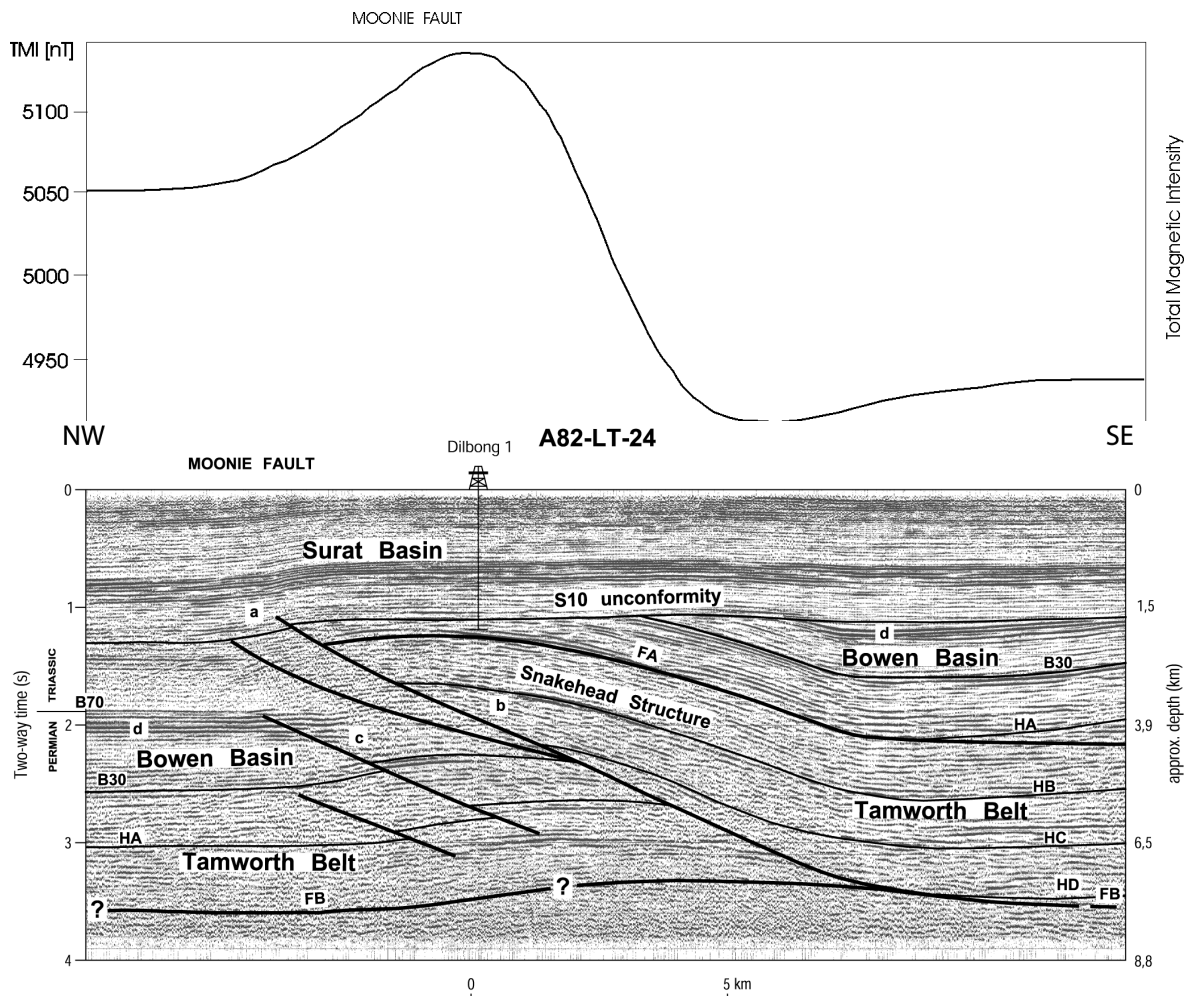


Fig. 5.3 (left): Schematic progressive development of fault-bend folds as a thrust sheet rides over a step in décollement (from SUPPE, 1985).

Fig. 5.4 (beneath): Interpretation of seismic reflection profile A82-LT-24 (final stack). Heavy solid lines represent faults, such as the Moonie Fault as it ramps up to the NW (marked as “b”) with its fault tip line cutting Mesozoic platform cover (marked as “a”, see text for details). Two synthetic faults are recognised (highlighted as “c”).

The light solid lines represent interpreted seismic horizons. HA, HB, HC and HD are within the Tamworth Belt succession. B30 and S10 represent the sequence boundaries at the base of the Bowen and Surat basins, respectively, and B70 represents the approximate position of the Permian-Triassic boundary. The clear-cut seismic reflections marked as “d” identify latest Permian Bowen Basin sedimentary sequences.

The aeromagnetic anomaly along this traverse (cf. Fig. 4.3) is illustrated above the seismic image.



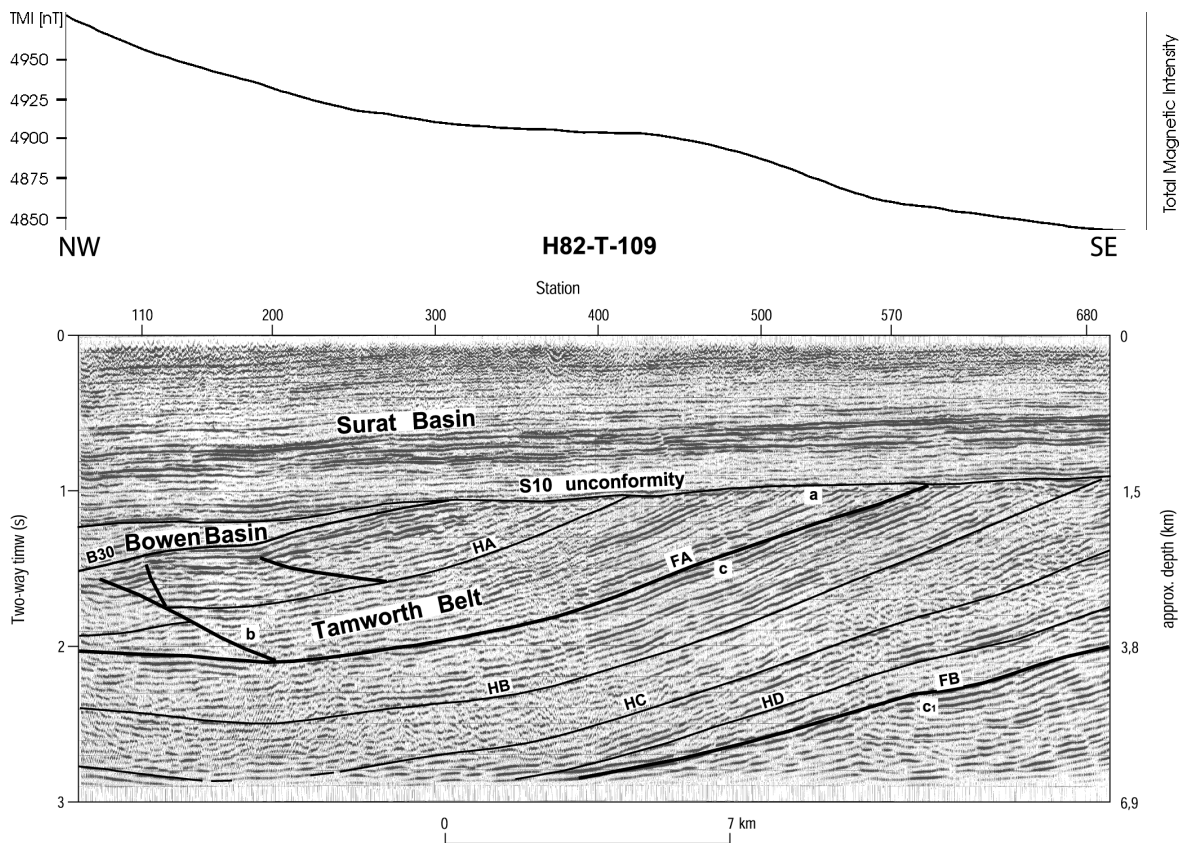
The top of the Tamworth Belt succession is defined by the *B30* reflection (which marks the transition to the Bowen Basin). Seismic data show that the folded Tamworth Belt succession appears to be stratigraphically conformable with the overlying Bowen Basin units (*Figs 3.4*; see also *Figs 5.7 & 5.8*), although there is evidence for some reflection truncation between the two.

Towards its northern tip, the Moonie Fault curves to the north-east (*Fig. 3.1*) and has a classic fault-bend fold geometry (cf. *Fig. 5.3*; for definition see SUPPE, 1983). The fault appears to transport part of the Bowen Basin and the upper half of the Tamworth Belt as a piggy-back structure in the hanging-wall of the thrust (see *Figs 5.4 & 5.5*).

Fig. 5.5: Interpretation of the seismic reflection profile H82-T-109 (migrated). The light solid lines represent interpreted seismic horizons. *HA*, *HB*, *HC* and *HD* are within the Tamworth Belt succession. *B30* and *S10* represent the sequence boundaries at the base of the Bowen and Surat basins, respectively. Beneath the *S10* discontinuity a weathering surface may be identified (marked as “a”).

Heavy solid lines represent interpreted faults. The fault marked as “b” depicts a back-thrust off a fault plane “c” that runs subparallel to the fore-arc basin sequences.

The aeromagnetic anomaly along this traverse is illustrated above the seismic image (cf. *Fig. 4.4*).



On the profile A82-LT-24 (*Fig. 5.4*), the Moonie Fault has a vertical displacement of over 3 kilometres. Geometrical restoration of the fault, prior to the phase of thrust movement, suggests that the Tamworth Belt succession possibly extends to the west within the Taroom Trough beneath the sedimentary rocks of the Bowen Basin (on seismic line A82-LT-24, reflector *HA* was identified to the west of the thrust fault, *Fig. 5.4*). However, the full western extent of the Tamworth Belt could not be determined. The seismic pattern of the Tamworth Belt southeast of the Moonie Fault is clearly of a different character to that of the succession on the north-western side of the fault (cf. *Figs 5.4, 5.5 & 5.6*). Within the hanging-wall, the upper Tamworth Belt succession is characterised by strong, more continuous reflections mimicking a snakehead structure (HATCHER 1995, figure 11-34), whereas in the foot-wall, the reflections are weaker and markedly less continuous (*Fig. 5.4*). This seismically imaged feature indicates that the fold is associated with a thrust

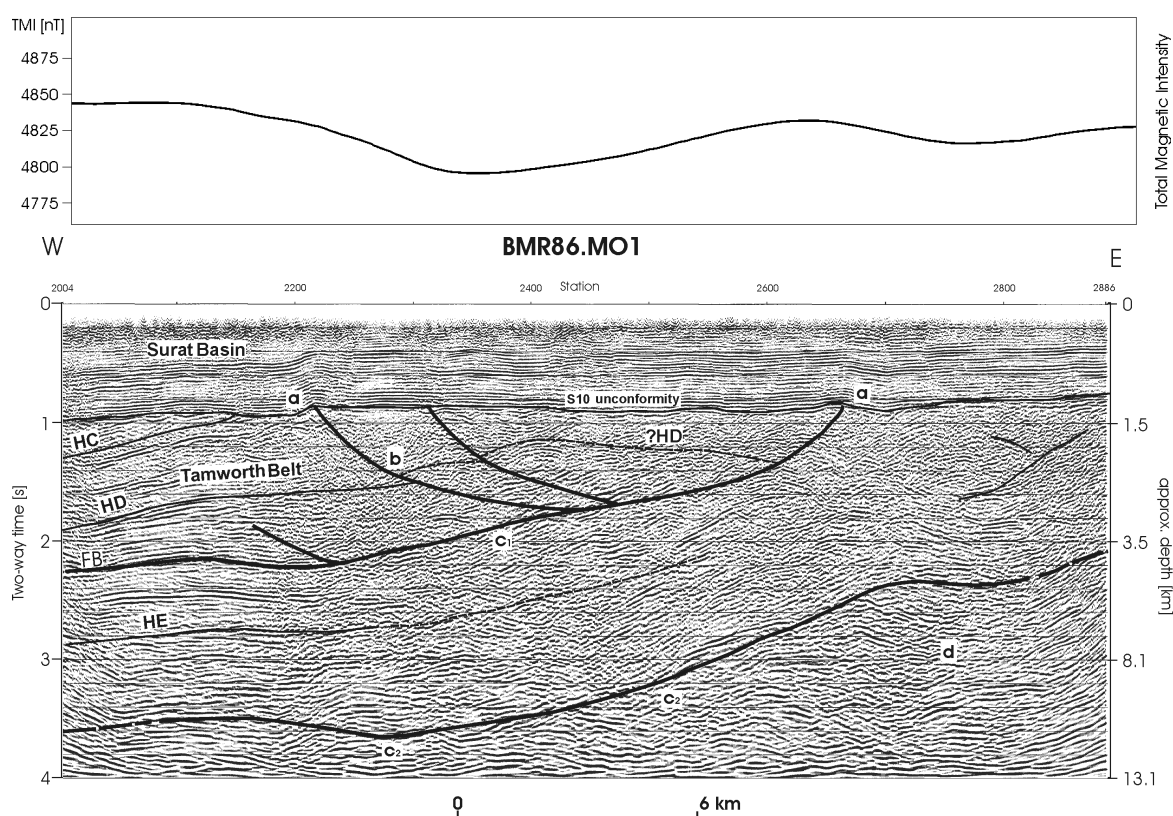


Fig. 5.6: Interpretation of the migrated seismic reflection profile BMR86.MO1 (“Millmerran” profile). Heavy solid lines represent interpreted faults. Two faults of major importance are marked as “*c*₁” and “*c*₂”, respectively. “*b*” is interpreted as a back-thrust off the westward-dipping fault marked as “*c*₁”. “*a*” identifies the reactivation of faults influencing the lowermost sequences of the Mesozoic Surat Basin cover (*S10* represents the base of the Surat Basin).

Light solid lines represent Tamworth Belt seismic horizons. *HE*, *HD* and *HC* are within the fore-arc basin succession. The ratio of vertical to horizontal scale approximately equals 1.

The aeromagnetic anomaly along this traverse is illustrated above the seismic image (cf. *Fig. 4.5*).

ramp (“b” in *Fig. 5.4*).

Tracing particular horizons across the thrust fault reveals that there is a distinct offset. For example, the *B30* reflection occurs at *c.*1650 ms TWT within the hanging-wall succession, whereas on the footwall side it is at a depth of *c.*2600 ms TWT. The offset, therefore, between the two reflections is *c.*950 ms TWT which equals approximately 2850 m (*Fig. 5.4*). Additionally, both reflections may be traced almost as far as the fault plane, revealing uplift in the hanging-wall, indicating a thrust sense of movement. Such a pattern suggests, perhaps, the presence of a fault ramp structure farther to the east of the seismic profile A82-L-24 (*Fig. 5.4*).

The two composite seismic profiles A82-LT-20/A82-WR-22 (to the north, *Fig. 5.7*) and A82-LT-29/H82-T-106 (to the south, *Fig. 5.8*) depict the asymmetric syncline that forms part of the larger fault-bend-fold structure and is related to NW-directed thrust movement with the synclinal axis trending NE-SW. If the *B30* reflection is taken as the marker, then the syncline is broad and flat bottomed in the southern part, but is narrower and more angular in the north, with its east limb measuring *c.*3 kilometres for A82-LT-20/A82-WR-22 and *c.*9 kilometres for A82-LT-29/H82-T-106 (*Figs 5.7 & 5.8*). However, in the study area, the overall geometry of the hanging-wall tends to broaden towards the north (cf. *Figs 5.4, 5.5, 5.7, 5.8 & 5.9*).

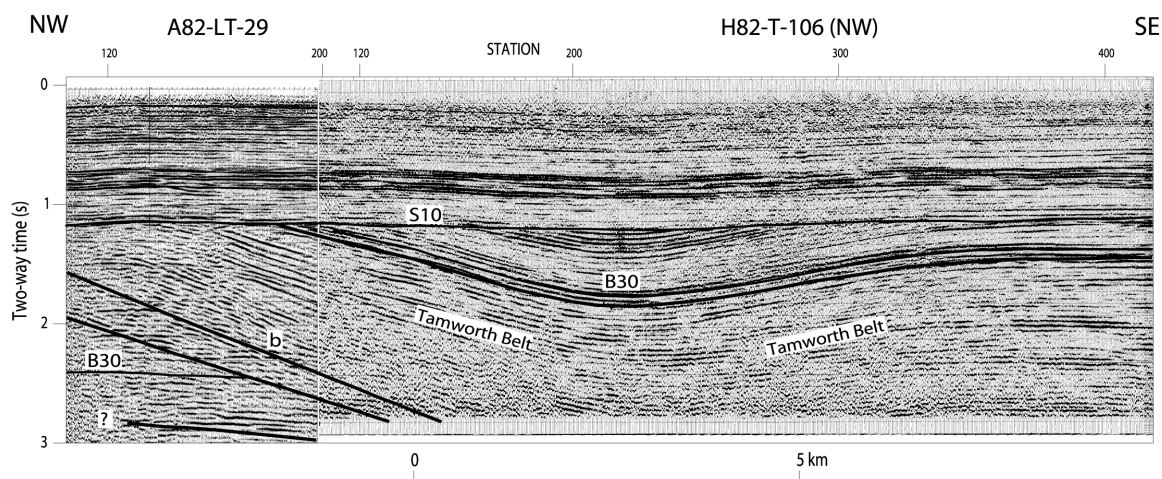
5.2. Fault Maps

Erosion and peneplanation occurred in the Late Triassic removing not only part of the sedimentary record of the Tamworth Belt and the Bowen Basin but also part of the thrust fault-related palaeomorphology in the area of interest. Thus, the thrust faults that intersect the Early Jurassic rocks of the basal Surat Basin succession (*Figs 5.4 & 5.7*) do not mirror the palaeogeometrical orientation of the thrust sheet as the fault tip-line cutting the *S10* reflection (“a” in *Fig. 5.4*) may be shortened differently in depth and angle. However, as the depicted thrust-faults of the study area predominantly have a flat-dipping character, the fault geometry may be interpreted as a trend. Most of these thrust faults appear to be NW- to W-directed, forming part of a foreland thrust-fold belt that deforms the entire Tamworth Belt succession. In the study area, the Tamworth Belt is uplifted as the hanging-wall of the Moonie Fault ramp (“b” in *Fig. 5.4*). The plane of the Moonie Fault is in-

terpreted to depict a detachment surface of major importance to the overall structural geometry in the subsurface. It is marked **FB** on some of the following figures imaging the Moonie Fault. For reasons of a better comprehensibility, the thrust sheet above the Moonie Fault shall be called “*Moonie thrust sheet*” in the following.

5.2.1. Moonie Fault plane

Tracing the tip line of the Moonie Fault plane in the western part of the study area, three different trends of fault-strike may be identified on the fault map for the eastward-dipping thrust. The major fault orientation is SW-NE (*Figs 5.10 & 5.11*; see *Figs 5.13 & 6.1*) and



so is the overall strike of the folded hanging-wall units (*Fig. 5.13*). Also, SE-NW-striking faults may be observed and, more rarely, near-N-S-striking faults (*Figs 5.11, 5.13 & 6.1*).

The study area is in an abnormal geometrical location in close, north-western vicinity to the Texas Orocline (*Fig. 3.1*; see **Chapter 3.1.**). Here, the strike of the major ramps is interpreted to vary from the near-longitudinal strike of the major ramps of the exposed Tamworth Belt to the south of the study area in northern New South Wales (see *Fig. 3.1*). As the ramp structures are inclined at other angles to the thrust sheet movement, it is important to identify (i) the orientation of the lateral thrust ramps, as they strike approximately parallel to the transport direction (ii) seismic lines along strike of the frontal ramp. Within the hanging-wall to the east of the Moonie Fault, most of the SW-NE-oriented seismic profiles show hardly any deformation with horizontal stratigraphy, implying that the transport direction is perpendicular to the profiles. Thus, the SW-NE-trending part of the Moonie Fault identifies the frontal ramp in the study area with the

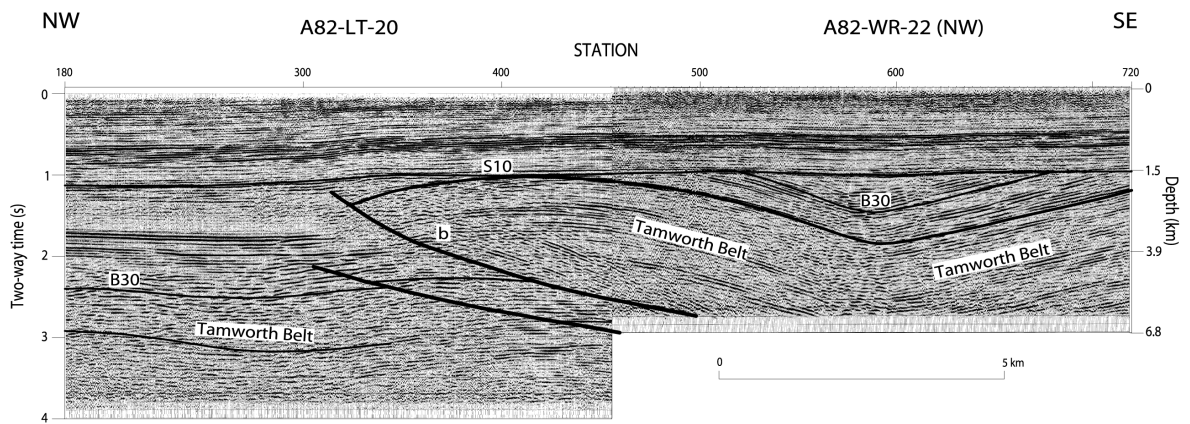


Fig. 5.7: Interpretation of the seismic reflection profiles (final stack) A82-LT-20 (to the north-west) and A82-WR-22 (to the south-east). The composite cross section is located in the northern study area across the strike of the subsurface Tamworth Belt (see Fig. 3.3 for location). Terminology as per figure 5.4.

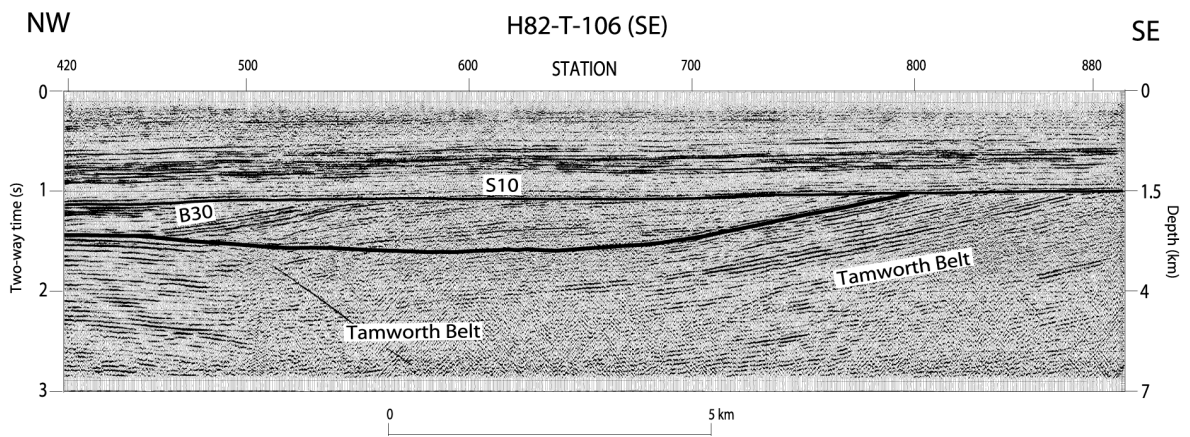


Fig. 5.8 (previous page and above): Interpretation of the seismic reflection profiles (final stack) A82-LT-29 (to the north-west) and H82-T-106 (to the south-east). The composite seismic profile is located in the southern study area across the strike of the subsurface Tamworth Belt (see Fig. 3.3 for location). To the west, on A82-LT-29, “b” identifies the Moonie Fault as it ramps up to the NW. Terminology as per figure 5.4.

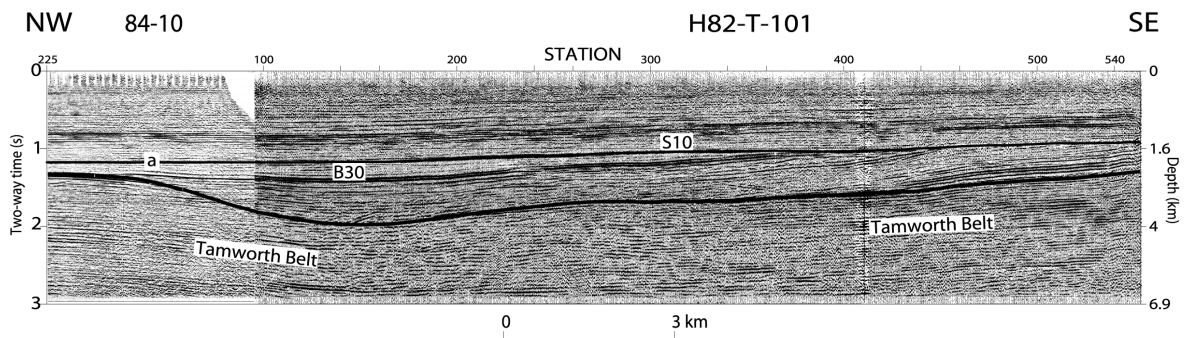


Fig. 5.9: Interpretation of the seismic reflection profiles (final stack) 84-10 (to the north-west) and H82-T-101 (to the south-east). The composite cross section is located in the southern study area across the strike of the subsurface Tamworth Belt (see Fig. 3.3 for location). “a” identifies a drag on the thrust fault that ramps up to the NW (see text for details). Terminology as per figure 5.4.

transport direction along the Moonie thrust plane from south-east to north-west (Fig. 5.10; see Fig. 5.11). Two lateral ramps are interpreted to strike SE-NW (Fig. 5.11). The N-S-striking thrust ramps are oblique ramps that are inclined at a different angle to the original transport direction (see Fig. 5.11).

5.2.2. Introducing another thrust horizon

As part of the foreland thrust-fold belt, the concealed Tamworth Belt is uplifted in the hanging-wall of the Moonie Fault ramp, bringing fore-arc strata to the pre-Late Triassic palaeo-surface. The gentle folding of the Tamworth Belt succession is a product of the thrusting (i.e. a cause of the fault-bend folding). However, within the study area, at least part of the shortening in the thrust belt seems to have been not only along the Moonie

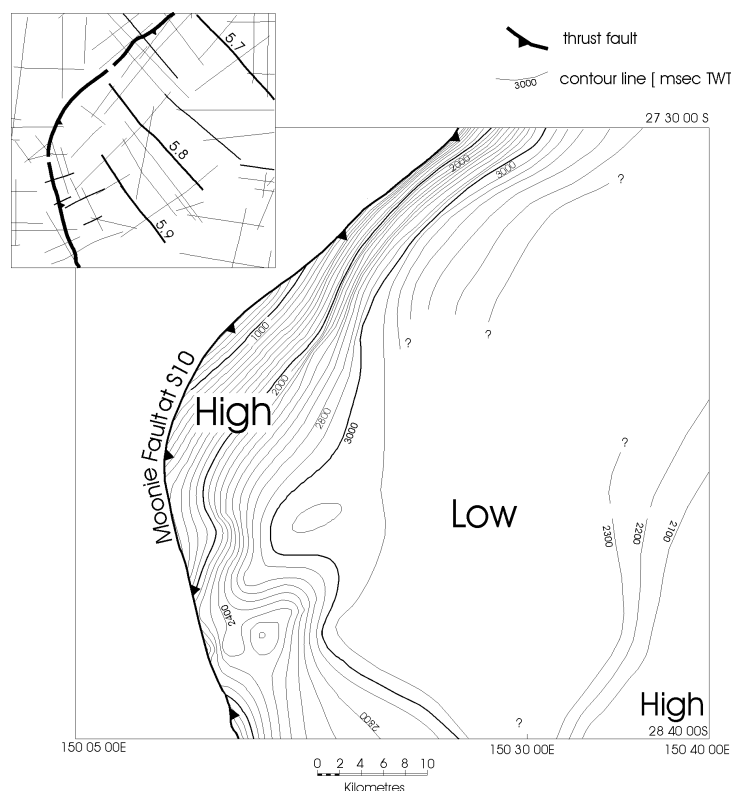
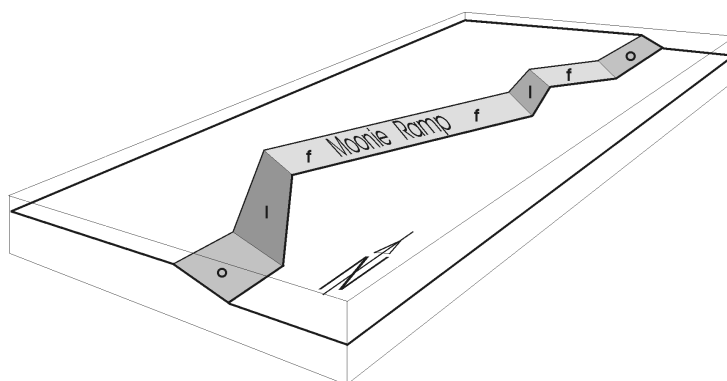


Fig. 5.10: Structure Contour Map of the Moonie thrust plane **FB** (based on the interpretation of the seismic profile network in the investigated area) identifying a NW-directed ramp structure to the west and a gently NW-dipping flat to the east (depths in milliseconds two-way-travel time). The fault azimuth dips towards the north-east. The black heavy solid line represents the position of the Moonie Fault cutting the *S10* reflection (base of the Surat Basin). In the top left corner, the seismic profile network is illustrated in light black solid lines.

Fig. 5.11: Schematic foot-wall morphology of the Moonie Fault to the west and to the north-west of the Texas Orocline as proposed from the interpreted seismic data. Note, that the cartoon shows the fault structure within the seismic study area and its continuation farther to the north (cf. Fig. 6.1). The ramp structures that are inclined at different angles to the Moonie sheet movement are designated “f” for frontal ramps, “o” for oblique ramps and “l” for lateral ramps. See text for further details.



Fault detachment. To the east of the Moonie Fault ramp, in the upper part of the hanging-wall block, another fault horizon is identified that can be traced parallel to the bedding of the fore-arc basin sediments beneath it (*Figs. 5.4 & 5.5*). This fault is interpreted to be a second thrust surface within the upper Tamworth Belt succession and from now on be referred to as the *FA thrust plane* (marked as **FA** on some of the seismic profiles).

On several seismic reflection profiles, the *FA* thrust plane can be traced, running more or less conformably with the *HB* Tamworth Belt reflection (*Figs 5.4 & 5.5*), with some sections even indicating the incorporation of Bowen Basin sediments in the thrusting process (*Fig. 5.8*). On the seismic profile H82-T-101, the *FA* horizon may be interpreted to identify an older ramp, showing the hanging-wall flat *B30* dipping slightly to the NW, forming the easterly border of the basin succession with *S10* truncating *B30* (*Fig. 5.9*). To the NW, at the eastern end of the neighbouring 84-10 seismic profile, the *B30* horizon is thrust upon itself with minor displacement. Here, a drag on the thrust fault may be observed with *B30* picking up the thrust shear movement.

5.3. Discussion

One of the main goals of this study was to establish the three-dimensional relations between the faults that are relevant for the structural evolution in the study area in southern Queensland. As stated by BOYER & ELLIOTT (1982), the geometric relations between thrusts give rise to two typical questions: will my interpretation change if this thrust fault joins that one? – and – what does the thrust map pattern imply for the cross section?

Seismically significant stratigraphic reflections and bounding thrusts of the Moonie Thrust Sheet allowed for mapping its subsurface geometry. Owing to the extremely sparse lithological, palynological and borehole-geophysical control within the Tamworth Belt succession (cf. **Chapter 3.2.2.**) it is pointed out that the final interpretation is based on the observed seismic stratigraphy and on aeromagnetic- and gravity data. This provides an understanding of the fore-arc basin geometry and an understanding of the evolution of the subduction-related units within the subsurface New England Orogen.

5.3.1. The concealed Tamworth Belt – post-depositional deformation

Following initial basin subsidence and deposition, the Tamworth Belt was subjected to contractional and oroclinal deformation. Evidence for this may be seen in the pattern of reflection offsets within the basin fill succession (Fig. 5.4). Two major fault sets developed in the Tamworth Belt - to the west the Moonie Fault (Figs 5.14 & 5.15) and to the east the two westward-dipping faults (“c₁” and “c₂” on Fig. 5.6), east of which the accretionary wedge is identified (“d” on Fig. 5.6; see **Chapter 5.3.2**). Owing to the lack of cross-cutting relationships it not possible to determine precisely which of the westward-dipping faults developed first. However, the easternmost faults define a zone between the fore-arc basin and the accretionary wedge succession (Fig. 5.6), suggesting that they were part of the original fore-arc basin-

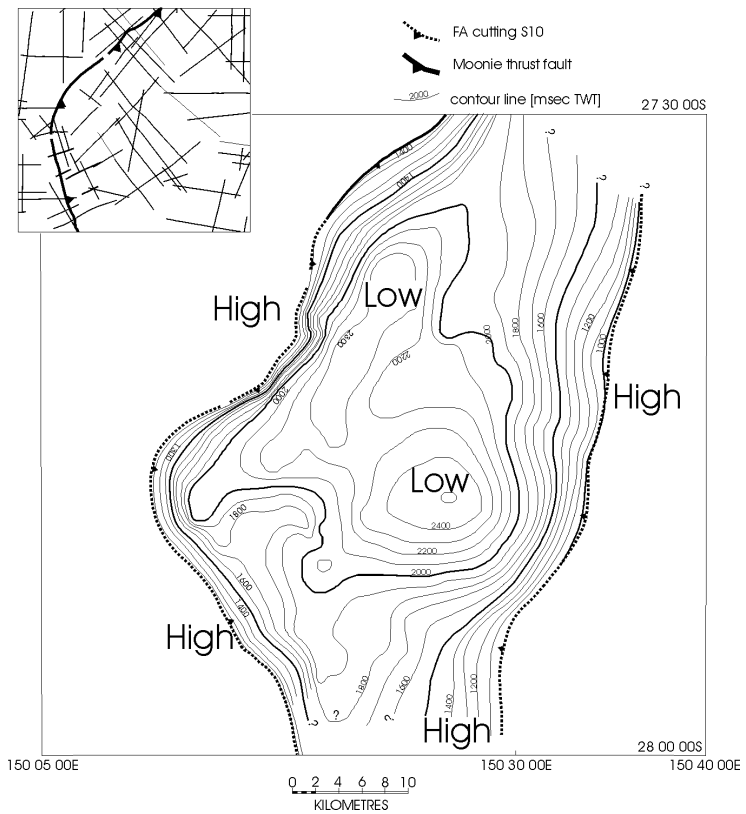
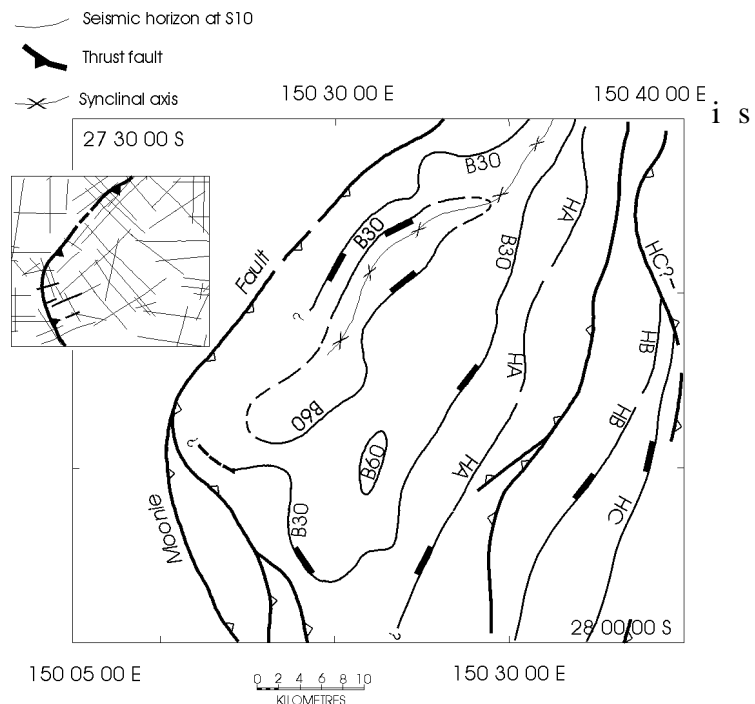


Fig. 5.12: Structure Contour Map of the thrust plane FA in the hanging-wall sequence of the subsurface Tamworth Belt based on the interpretation of the seismic profile network in the study area. The dotted line illustrates FA being truncated by S10.

Fig. 5.13: Map of the seismic study area showing thrust faults and Tamworth Belt and Bowen Basin horizons at the S10 base of the Surat Basin.



bounding structures. In contrast, the Moonie Fault is a later structure, related to Middle to Late Triassic deformation, which offsets basin infill reflections (see above). Nevertheless, the author can not rule out the possibility that the westward-dipping faults may have formed during a post-depositional contractional event.

5.3.2. Defining the eastern limit of the subsurface Tamworth Belt

Two major westward-dipping faults, “c₁” and “c₂”, form a zone that defines the eastern margin of the Tamworth Belt on the seismic reflection profiles (*Fig. 5.6*). On the western side of this fault zone, the Tamworth Belt shows a nice stratigraphy (*Figs 5.6 & 5.5*). If the easternmost of the faults is projected upwards beyond the limits of the seismic line, it intersects the base of the Surat Basin at the position of the northern extension of the Peel Fault (as interpreted from the aeromagnetic data) (see “c₂” on *Fig. 4.6*; cf. *Fig. 4.8*). To the south of the study area, the surface expression of the Peel Fault contains serpentinites and mafic related rocks which result in higher magnetic intensity along the fault trace. Thus, the aeromagnetic data suggest that the true limit of the subsurface Tamworth Belt lies along the eastern westward-dipping fault “c₂” (*Fig. 5.6*). Deformation within the fault zone precludes precise definition on the seismic profiles of the margin of the Tamworth Belt, but the aeromagnetic data suggests that the boundary is coincident with the easternmost limit of the fault array (*Figs 4.2a, 4.5 & 5.6*) (see above).

5.3.3. Structure of the concealed Tamworth Belt

Fault initiation and propagation as a result of externally-controlled tectonic activity, led to deformation of the basin fill of the Tamworth Belt succession. Although the precise base of the Tamworth Belt is difficult to determine, it can be locally constrained in the area by the two basin fault sets, namely, the Moonie Fault and the northern extension of the Peel Fault (*Figs 5.4 & 5.6*). In the southern part of the study area, the Moonie Fault is approximately oriented north-south, curving to the NE (from approximately 28° 05' S), with the highest part of the fore-arc succession located along the concave part of the fault curve (*Figs 5.10 & 5.11*). The internal geometry of the Tamworth Belt can be determined only by a more detailed examination of the hanging-wall succession which developed between the Moonie Fault and the Peel Fault extension. The top of the hanging-wall succession, as

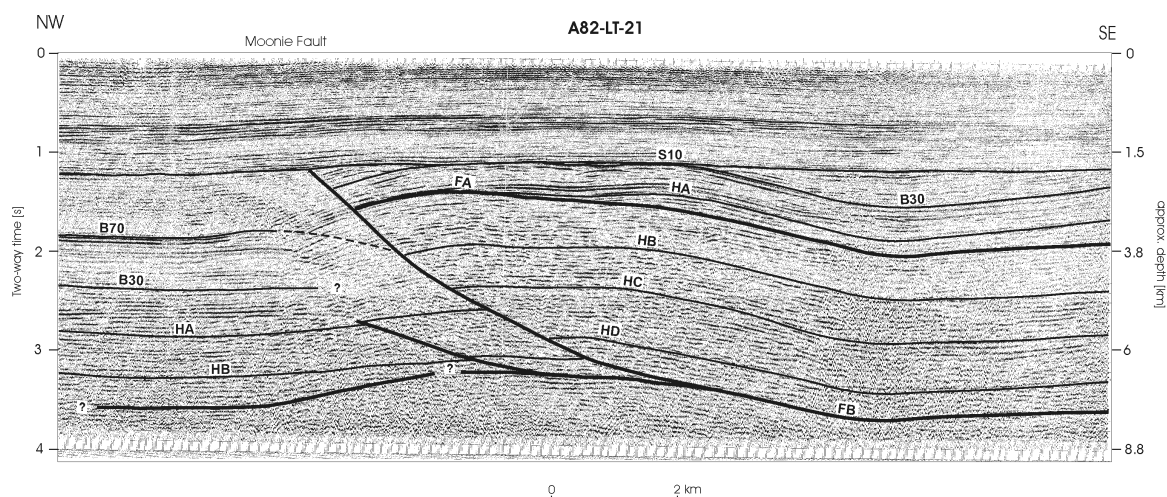


Fig. 5.14: Interpretation of the seismic reflection profile A82-LT-21 (final stack) perpendicular to strike of the subsurface Tamworth Belt in the northern study area (see Fig. 3.3 for location). Heavy solid lines represent faults, such as the *FB-Moonie Fault plane*, here identifying a flat in the ramp-flat geometry of which the *Moonie Fault* ramps up towards the NW. The *FA-roof thrust* is identified within the hanging-wall sequence.

The light solid lines represent the interpreted seismic horizons *HA*, *HB*, *HC* and *HD* within the Tamworth Belt succession. *S10* and *B30* represent the sequence boundaries at the base of the Surat and Bowen Basins, respectively.

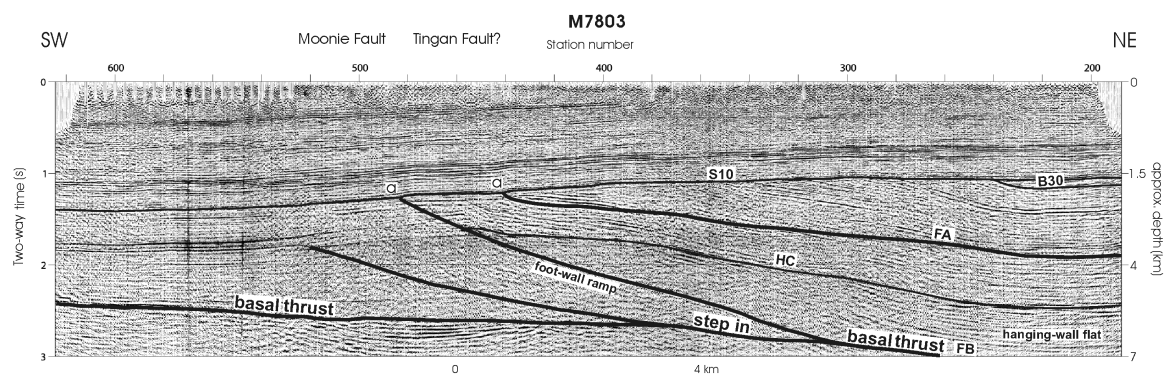


Fig. 5.15: Interpretation of the seismic reflection profile M7803 (final stack) oblique to strike of the subsurface Tamworth Belt in the southern study area (see Fig. 3.3 for location). Heavy solid lines represent faults, such as the *FB-Moonie Fault plane*, here identifying a flat from which the *Moonie Fault* ramps up to the SW (marked as “*foot-wall ramp*”) with its fault tip line at the base of the Surat Basin (marked as “*a*”). The *FA-roof thrust* is identified within the hanging-wall sequence. Its fault tip (at *S10*, marked “*a*”) can be traced to the south of the study area, possibly identifying the thrust fault to be the *Tingan Fault* equivalent. The timing of thrusting occurred during the Middle to Late Triassic Goondiwindi Event. Both thrust faults were reactivated during the early Late Cretaceous Moonie Event (“*a*”), uplifting the Mesozoic platform cover NE of the Tingan Fault relative to the same succession SW of the Moonie Fault.

The light solid line represents the interpreted seismic horizon *HC* which is within the Tamworth Belt succession. *S10* and *B30* represent the sequence boundaries at the base of the Surat and Bowen Basins, respectively.

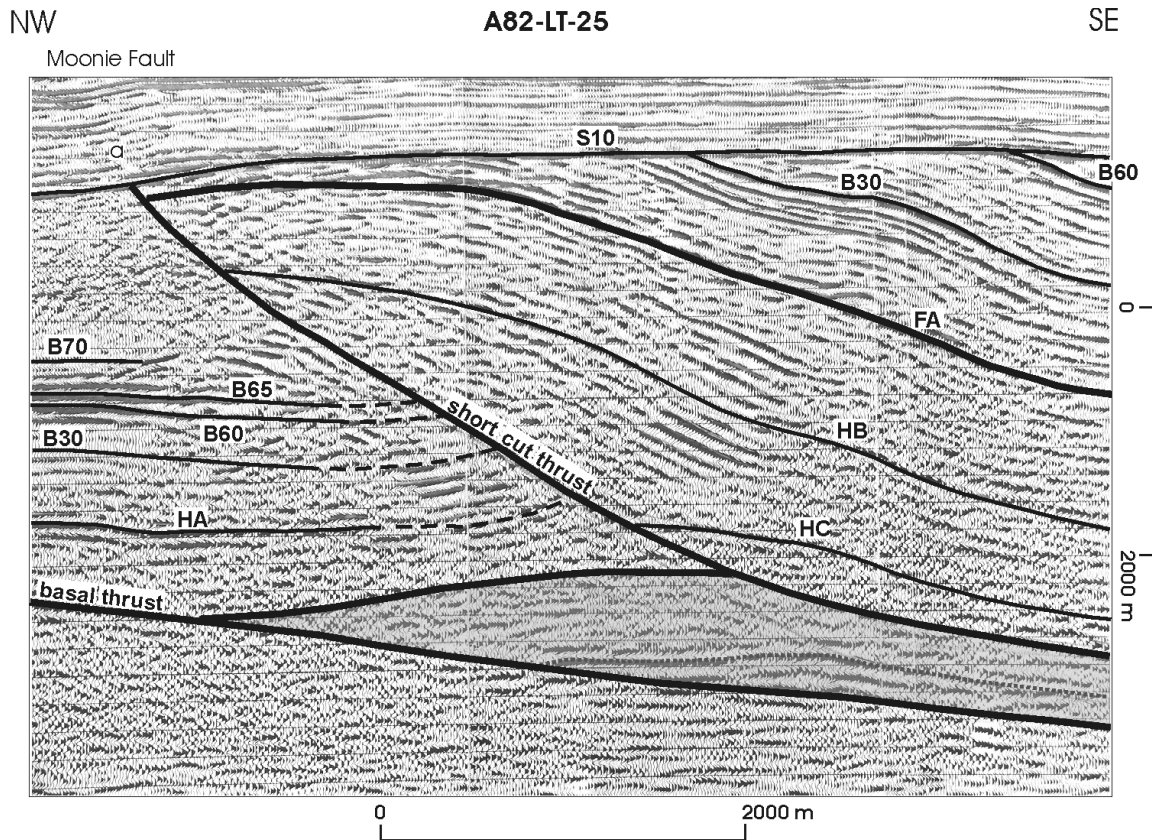


Fig. 5.16: Interpretation of the seismic reflection profile A82-LT-25 (migrated) perpendicular to strike of the subsurface Tamworth Belt (see Fig. 3.3 for location). Heavy solid lines represent fault surfaces. Two imbricates marked in light grey form a horse. (see text for details).

The light solid lines represent the interpreted seismic horizons within the Bowen Basin and the Tamworth Belt succession, respectively. *S10* and *B30* represent the sequence boundaries at the base of the Surat and Bowen Basins, respectively.

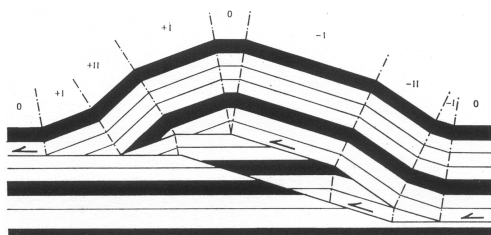


Fig. 5.16a: Cartoon showing the panels of forward and back dip in a simple-step fault-bend fold with two imbrications (from SUPPE, 1983) (cf. Fig.5.3).

defined by the Moonie Fault, lies less than 1 second TWT beneath the surface (c.700 ms TWT on Fig. 5.6), while the deepest part is to the east, at a depth of c.3400 ms TWT (Fig. 5.4). The overall geometry of the hanging-wall succession tends to broaden towards the north, that is, the farther away the hanging-wall succession is from the Texas Orocline, the wider it stretches west-east. The map, showing the uppermost three Tamworth Belt reflections *HA*, *HB* and *HC* (Fig. 5.13), depicts an asymmetric syncline that trends NE-SW and is broad and flat bottomed in the southern part of the study area, while steep-

ening to the north (cf. **Chapter 5.1.2.**). This feature, which forms part of the larger fault-bend-fold structure (as seen elsewhere in the region), is related to NW-directed thrust movement (*Fig. 5.13*). On the migrated seismic profile A82-LT-25 (*Fig. 5.16*), the Moonie Fault is interpreted to be a short cut thrust that roots on to the upper of two imbricates. The imbricates form a horse that is located beneath the simple-step fault-bend fold in the hanging-wall sequence to the east of the fault (shaded area in *Fig. 5.16*).

The NE-SW-trending steep asymmetric syncline that broadens to the south, together with the change in trend of the Moonie Fault from N-S (to the south of the study area) to NE-SW (within the study area) underlines the anomalous geometric situation within the study area. Here (Texas Orocline), the Tamworth Belt sediments underwent oroclinal bending that influenced the geometry of the basin. To the south, the fore-arc basin geometry is described by the faulted character of the Tamworth Belt succession with the eastward-dipping Moonie Fault to the west and the westward-dipping northern extension of the Peel Fault to the east. Farther north, however, the basin geometry widens along strike, as can be seen in the deep seismic line BMR84.14 farther north (*Fig. 4.12*; WAKE-DYSTER *et al.*, 1987).

The relationship between the Bowen Basin and the Tamworth Belt

The previously noted apparent conformable stratigraphic relationship between the successions in the Tamworth Belt and Bowen Basin raises an interesting issue. The Tamworth Belt has been interpreted as a fore-arc basin succession (e.g. KORSCH & TOTTERDELL, 1996), whereas the Bowen Basin is considered to have formed in a back-arc setting (e.g. MCKELVEY & MCPHIE, 1995). This relationship would imply that there was little deformation of the Tamworth Belt succession during the period when subduction migrated (KORSCH *et al.*, 1997) or jumped (AITCHISON & FLOOD, 1995) eastwards, and the magmatic arc relocated to the east of the current position of the Bowen Basin. In the vicinity of the seismic lines A82-LT-24 (*Fig. 5.4*) and A82-WR-22 (*Fig. 5.7*), a small remnant of the Bowen Basin is preserved to the east of the Moonie Fault. The presence of this remnant of the Bowen Basin in a thrust sheet to the east of the main basin suggests that the original area covered by the basin extended much farther to the east than its present limits. It also indicates that the original eastern margin of the Bowen Basin has been destroyed and has been incorporated into the Late Permian to Middle Triassic retro-foreland

thrust belt of the New England Orogen. In the eastern part of the investigated region, the situation is less clear, partly due to the lack of sufficient seismic profile coverage (see *Fig. 3.3*), and partly due to seismic record depths of only 3 seconds TWT.

Balancing of the above discussed cross sections has not been accomplished (a) due to the strong internal deformation within the seismic fore-arc basin sequences and (b) due to the strongly curved and low-angle folded character of the subsurface Tamworth Belt segments, especially in the easternmost area of interest (*Figs 3.7 & 5.6*).

5.3.4. The concealed Tamworth Belt – fault history

Three significant deformational events are recorded in the study area. Following initial formation and infill of the Tamworth Belt fore-arc basin, these tectonic events mark the various stages of subsequent thrusting (*Figs 5.4, 5.5, 5.6, 5.15, 5.16, 5.17 & 5.18*).

On several SW-NE-oriented seismic profiles, structural features may be identified that show evidence for the oldest observed deformational phase in the study area. Thrust faults of minor displacement offset the uppermost Tamworth Belt succession and the lowermost sedimentary sequences of the Bowen Basin (*Fig. 5.17*). These faults are often observed to be combined with backthrusts, identifying pop-up structures as to be seen on the seismic profile H82-T-110 (*Fig. 5.17*).

This seismic survey was shot approximately along strike of the fore-arc basin unit (and therefore perpendicular to the earlier described composite seismic traverse; cf. *Fig. 3.3*). Here, the main thrust is NE-directed and seems to root onto the *HA* reflection of the youngest Tamworth Belt succession. The fault offsets the base of the Bowen Basin (*B30*) with a maximum of *c.*150 metres to the northeast of the seismic profile (70 ms TWT in *Fig. 5.17*). Above the *B30* reflection - and beneath the base of the Surat Basin (*S10*) - three strong seismic reflections may be identified, that are slightly folded but not influenced by the fault displacement. The uppermost of these seismic reflectors is identified as the Early Triassic *B70* horizon and assigned to the Late Permian-Early Triassic base of the *Rewan Group*. The two underlying seismic horizons are very distinctive on seismic profiles throughout the study area. The horizons are identified as the Late Permian *B60* horizon (base of the *Burunga Formation*) and the early Late Permian *B65* horizon (which defines the base of the *Baralaba Coal Measures*) (see *Tab. 2.1*). A non-reflective pile

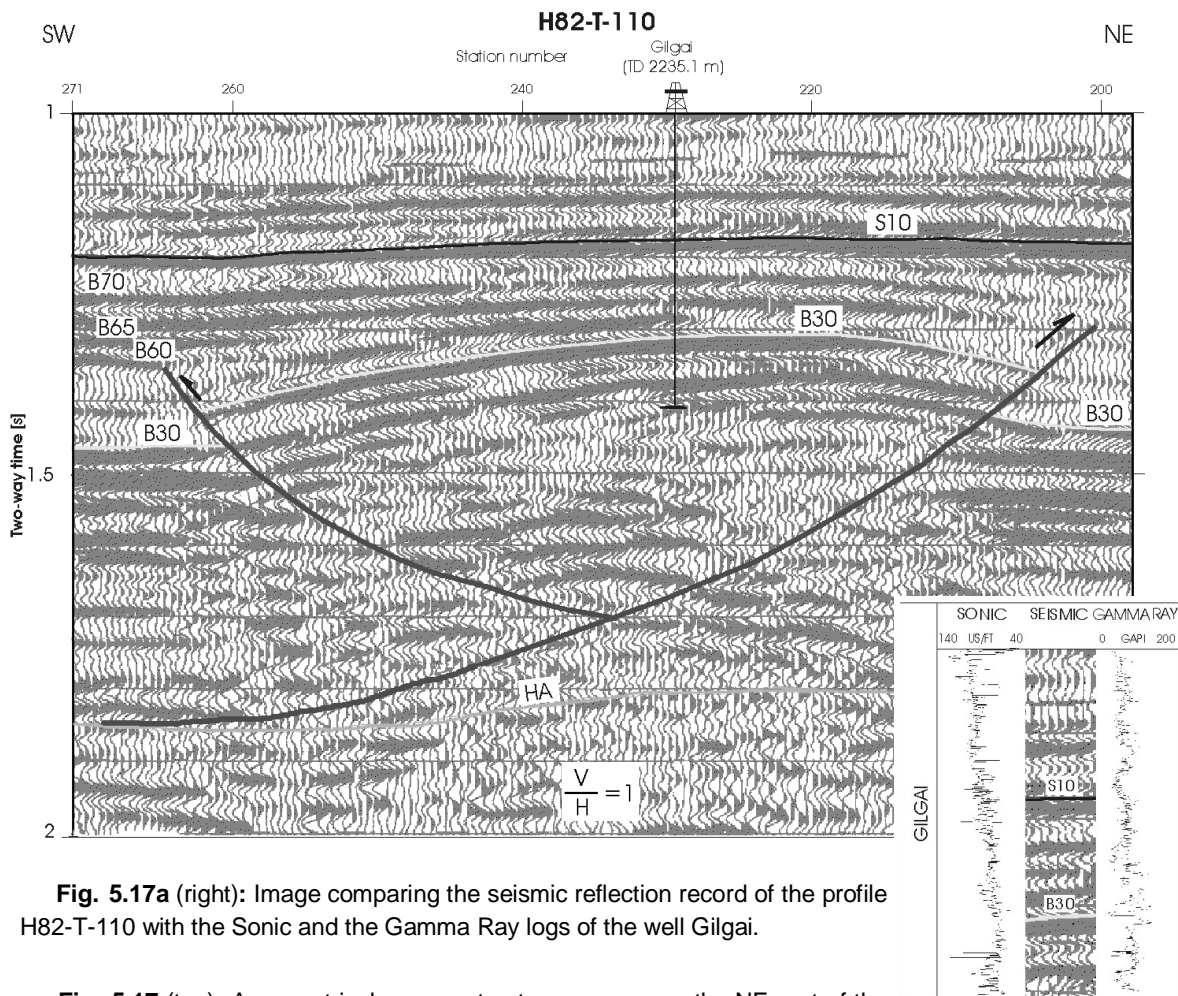
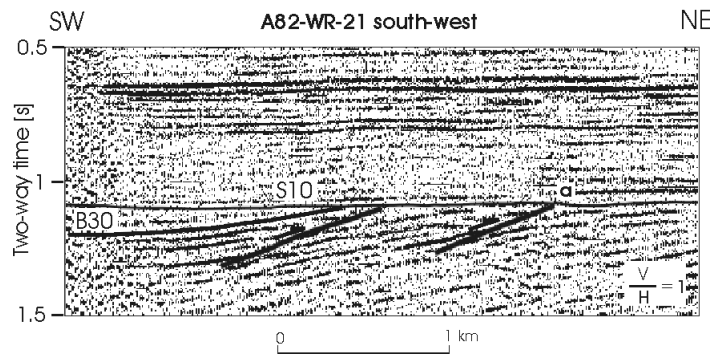


Fig. 5.17a (right): Image comparing the seismic reflection record of the profile H82-T-110 with the Sonic and the Gamma Ray logs of the well Gilgai.

Fig. 5.17 (top): Asymmetrical pop-up structure as seen on the NE-part of the seismic profile H82-T-110, offsetting the *B30* base of the Bowen Basin. The seismic interpretation shows a thrust - back-thrust geometry that occurs at high structural levels in the brittle field (see HAYWARD & GRAHAM, 1989). The main thrust is NE-directed and seems to root onto the *HA* reflector of the Tamworth Belt. For location of the seismic line H82-T-110, see Fig. 3.3.

zone is seen above the *B30* horizon on either side of the above mentioned pop-up structure (Fig. 5.17). In between the two structure-defining thrust faults, this pile zone has been removed. Here, the borehole data of the well Gilgai intersect the lowermost Bowen Basin sequences. A higher amplitudinal signal of the Gamma Ray log can be observed directly above the *B30* seismic horizon (Fig. 5.17a). This high amplitudinal signal of the Gamma Ray log corresponds with a distinct unconformity as seen in the Bowen Basin. The geology anywhere else in the basin shows, that between the *B30* and the *B60* seismic horizons a big unconformity occurs at the base of the *Oxtrack Formation* and is identified on the seismic profiles as the *B45* horizon (Tab. 2.1). On the H82-T-110 seismic profile, the *B45* horizon may be located directly on top of the pile zone that has been removed,

Fig. 5.18: Detail of the SW-part of the seismic reflection profile A82-WR-21 (final stack) (for location, see Fig. 3.3). The sedimentary succession beneath the B30 base of the Bowen Basin is dominated by minor, NE-directed thrust faults (solid black lines). To the right of the profile, "a" marks that part of the Surat Basin that is slightly effected by a later, post-S10 fault movement.



providing evidence for thrusting processes at least during Mid Permian times (Fig. 5.17; cf. B30 to B70 of Table 2.1).

Various seismic profiles in the study area show evidence for the second phase of thrusting - the Goondiwindi Event of KORSCH *et al.* (1998) - where strata of the Tamworth Belt are thrust over Middle Triassic rocks of the Bowen Basin along the Moonie Fault. Line A82-LT-24 (Fig. 5.4) provides convincing evidence for at least 3 kilometres of vertical displacement on the Moonie Fault. Erosion and peneplanation occurred in the Late Triassic before the Tamworth Belt and Bowen Basin were overlain by Early Jurassic rocks of the Surat Basin. Thus, the major period of fault movement was Middle-Late Triassic, cutting Middle Triassic rocks. Deposition could have been synchronous with thrusting but it is also possible that sediments were removed during the peneplanation and prior to the depositional phase in the Early Jurassic within the Surat Basin.

During the Late Cretaceous, there is evidence for the third deformational phase - the Moonie Event of KORSCH *et al.* (1998) - again seen on several seismic sections in the study area (e.g. Figs 5.4 & 5.6). Of note is the reactivation of the Moonie Fault, with the fault tip propagating into the Surat Basin succession and uplift of the Surat Basin on the hanging-wall side of the fault relative to the footwall (cf. Fig. 5.4). Further evidence for the Moonie Event is provided by folding and uplift of the Surat Basin succession above an eastward-dipping fault near station 2200 in seismic line BMR86.M01 (Fig. 5.6). Although the faults were reactivated in the basement, in most cases they have not propagated upwards into the Surat Basin succession, and usually there is no displacement of the Surat Basin succession above the faults.

5.3.5. The concealed Tamworth Belt – fault orientation

Throughout the study area, various seismic reflection profiles show different effects of the change in fault spacing on fold shape.

The discussion above on the overall geometry has shown that the movement of the Moonie thrust sheet took place over irregularly oriented flats and ramps, resulting in a moderate, asymmetric fold in the thrust sheet. The axial surface of this fold - best defined by its synclinal axis (see *Fig. 5.13*) - is controlled by the location of the changes of orientation of the fault surface.

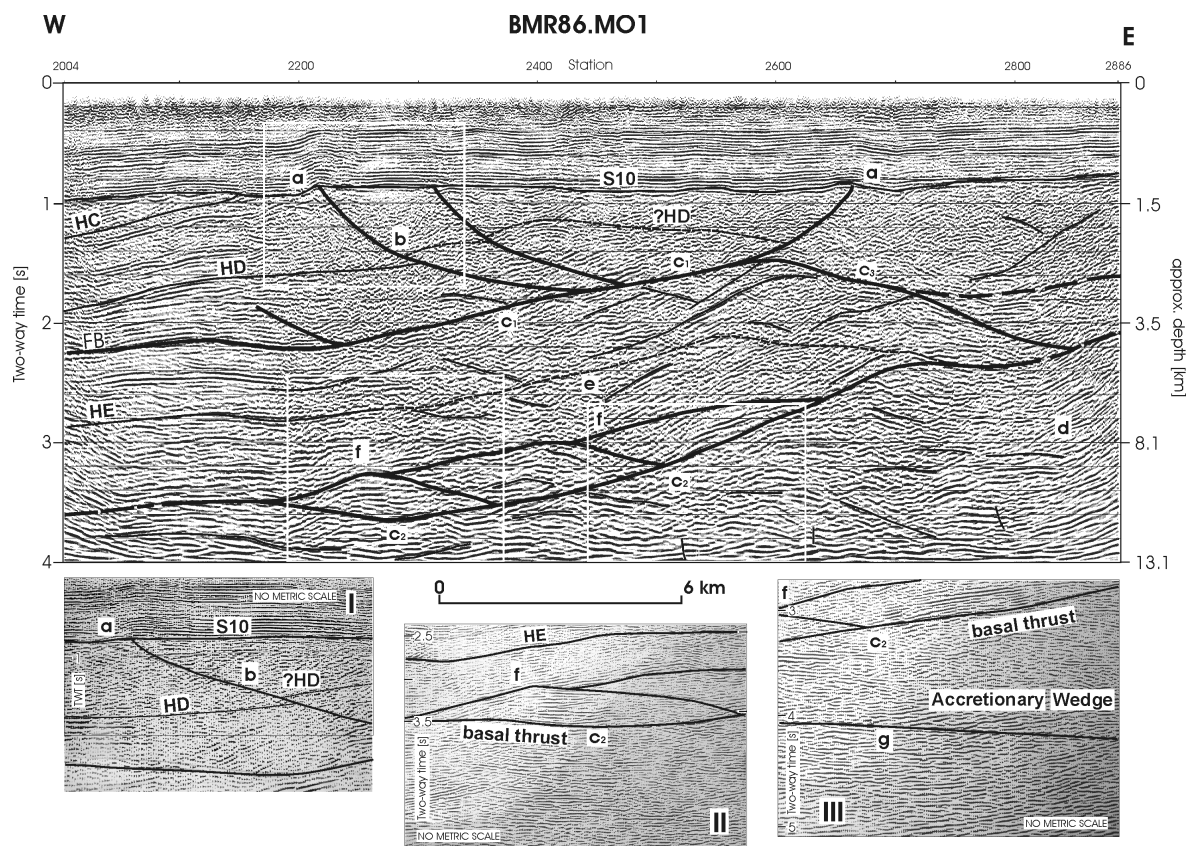


Fig. 5.19: Migrated seismic reflection profile BMR86.MO1 (Millmerran) with reprocessed data illustrated on boxes I, II and III. Heavy solid lines depict fault surfaces. Two faults of major importance are marked as “*c*₁” and “*c*₂”, respectively. “*b*” is interpreted as a back-thrust off the westward-dipping fault marked as “*c*₁”. “*a*” identifies the reactivation of faults affecting the lowermost sequences of the Mesozoic Surat Basin cover (*S10* represents the base of the Surat Basin). “*d*” marks the discontinuous seismic reflection pattern that may be assigned to the seismic resonance of the accretionary wedge assemblage. “*e*” marks the proposed continuation of the *HE* Tamworth Belt reflection in between the two major fault surfaces described above. “*f*” highlights the top of a series of fault surfaces possibly due to basal shearing (basin evolution approach) or as a consequence of footwall horses (thrust mechanics approach) (see text for details).

Light solid lines represent Tamworth Belt seismic reflections. *HE*, *HD* and *HC* are within the fore-arc basin succession. The ratio of vertical to horizontal scale approximately equals 1.

5.4. Subsurface geometries from reprocessed seismic data – a different approach

As described in **Chapter 5.1.**, a series of major NW– to W-directed thrusts may be recognised on the seismic sections (*Figs 5.4 & 5.7*) with the most significant of these structures being the Moonie Fault (*Fig. 5.4*). The complexity of this thrust belt is indicated by the presence of east dipping synthetic thrusts on the western side of the belt (*Fig. 5.4*) and east dipping structures that are interpreted as west-directed backthrusts on the eastern side of the belt (*Fig. 5.6*). On the Millmerran seismic profile (BMR86.MO1) the eastern boundary of the Tamworth Belt is identified by a major westward-dipping fault (*Fig. 5.6*) that may be interpreted as the boundary between fore-arc basin and accretionary wedge sequences.

Geoscience Australia (formerly AGSO) undertook further processing of the two seismic surveys BMR86.MO1 and BMR84.14 down to 6 seconds TWT to improve the display in order to better integrate the data into the existing database. The reprocessed seismic data was subsequently redisplayed at the same vertical scale as most of the industrial shallow seismic lines. This has led to a more detailed interpretation of the overall subsurface geometry of the Tamworth Belt beneath the Surat Basin cover.

5.4.1. Reprocessed seismic data – BMR86.MO1 (Millmerran profile)

At the western end of the Millmerran seismic profile (Station 2004 to 2200 on *Fig. 5.19*) strong, westward-dipping reflections may be seen beneath the *S10* reflection – at *c.*1000 ms TWT – down to a recording depth of *c.*2300 ms TWT. Beneath this depth, the seismic pattern changes and may be characterised by strong, shallow curved reflections down to a recording depth of at least *c.*3200 ms TWT (*Fig. 5.19*). This change in the seismic reflective orientation marks the position of the seismic reflection *HE* (cf. *Fig. 3.6*).

The thrust reflection (*FB* equivalent) of the base of the Moonie thrust sheet is positioned at *c.*2300 ms TWT at the western end of the seismic profile, whereas the basal thrust of the thrust sheet beneath it (from now on, this thrust sheet shall be simply called the “main thrust sheet”) is at a recording depth of *c.*3600 ms TWT, implying that the offset between the two thrusts is *c.*1300 ms TWT (*Fig. 5.19*). As a result from the reprocessing of the seismic data, the base of the Moonie Thrust Sheet (*FB* horizon) is considered to be the

same fault as the above mentioned c_1 fault. Above the base of the main thrust sheet (“ c_1 ” on *Fig. 5.19*), a series of fault surfaces are depicted (see “f” on *Fig. 5.19*) that may be interpreted as (i) footwall horses resulting from contraction or as (ii) residuals of basal shearing processes during the time of fore-arc basin subsidence (see **Chapter 5.5.** for further details).

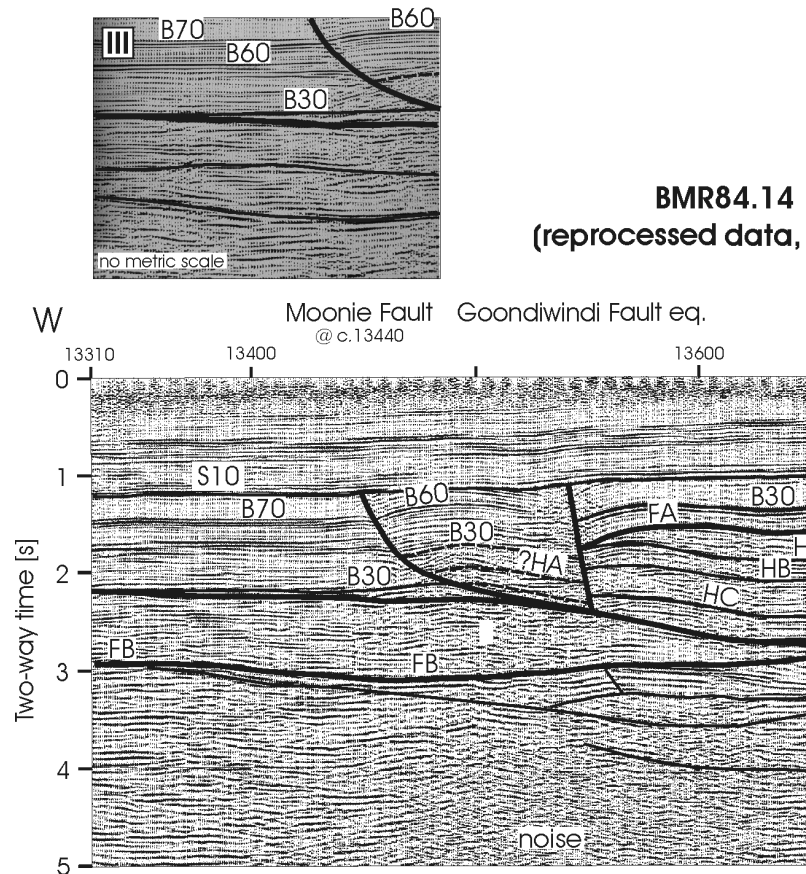
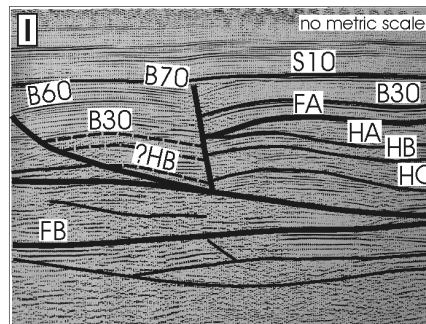


Fig. 5.20: Upper, reprocessed part (upper 1 - 5 s TWT) of the deep seismic survey *BMR84.14* in southern Queensland (cf. *Fig. 5.1*). The boxes shown above and beneath the seismic profile are “zoom ins” that identify structures of greater importance.



5.4.2. Reprocessed seismic data – BMR84.14

The reprocessed data of line BMR84.14 (recording length down to 6 s TWT) has provided a more detailed image of the uppermost crustal seismic reflections.

On the deep seismic profile, the Moonie Fault ramp is interpreted to derive from the thrust base *FB* (*Fig. 5.20*). In contrast to several other seismic sections in the study area, the Moonie Fault is noted not to have been reactivated during the early Late Cretaceous Moonie Event (*Fig. 5.20*; cf. “*a*” on *Fig. 5.4*).

To the east of the Moonie Fault (at SP *c.13530* on *Fig. 5.20*, at *c.3000* m to the east of the fault), a fault has been identified within the hanging-wall sequence that shows a

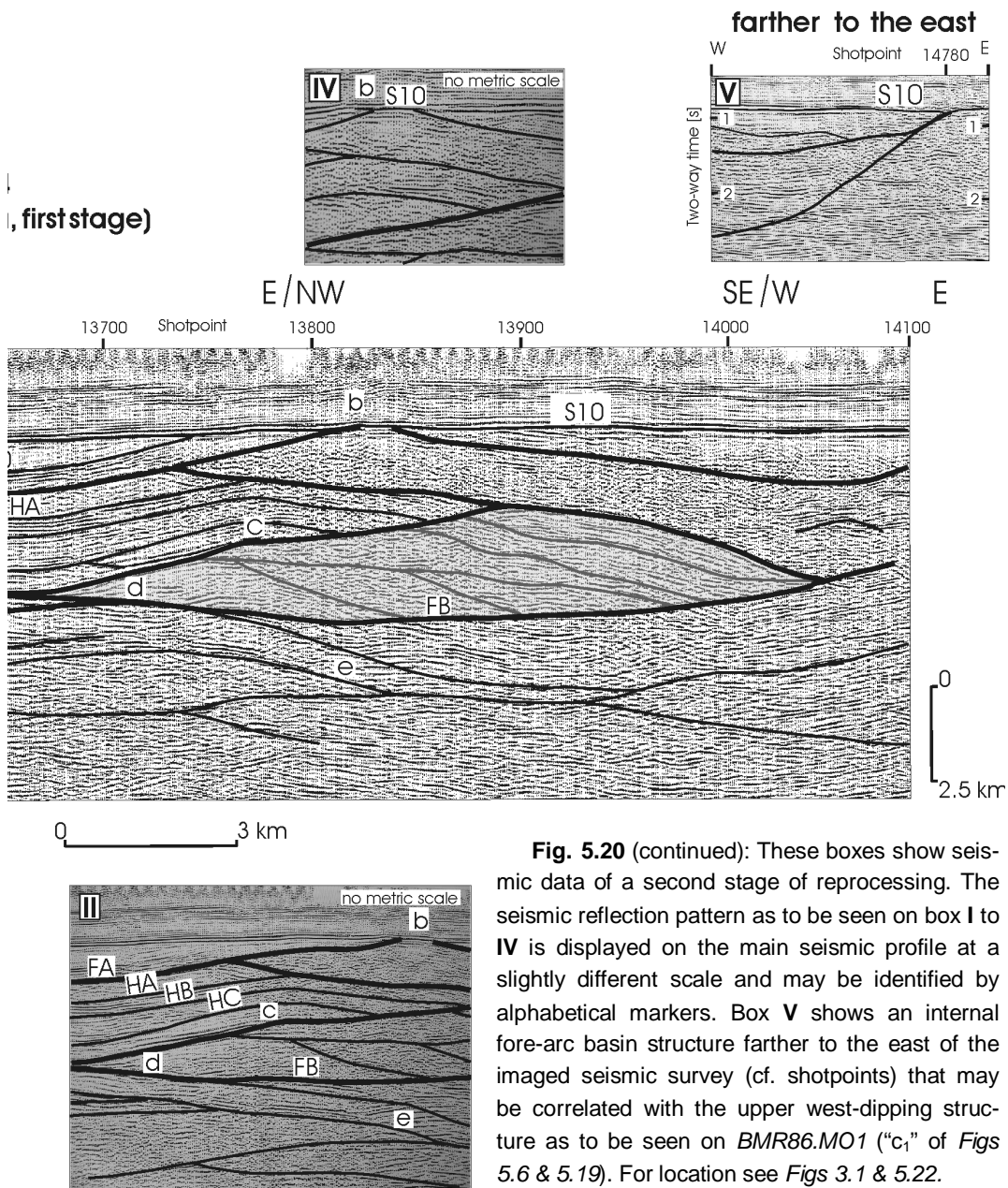
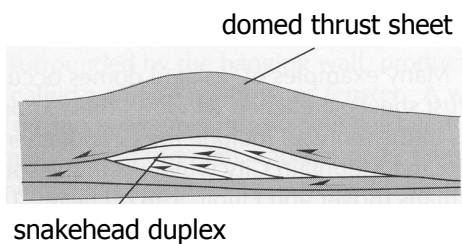


Fig. 5.20 (continued): These boxes show seismic data of a second stage of reprocessing. The seismic reflection pattern as to be seen on box I to IV is displayed on the main seismic profile at a slightly different scale and may be identified by alphabetical markers. Box V shows an internal fore-arc basin structure farther to the east of the imaged seismic survey (cf. shotpoints) that may be correlated with the upper west-dipping structure as to be seen on *BMR86.MO1* ("c₁" of Figs 5.6 & 5.19). For location see Figs 3.1 & 5.22.

Fig. 5.20a: Cartoon of a snakehead duplex beneath a domed thrust sheet (from HATCHER, 1995) (cf. shaded area on Fig. 5.20 above).



near-vertical east dip with small vertical displacement (Fig. 5.20). The fault is considered to be the *Goondiwindi Fault equivalent* (cf. *Tingan Fault* on Fig. 5.15) and, as the Moonie Fault, does not show any reactivation during Late Cretaceous time. As there are no other seismic data crosscutting the deep seismic survey near to this fault, it is uncertain whether this near-vertical structure is (i) transfer fault-related (which is, due to the

fault's steep dip and overall geometry, the preferred explanation in this study) or (ii) a short cut thrust that roots onto the Moonie Fault ramp. The reprocessing of the seismic data shows that this steep east-dipping fault ends at the Moonie Fault ramp at a depth of *c.* 6300 m (*c.* 2500 ms on *Fig. 5.20*). However, in case of the near-vertical fault being a short cut thrust (the latter approach), this would imply that the fore-arc basin sequence beneath the Surat Basin cover has been influenced by multiple deformational phases during the Middle to Late Triassic Goondiwindi Event (with the near-vertical fault being of post-Middle Triassic but pre-Jurassic age).

To the east of the Goondiwindi Fault equivalent, the seismic image shows a non-reflective zone directly beneath the Surat Basin cover that is based on two strong, parallel running seismic reflectors. This seismic reflection pattern is derived from the basal Bowen Basin sequence, as seen elsewhere in the region in the hanging-wall (*B30* on *Fig. 5.20*, cf. *Fig. 5.4*). To the west of the Moonie Fault, in the foot-wall, and in between the two faults, these reflections can not be identified. Here, the sedimentary succession is considered to be influenced by the contractional movement of the thrust belt, showing the juxtaposition of sediments of similar age but of dissimilar facies and indicating major telescoping (*Fig. 5.20*; cf. *Figs 5.4, 5.7, 5.14, 5.16 & Fig. 21*). Thus, the *B30* seismic reflection is at a lower position in between the two faults relative to *B30* to the east and at a higher position relative to *B30* to the west (*Fig. 5.20*). Therefore, the Moonie Fault together with the equivalent of the Goondiwindi Fault is responsible for the uplift of the base of the Bowen Basin (*B30*) on the hanging-wall side of the fault relative to the foot-wall (a total of *c.* 600 ms on *Fig. 5.20*).

To the east of the Goondiwindi Fault equivalent, between shot-point *c.* 13650 and *c.* 14050, a lens-shaped structure is recognised at a depth of *c.* 2-3 s TWT and interpreted as a snakehead duplex (as defined by HATCHER, 1995, figure 11-26) beneath a domed thrust sheet (shaded area on *Fig. 5.20*). The branch line ("*d*" on *Fig. 5.20*) identifies the westernmost part of the duplex. This duplex indicates that there is a space problem in the thrust fold system (cf. **Chapter 5.3.4.**) even in the anomalous region where the fore-arc basin unit is extremely broad and flat bottomed (cf. *Fig 5.1*), underlining the great complexity of the pre-Jurassic tectonic history.

Above the duplex, an eastward-dipping, west-directed fault is recognised at the *S10* seismic reflection at SP *c.* 13900 ("*b*" on *Fig. 5.20*). This fault can be linked to a fault that has been identified within the easternmost study area (e.g. on seismic profile BMR86.

MO1), cutting the Moonie thrust sheet by west-directed back-thrusting (*Fig. 5.19*; see *Fig. 6.1*).

5.5. Seismic data – Discussion

The development of the Tamworth Belt was influenced both by the initial period of subduction-related activity and subsequent tectonic intra-plate deformation. The reprocessed seismic data of lines BMR84.14 and BMR86.MO1 suggests that the earlier discussed vertical displacement of *c.*3000 m (*c.*1000 ms TWT) of the Moonie Fault (cf. *Fig. 3.4*) may be explained according to two different thrust sheets within the hanging-wall, with the *FA* thrust sheet overriding the Moonie thrust sheet. Thus, the tip line of the Moonie Fault ramp (see “*b*” in *Fig. 3.4*; *Figs 5.7 & 5.15*) may identify a short cut thrust offsetting a domed thrust sheet rather than a thrust fault of major displacement. In the study area, e.g. on the seismic profile A82-LT-25 (*Fig. 5.16*), the Moonie Fault (*sensu stricto*) is seen to root onto the upper imbricate of a horse structure situated to the west of the Moonie Fault ramp and, as seen on the seismic profile A82-LT-24 (*Fig. 5.4*), to the east of the synthetic thrusts that may be identified in the foot-wall sequence. The occurrence of imbricates forming a horse is dependant on the tectonic processes within the foreland-fold thrust belt and may influence the intensity of the aeromagnetic anomaly signals (see *Fig. 6.1*, cf. A82-LT-24 and A82-LT-25). As the shallow seismic lines (4 s TWT) do not show any evidence for intrusive rocks being emplaced at the base of the Moonie thrust (as proposed for the Mooki thrust to the south of the study area; RAMSAY & STANLEY, 1976), the cause for the Moonie magnetic anomaly seems to be more likely located near the thrust ramp within the sedimentary succession (see **Chapter 4.4**). Which part of the sedimentary succession causes the asymmetric magnetic anomaly high along the Moonie Fault stays speculative (for A82-LT-20 and A82-LT-24, different depths were calculated for the causing magnetic anomaly along the thrust ramp; see **Chapter 4.2.2.2**). However, on the BMR84.14 reprocessed data, noise of uncertain cause can be seen on the seismic record at a depth beneath *c.*4000 ms TWT (*c.*10+ km depth) (see “noise” on *Fig. 5.20*).

Reactivation of faults

The reactivation of the Moonie Fault, with the fault tip propagating into the Surat Basin succession and the uplift of the Surat Basin on the hanging-wall side of the fault relative

to the footwall (cf. *Fig. 3.4*), is restricted to the area immediately west of the Texas Orocline (and cannot be observed in the anomalously wide region to the north that is depicted by the BMR84.14 survey; *Fig. 5.20*). Thus, the contractional forces that effected the reactivation of faults during the early Late Cretaceous Moonie Event seem to be related to the spatial distribution of the Tamworth Belt succession, showing the effect on the fore-arc basin unit in the south where it is narrow and steeply inclined. Here, the mechanism that initiated earlier fault structures generally seems to be camouflaged by the above mentioned Goondiwindi event and the earlier discussed Mid Permian deformational phase, which negatively influences the palinspastic restoration of the geometric relationships that once initiated the thrust-development within a compressional tectonic regime.

Faults of major importance

The deep seismic survey BMR84.14 was shot at the northern end of the Moonie Fault (for location see *Fig. 3.1*), to the north of the study area. On the reprocessed part of the profile (upper 6 s TWT) the Moonie Fault has less influence on the overall subsurface geometry than seen on the investigated shallow seismic profiles farther south (compare *Fig. 5.20* with *Fig. 5.4*). The characteristic west-directed thrust sense for the Moonie Fault is expressed mainly by folding of the hanging-wall sequence (*Fig. 5.20*) than by a distinctive vertical and horizontal displacement as to be seen on various seismic profiles within the study area (cf. *Fig. 5.4*). On the BMR84.14 seismic profile, the fault offsets the base of the Burunga Formation (*B60*) with a maximum of vertical displacement of c.400 metres on the seismic profile (200 ms in *Fig. 5.20*), and has been removed by erosion in the Late Triassic to the east of the Goondiwindi Fault equivalent (*Fig. 5.20*). Moreover, the - subhorizontal - fault beneath the above mentioned duplex structure (see *FB* on *Fig. 5.20* at c.3500 ms) is recognised as the more important fault structure relevant to the subsurface geometry of the Tamworth Belt succession. This fault is considered to be the equivalent of the *FB* horizon that is identified to the south. Furthermore, the fault may be identified as the foot-wall ramp of the Moonie thrust sheet and may be connected with fault structures to the west of the Moonie Fault that are noted on various seismic profiles within the study area (*Figs 5.4 & 5.14*). The fault is interpreted as part of the westward-propagating thrust belt, with the Leichhardt Fault most likely to be the westernmost extension of the fore-arc basin sequence, approxi-

mately 33 kilometres farther to the west of the Moonie Fault (where the Leichhardt Fault cuts *S10* on the deep seismic survey at SP c.12650). This is not displayed on the seismic profile within the study area, but occurs farther to the west (see *Fig. 5.1*).

Earlier in this study, the author identified at least one of the Tamworth Belt seismic reflections to the west of the Moonie thrust (*HA*). Discussing the overall tectonic architecture of the subsurface Tamworth Belt, this may result in the Moonie Fault (*sensu lato*) being the trailing fault and the Leichhardt Fault the leading thrust fault, forming the westernmost boundary of the Tamworth Belt succession. Another explanation is that these faults are all part of one fault system with the individual faults separated by relay zones. The western extent of the fore-arc basin, however, lies far to the west of the study area, but probably is bounded by the Leichhardt Fault, a thrust fault that seems to root onto the same thrust flat at depth as the Moonie Fault farther to the east.

A major westward-dipping structure forms the eastern margin of the subsurface Tamworth Belt. The reprocessed Millmerran seismic data (*Fig. 5.19*) including the aeromagnetic anomaly database (*Figs 4.1, 4.6 & 4.8*) clarifies, that the “*c*₂” fault is the boundary between the fore-arc basin to the west and the accretionary wedge to the east.

A second thrust sheet is identified

The *FA*-seismic reflection, as seen farther south in the study area, can be interpreted as the thrust plane which separates the adjacent Tamworth Belt sheets, representing the roof thrust of the Moonie thrust sheet (*Figs 5.4, 5.5, 5.19 & 5.20*). The location of its root zone is unknown, but on seismic line BMR84.14 it may be traced to lie far to the east of the identified duplex (*Fig. 5.20*). The shaded areas on WOODWARD’s (1995) cross-sections highlight a similar scenario for the exposed Tamworth Belt to the south of the study area, with thrust sheets sliding on top of each other (*Fig. 5.21*).

Subsidence history or tectonic evidence?

Three trapezoidal shaped bodies were identified on the Millmerran seismic reflection profile at c.3000 - 3700 ms TWT (faults beneath “*f*” on *Fig. 5.19*). These seismically imaged bodies as seen on the profile may be interpreted depending on the postulated idea of origin.

The mechanism that affected the foreland thrust belt during times of contraction gives tectonic evidence. In the thrust-fold system, the faults can be explained to be the result of a possible solution to the room problem. On the Millmerran seismic profile, the author postulated that their seismic reflection pattern identifies duplexes, with the major westward-dipping fault (“ c_2 ” on *Fig. 5.19*) representing the basal thrust.

A different, speculative explanation for the trapezoidal shape of the seismically imaged body, however, may be given by the basin history itself, asking for basal shearing (cf. faults beneath “ f ” on the reprocessed data of *Fig. 5.19*) at the base of the fore-arc basin.

However, a final explanation for the faults above the basal thrust (“ f ” above “ c_2 ” on *Fig. 5.19*) that continues to the east, to become the northern extension of the Peel Fault, cannot be stated because of the highly deformed succession above the structures and the depth they occur (c.7 km to c.12 km, *Fig. 5.19*).

Configuration of the Tamworth Belt related to its evolution - a hypothesis

As the subsidence history of fore-arc basins is generally very complicated - i.e. there are specific variations in the configuration of fore-arc basins - it stays uncertain, which type of fore-arc basin the Tamworth Belt has to be categorised in. Three major questions can be raised about the tectonic history of the fore-arc basin succession in the

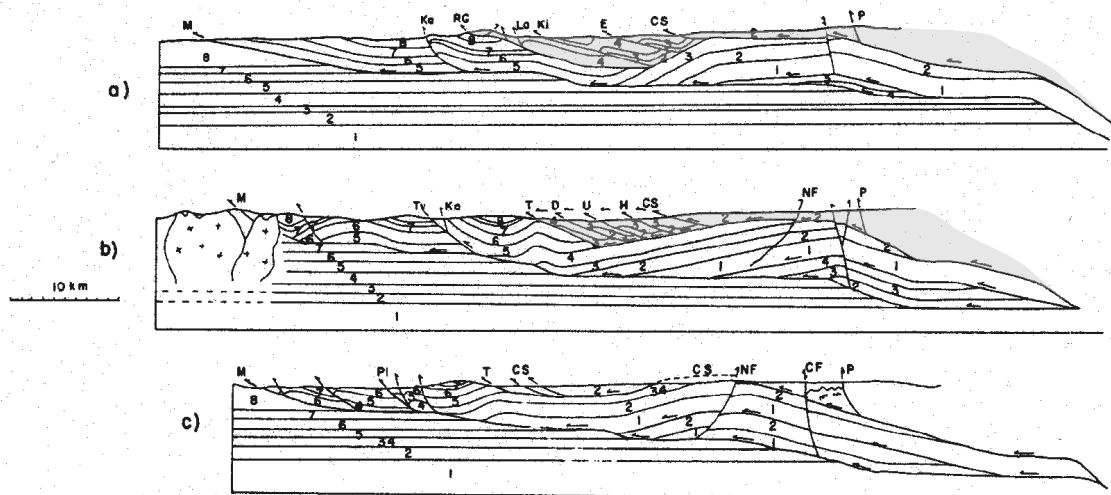


Fig. 5.21: Three balanced cross sections across the northernmost exposed part of the Tamworth Belt in northern NSW (after WOODWARD, 1995). The cross sections are displayed in latitudinal order, with (a) located to the north, (c) to the south and (b) in between. The thrust marked as “ M ” and located to the west depicts the Mooki Fault, the New South Wales-thrust fault equivalent to the Moonie Fault in southern Queensland (cf. *Fig. 3.1*).

subsurface in southern Queensland: (1) what were the original characteristics of the fore-arc basin type, (2) where is the accommodation space that is needed for the proposed thickness and (3) how can the absence of the volcanic arc be explained?

The following scenario may explain the overall thrust-related geometry that is seen throughout the investigated area. (1) A ridged fore-arc basin configuration at a later basin stage (and here to the eastern end of the Tamworth Belt) may have developed on top of the accretionary wedge in a back-tilted fore-arc regime (see *Fig. 5.22*). This scenario would (2) accumulate sediments of substantial thickness during basin evolution whilst the sedimentary fill may become deformed stronger as seen in the study area and (3) explain the “missing arc” as the volcanic arc may have been submerged below sea level. Moreover, this scenario could create an initial position of the fore-arc basin and the back-arc basin sediments at which the two basin successions could have been pushed on top of each other during times of contraction and thus explaining the apparently conformable behaviour between the Bowen Basin and Tamworth Belt successions farther to the west (that is, the volcanic arc would not need to be a “physical barrier” that separates Bowen Basin sediments from Tamworth Belt sediments).

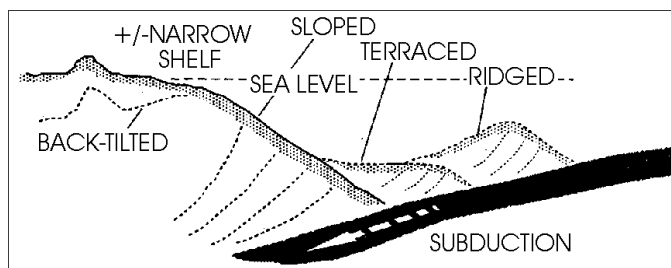


Fig. 5.22: Cartoon showing the configuration of a fore-arc basin related to its evolution, depicting a ridged basin type (from EINSELE, 2000).

5.5.1. Structural Geometry – conclusion

The configuration of the original Tamworth Belt fore-arc basin related to its evolution stays subject to speculation.

However, the apparently conformable behaviour between the Tamworth Belt and the Bowen Basin sequences can - at least in parts - be explained by the thrust tectonic processes that occurred during three deformational events. The *FA*-thrust horizon is interpreted to have transported the Bowen Basin and Tamworth Belt successions with westward-directed movement by sliding on top of the Moonie sheet. The back-arc ini-

tiated Bowen Basin originally extended farther to the east than its recent position suggests. The fore-arc Tamworth Belt continues in the subsurface beneath the foreland positioned Bowen Basin system to the west of the Moonie Fault and hence is not bounded to the west by the Middle Triassic thrust fault. The western extent of the fore-arc basin unit is probably bounded by the Leichhardt Fault (*Fig. 3.1*), a thrust fault that is interpreted on the new BMR84.14 seismic data (see **Chapter 5.5.**) to root onto the same thrust flat at depth (“*FB*” at the western end on *Fig. 5.20*).

The question, which tectonic processes left the Bowen Basin in a foreland position cannot be answered here. However, as the author can not rule out the possibility that the sequence above the *HA* seismic horizon depicts oldest Bowen Basin sediments, this - on reflection truncation geometries based - *HA* horizon may be considered to be the possible equivalent to the *B15* seismic reflection of the Bowen Basin (as defined by TOTTERDELL *et al.*, 1995) (see **Chapter 3.2.3.**). Moreover, the *FA* seismic reflection depicts a pronounced angular relationship between the Moonie sheet and the sedimentary succession above the *FA* reflection, identifying a second thrust horizon above the *FB* basal thrust. Thus, the *FA* thrust plane may be considered to identify a thrust of major importance that may have transported the back-arc Bowen Basin succession with westward-directed movement on top of the fore-arc basin unit.

Die Hauptschwierigkeit der Geologie beruht auf der Ansicht;
darauf nämlich, daß man das Atomistische und Mechanische,
welches in gewissen Momenten freilich sich wirksam erweist,
solange als möglich zurückdrängt,
dem Dynamischen dagegen, einem gesetzmäßig bedingten Entstehen,
einem Entwickeln und Umgestalten,
sein Recht gibt.

Johann Wolfgang Goethe

6. SYNTHESIS

The tectono-stratigraphic evolution of Eastern Australia during Silurian to Carboniferous times involves the subduction of the Panthalassan Ocean plate beneath the eastern margin of Gondwanaland. This was accompanied by the development of a series of subduction-related sedimentary basins, where individual basin stratigraphy was strongly influenced by the ongoing orogenic activity. Such changes included possible conversion from an island arc to continental margin arc subduction system (KORSCH *et al.*, 1997) or reversals in subduction polarity (AITCHISON & FLOOD, 1995) from Late Devonian to Late Carboniferous.

In the Early Permian, the region was subjected to oroclinal bending producing the Texas and Coffs Harbour oroclines, which resulted in the development of a complex structural pattern. As noted above, the study area is located immediately to the west of the Texas Orocline. Thus, the development of the Tamworth Belt was influenced both by the initial period of subduction-related activity (which included basin formation and infill) and subsequent tectonic deformation during oroclinal bending. The study area with its location adjacent to the oroclinal bend is, therefore, of key interest in elucidating both the pre-deformation history of the area, and the nature of later tectonic activity.

Initiation of the fore-arc succession

Initial formation of the Tamworth Belt fore-arc basin began in the Late Devonian (*Table 2.1*). The precise dimensions and extent of the original basin are uncertain, however, due to subsequent tectonic deformation and sequence repetition by thrusting (see **Chapter 5.3.4.**). LEITCH (1975) suggested

for the Tamworth Belt a possible length of c.400 km and a width of c.50 km. The total length of the fore-arc basin including both, the Tamworth and the Yarrol Belt must be at least 1000 km (see *Fig. 2.2*), which is considerably larger than values obtained for current fore-arc basins (see DICKINSON, 1995). Fore-arc basin environments are extremely complex and variable both in terms of the basin architecture and the infill pattern (see DICKINSON, 1995), who recognises a range of morphological types (DICKINSON, 1995, figure 6.4). The limited Tamworth Belt database precluded the recognition of any specific morphology.

A ridged fore-arc basin configuration (see *Fig. 5.22*) at a later basin stage, however, may explain the apparently conformable behaviour between the Tamworth Belt fore-arc basin and the Bowen Basin sequences. Following up this hypothetical scenario, the potential basin configuration may have developed on top of the accretionary wedge in a back-tilted fore-arc regime, that is, the volcanic arc would not need to be a “physical barrier” that separates Bowen Basin sediments from Tamworth Belt sediments (see **Chapter 5.5**).

Age control

Precise dating of the sequences in the study area is difficult since palynological control is sparse, and provided by only a few drill core samples across the entire region (see **Chapter 3.2.2**). The oldest palynoflora dated is Visean in the Early Carboniferous (DE JERSEY, in MURRAY, 1994), confirming the correlation with the exposed Tamworth and Yarrol belts. Palynological samples from five wells to the west of the study area have been dated as Late Carboniferous to earliest Permian (MURRAY, 1994). These are equivalent to the uppermost parts of the exposed belts. In three other wells (pers. comm. MCKELLAR, 1998), the palynoflora was dated as Early Permian (APP2.1 stage of PRICE, 1997, see *Table 2.1*), which provides a correlation with the sequence at the base of the Bowen Basin (cf. Supersequence A in *Table 2.1*, defined by BRAKEL *et al.*, in press; KORSCH *et al.*, 1998).

In the Bowen Basin, *Supersequence A* occurs immediately below the *B30* sequence boundary, implying that the seismic sequence in the subsurface Tamworth Belt between *B30* and reflector *HA* is its equivalent (*Table 2.1*) (cf. **Chapter 3.2**). Nevertheless, the stratigraphic relationship between the Supersequence A section and the upper-

most Tamworth Belt succession is unclear as no seismic lines tie the two successions. Unfortunately, interpretation of well information associated with the grid of seismic lines across the eastern Surat Basin did not provide further estimates of the ages of the sequences as the base of the Bowen Basin that has been identified on some of the seismic profiles to the west of the study area - the seismic reflector *B15* (cf. TOTTERDELL *et al.*, 1995; BRAKEL *et al.*, in press) - could not be picked within the reflective package that underlies *B30*.

Comparison with previous studies

The concealed Tamworth Belt has been deformed by a series of major thrust faults, most of which appear to be westward-directed, and probably form part of a westward-propagating foreland thrust belt (*Figs 5.4, 5.5, 5.6, 5.7, 5.14 & 5.15*). Based on the interpretation of the seismic profile network in the investigated area, the thickest vertical succession of the Tamworth Belt is situated between the Moonie Fault to the west and the northern extension of the Peel Fault to the east. However, the western boundary of the Tamworth Belt is not defined by the Moonie Fault. Fore-arc basin sediments were also deposited to the west of this structure but are now mainly deeper than the seismic resolution (see *Figs 5.4, 5.14 & 5.16* where the uppermost reflectors can be traced west of the fault). Due to the shallow character of the seismic profile network (most surveys were shot down to 3 s TWT), the basement is not always clearly imaged within the Tamworth Belt itself (see *Figs 5.5, 5.7, 5.8, 5.9 & 6.1*). Thus, the elaborated distribution of structures illustrates the broad, rather than the detailed basin trend.

The overall geometry in the study area is best seen on the longest composite seismic cross section (66 km) perpendicular to the subsurface Tamworth Belt (*Fig. 6.2*). It is completed by two deep seismic surveys to the north and to the south of the study area. In the vicinity of seismic line A82-LT-24, in the hanging-wall of the Moonie Fault, the sedimentary succession is folded into an anticline-syncline pair (see also seismic lines of *Figs 3.7 and 5.7*) with the crest of the anticline being planed off by subsequent erosion. Farther east, on seismic line H82-T-109, the Tamworth Belt succession dips moderately to the west and forms the eastern limb of the syncline, being interrupted by a west-directed thrust with minor vertical displacement (*Fig. 5.5*). On the eastern side of the belt, a series of minor eastward-dipping thrusts appear to be backthrusts which sole onto a major west-

ward-dipping fault, with the amount of displacement on the backthrusts decreasing to the west (*Figs 5.6 & 5.19*). Farther north, on the reprocessed deep seismic line BMR84.14, an eastward-dipping fault (SP c.13840 on *Fig. 5.20*) may be taken to track the westernmost back-thrust that hits the base of the Surat Basin on the Millmerran profile (“a” on *Fig. 5.19*, cf. *Fig. 6.1*). The overall geometry of the subsurface Tamworth Belt in the study area is similar to that seen on the deep seismic line BMR91.G01 in the Bogabri-Manilla area (GLEN *et al.*, 1993; KORSCH *et al.*, 1993, 1997) (*Fig. 4.2*; see *Fig. 3.1* for location) and on geological cross sections (see *Fig. 21*) from the same region (LIANG, 1991; GLEN & BROWN, 1993; WOODWARD, 1995).

Comparison with previous studies – assigning of structural units

The fault-bend fold in the hanging-wall of the Moonie Fault (*Figs 3.4, 3.5, 3.6 & 5.7*) is similar to the ramp anticline forming the Tulcumba Ridge, as described by LIANG (1991), whereas the hanging-wall syncline (*Figs 5.7, 5.8*; see *Fig. 6.1 & 6.2*) is equivalent to the Rocky Creek Syncline seen in the deep seismic profile BMR91.G01 (KORSCH *et al.*, 1997, fig. 4) and to the Belvue Syncline in the cross-section of LIANG (1991). The westward-dipping east-limb of the asymmetric syncline that has been identified within the study area, however, tends to widen as we approach the southern part of the investigated area (cf. *Figs 3.5 & 3.7*). Farther east, the eastward-dipping faults in the Millmerran profile appear to be in the same structural position and equivalent to the Baldwin Fault in BMR91.G01 (*Fig. 2.3*) (KORSCH *et al.*, 1997, figure 3).

Comparison with previous studies – major faults

Two major westward-dipping faults can be identified within the study area, and the westerly structure appears to die out just to the northeast of the investigated area at a latitude of approximately 27° 20'S (*Figs 3.6 & 4.4*). This may be due to the stronger influence of the oroclinal bending to the east. The cross sections constructed by LIANG (1991) and WOODWARD (1995) invoke an eastward-dipping thrust system associated with the eastern limit of the Tamworth Belt, whereas the seismic sections of this study suggest that this boundary is defined by a major westward-dipping fault zone, reaching a depth of at least 3.5 s TWT (approximately 11 km) (c_1 and c_2 on *Fig. 5.19*) (see also KORSCH *et al.*, 1997).

The BMR84.14 deep seismic line (*Fig. 5.1*; for location see *Fig. 3.1*) imaged a prominent series of mid-crustal reflections at a depth of *c.*20 km with westward-dipping orientation (KORSCH *et al.*, 1997). MURRAY (1997c), with respect to depth and dip of the strata, questioned whether this seismic marker represented the detachment surface along which movement of the fore-arc succession took place. Within the study area, however, thrusts that developed at the eastern boundary of the subsurface Tamworth Belt form a major westward-dipping fault zone (c_1 and?) c_2 on *Fig. 5.19*) that may continue to greater depth (see KORSCH *et al.*, 1997). This fault zone can be interpreted to root onto the mid-crustal reflections as indicated by FINLAYSON *et al.* (1990). Nevertheless, the precise character of this fault zone is uncertain due to the sparse seismic data and its poor quality within the eastern part of the investigated area (*Fig. 3.3*).

Comparison with previous studies – the youngest fore-arc basin seismic reflection

During this study, the uppermost Tamworth Belt seismic reflection *HA* was traced on the seismic profiles to be conformably overlain by the *B30* horizon with over one kilometre of section between the two reflections (*c.*400 ms TWT = *c.*1200 m on seismic line A82-WR-21, *Fig. 3.7* and *c.*450 ms TWT = *c.*1350 m on seismic line H82-T-109, *Fig. 5.5*). In the lithological record for the Deep Crossing well (**Chapter 3.2.2.**), ADAMSON & DORSCH (1988) did not identify any rocks of the Early Permian Back Creek Group (*c.*280-259 Ma; cf. *Table 2.1*), leaving their lithostratigraphic equivalent to the *HA* seismic reflection (Block I) to be of Earliest Permian age (pre-280 Ma) if not Late Carboniferous (*Fig. 3.12*, *Table 2.1*). Hence, the author can not rule out the possibility that the sequence above the *HA* horizon depicts oldest Bowen Basin sediments, that is, the *HA* Tamworth Belt seismic reflection may be considered to be the possible equivalent to the *B15* seismic reflection of TOTTERDELL *et al.* (1995).

Comparison with previous studies – eastern boundary

The eastern boundary of the Tamworth Belt, the Peel Fault in New South Wales, is known to dip steeply to the east at the surface. On the deep seismic line BMR91.G01 (*Fig. 2.3*; for location see *Fig. 3.1*) the fault is interpreted as an east-dipping splay off a major west-dipping structure that corresponds with a mélangé zone of serpentinite and re-

lated mafic igneous rocks and extends to the base of the crust (KORSCH *et al.*, 1993, 1997). This would suggest that the entire Tamworth Belt has been thrust eastwards over rocks of the accretionary wedge.

In the subsurface, in southern Queensland, the curved magnetic (*Fig. 4.8*) and gravity anomaly (*Fig. 4.10*) represents the northern continuation of the fault (see also WELLMANN, 1990). Evidence for the fore-arc basin succession having been influenced by thrust faults is here given by the seismic record of the seismic reflection profiles mentioned in the geometry chapters of this thesis (*Figs 3.4, 5.7, 5.15 & 5.20*; cf. *Fig 6.2*), identifying the Moonie thrust sheet with its base, the *FB* seismic horizon, and its top, the roof thrust that may be picked as the *FA* seismic horizon. The interpretation of these seismic profiles postulates a westward-directed transport of the Moonie thrust sheet for at least 10 kilometres.

Comparison with previous studies – western boundary

The western boundary of the Tamworth Belt is commonly described as being represented by the Goondiwindi-Moonie Fault (MURRAY, 1997c). As seen on the seismic profiles BMR84.14 (*Fig. 5.20*), M7803 (*Fig. 5.15*) and A82-LT-25 (*Fig. 5.16*), however, it is more likely that sediments of the Tamworth Belt continue farther to the west of the Moonie fault system, with at least the two seismic horizons *HA* and *HB* being identified beneath the Bowen Basin seismic horizons (*Figs 5.4 & 5.14*). ELLIOTT (1993, *Fig. 12*) noted a fundamental change in structural style towards the northern end of the Moonie Fault. To the south, he postulates basement rocks being thrust westwards over the Taroom Trough, whereas to the north, Taroom Trough sediments have been thrust eastwards over basement along back-thrusts that are related to large-scale duplex structures. It is at the northern end of the Moonie Fault, where the deep seismic survey BMR84.14 was shot by Geoscience Australia. The upper 6 s TWT that have been reprocessed and displayed in this study, suggest a major duplex structure with westward thrust movement (*Fig. 5.20*).

On the deep seismic survey BMR84.14 WAKE-DYSTER *et al.* (1987) and KORSCH *et al.* (1997) recognised the westernmost fore-arc basin boundary to be the Leichhardt Fault to the west of the Moonie Fault. The occurrence of at least two Tamworth Belt sequences to the west of the Moonie Fault, described in this study, used the information given by a number of industry shallow seismic data to link the fault behaviour from the

narrow fore-arc basin geometry in the southern study area (*Figs 5.7, 5.8*) to the anomalously wide basin architecture to the north of it (*Fig. 5.20*). The interpretation here of the reprocessed BMR84.14 seismic data supports WAKE-DYSTER's and KORSCH's interpretation (see **Chapter 5.4.2.**, *Fig. 5.20*).

Comparison with previous studies – overall geometry

In the vicinity of seismic line BMR91.G01, the intensity of deformation within the Tamworth Belt increases eastwards towards the Peel Fault, while surface studies have indicated that cleavage development also increases markedly (DURNEY & KISCH, 1994). This eastward increase in deformational intensity, together with a concomitant steepening of the structures, is the probable explanation for the decrease in the quality of the seismic data seen on both lines BMR91.G01 and BMR86.M01 (*Fig. 5.19*).

The interpretation of the seismic profiles in the southern part of the study area postulates a westward-directed transport of the Moonie thrust sheet (*Figs 5.8 & 5.15*). Farther south, in the vicinity of the deep seismic line BMR91.G01 (*Fig. 5.2*), the Tamworth Belt forms

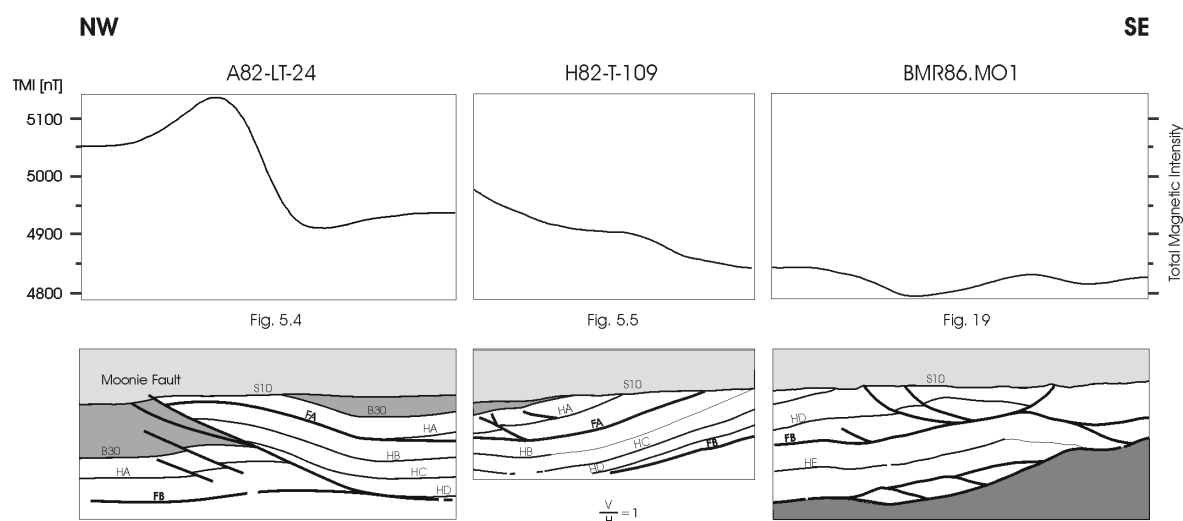


Fig. 6.2: Cartoon of the composite seismic cross-section across the subsurface Tamworth Belt in southern Queensland. Heavy solid lines represent interpreted faults. The light solid lines represent interpreted seismic horizons. HA, HB, HC, HD and HE separate the recognised Tamworth Belt seismic sequences and are within the fore-arc basin succession.

The overlying Jurassic to Cretaceous Surat Basin succession is marked in light grey. Shown in grey and located beneath the Surat Basin and above the Tamworth Belt succession is the Bowen Basin succession. The accretionary wedge assemblage is located to the SE of the composite cross-section and is highlighted in dark grey. Above it, a westward dipping major fault (c_2 on the seismic profile BMR86.MO1, *Fig. 5.19*) identifies the eastern boundary of the Tamworth Belt in the subsurface in southern Queensland.

part of a doubly vergent orogen, with its western side being thrust to the west and its eastern side being thrust to the east at the same time (pers. comm. KORSCH, 2004).

– *overall geometry: width and shortening*

From south to north, the Tamworth Belt shows great variability in its width, ranging from over 90 km in the far south, to only about 25 km near the border between Queensland and New South Wales (*Fig. 1 & Fig. 4.8*).

In the subsurface, in the vicinity of the composite seismic cross-sections (as described in **Chapter 3.1.2.**), the belt is just over 75 km wide, and it is here estimated (geometrical reconstruction of the composite cross section based on the interpreted seismic faults) that, across the belt, there has been a minimum of at least 10 km (*c.14%*) of shortening due to thrust movement along the Moonie thrust. The existence of the *FA* thrust plane (*Figs 5.8, 5.9, 5.15*) and footwall horses beneath the Moonie thrust sheet (*Fig. 5.19*) suggests at least another 25 km (*c.33%*) of shortening. Therefore the total estimated amount of shortening across the Tamworth Belt has been at least ~35 km (~44%).

In the southern part of the study area, the width of the belt is just over 50 km, very similar to the width where seismic line BMR91.G01 crosses the belt (see *Fig. 3.1* for location). In that area, LIANG (1991) estimated that the belt had been shortened by 25% (*c.12.5 km*). LIANG's result is significantly less than the 48% (75 km) shortening determined by WOODWARD (1995) in the vicinity of BMR91.G01. Woodward (1995) showed much greater complexity in his balanced cross sections (see *Fig. 5.21*), including a series of footwall horses in his section closest to BMR91.G01.

– *overall geometry: thrust-related structures*

On the reprocessed seismic profile BMR84.14, a snakehead duplex structure (as defined by HATCHER, 1995) is recognised beneath the domed Moonie thrust sheet. This seismic feature, perhaps, may be linked to a distinct magnetic high farther south (“*d*” on *Fig. 4.8*). Hence, the observed magnetic high depicts a domed thrust sheet above a thrust-related structure. The base of the thrust sheet may be traced southwards into the seismic study area, where it defines the base of the Moonie thrust sheet. However, within it, the precise location of the Tamworth Belt seismic reflections *HD* (older) to *HA* (younger) stays uncertain and can not be linked precisely to the reflections that have been identified within the study area.

The horses that have been interpreted on the Millmerran seismic profile (*Fig. 5.19*) and the snakehead duplex on the reprocessed upper 6 s TWT of deep seismic survey BMR84.14 (*Fig. 5.20*) indicate that the tectonic history of the Tamworth Belt is much more complex than WARTENBERG *et al.* (2003) had proposed. They proposed a fault-bend-fold in the hanging-wall sequence with a ramp to the east of the Moonie Fault associated with the geometrical room problem.

– *overall geometry: status of the Moonie Fault*

The seismic data in the investigated area suggest that the enormous vertical displacement of the Moonie Fault (e.g. *c.*3000 m, which equals *c.*1000 ms TWT in *Fig. 3.4*) may possibly be explained by the *FA* thrust sheet overriding the Moonie thrust sheet, recognising the tip line of the Moonie Fault as a short cut thrust (see **Chapter 5.4.2**). Moreover, the Moonie short cut thrust - in some seismic profiles - roots on to the upper of a total of two imbricates that cause the simple-step fault-bend fold in the hanging-wall sequence to the east of the Moonie Fault (*Fig. 5.16*). This broadens the understanding of the cause for the fault-bend fold with the easiest explanation being a flat-ramp geometry on a single thrust (see *Fig. 5.3*). However, the identification of two thrust sheets stapled upon each other (*Figs 5.4, 5.5, 5.8, 5.15 & 5.16*) improves the argument of WARTENBERG *et al.* (2003). Facing the offset on either side of the Moonie thrust, they asked for a tectonic ramp to the east of the Moonie Fault to explain the distinct vertical displacement of the fault itself (with *B30* to the west being adjacent to *HC* on the east side of the Moonie Fault).

– *overall geometry: the subsurface Bowen Basin – an indicator for thrusting*

Thin-skinned thrust deformation occurs throughout the study area, as seen within the defined seismic Bowen Basin and Tamworth Belt sequences. For the Bowen Basin further north, in central Queensland, FIELDING *et al.* (1997a) define the time span of thin-skinned thrust deformation at around 235-230 Ma, terminating the Bowen Basin sediment accumulation. KORSCH *et al.* (1998) identified the period of deformation from 265 to 230 Ma. This time span also identifies the deformational event of major importance within the study area.

The presence of Bowen Basin sequences in the hanging-wall sequence to the east of the main basin suggests that the original area covered by the basin extended

much farther to the east than its present limits (*Figs 5.4 & 5.8*). On the deep seismic survey BMR84.14, Triassic sequences occur *c.*70 km to the east of the Moonie Fault within the Cecil Plains Syncline (*Fig. 5.1*). The interpretation of the seismic data of this study suggests that these Triassic sediments may be a remnant of the - elsewhere eroded - Triassic unit within a synclinal upper part of the broad and slightly folded thrust sheet (cf. seismic reflectors beneath *S10* at the eastern side of the reprocessed data – *Fig. 5.20*) and thus part of the west-directed thrust system. Due to the tectonically unusual location of BMR84.14 to the north of the Texas Orocline and due to the sparse seismic data in this area, however, it remains uncertain whether the Permian-Triassic conglomerates in the Horrane Trough (to the east of the BMR84.14 seismic profile) described by O'BRIEN *et al.* (1990) are involved in, and explained by, the same thrusting process.

– *overall geometry: a third deformational phase has been depicted*

Another deformational phase was depicted on various seismic profiles in the study area within the Moonie Fault hanging-wall sequence, offsetting Early to Mid Permian sediments. The observed faults do not influence Late Permian and Early Triassic sequences and therefore may be interpreted to describe a period of compressional deformation at around 265-250 Ma. During this time span, thrust faults developed that root onto the uppermost *HA*-Tamworth Belt horizon (*Fig. 5.17*) or onto the *FA*-roof thrust (*Fig. 5.4*). Most likely, this deformational phase occurred during Mid Permian times, tracing a distinct unconformity in the Bowen Basin beneath the seismic horizon *B45* which identifies the base of the *Oxtrack Formation* (cf. *Table 2.1*). To the north-west of the study area -and thus to the north-west of the Moonie Fault - evidence for this seismically distinct *B45* unconformity is best seen within the Denison Trough succession (for location, see *Fig. 1*), identifying the *Aldebaran Event*, dated 265-260 Ma (KORSCH, 2004).

As seen elsewhere in the study area, the Mid Permian faults – where being cut by the disconformably overlying Surat Basin sediments – slightly folded the *S10* seismic reflector, and thus identify the Late Cretaceous Moonie Event by reactivation of the thrust movement during a later phase of compression (see “a” in *Figs 5.6 & 5.18*).

Final statement

The arguments discussed above shall be used in an attempt to speculate on the nature and mechanics of the thrust-fold system within the study area and the overall thrust-mechanics that has led to the recent subsurface Tamworth Belt geometry. However, the outcome of this study highlights the need for further research on this matter to increase the understanding of the structural evolution not only of the Tamworth Belt concealed by Surat Basin sediments, but of the New England Orogen as a whole.

Alles ist, was es ist, weil es so geworden ist.

D'Arcy Thompson

7. CONCLUSIONS

1. Interpretation of seismic and aeromagnetic profiles within the study area, the eastern Jurassic-Cretaceous Surat Basin of southern Queensland, has led to an increase in the understanding of the geometry of the Devonian-Carboniferous Tamworth Belt which occurs beneath the younger sedimentary cover.

2. The succession in the Tamworth Belt is at least 12 km thick and is moderately folded. Within it, six seismic sequences have been identified. Each sequence is separated by a significant sequence boundary. Due to poorer resolution of the seismic data in the eastern part of the study area, it is likely that there are other sequence boundaries not imaged seismically.

3. The succession in the Tamworth Belt – which is part of a large foreland fold-thrust belt – has been subjected to large-scale thrusting, with the Moonie thrust sheet having been transported westwards for at least 8 kilometres.

4. In the vicinity of the seismic profiles, the subsurface Tamworth Belt is over 75 km wide. It has been shortened by at least 35 km. Its overall geometry is similar to that observed farther south in the exposed part of the belt, with an anomalous increase in the width of the belt across strike to the north. The major thrust movement was NW-directed.

5. Two major deformational events have been recognised, (a) the Mid-Late Triassic Goondiwindi Event and (b) the Late Cretaceous Moonie Event.

6. An early deformational phase has been identified, that occurred before the Goondiwindi- and the Moonie events,

most likely during Mid Permian times, tracing a distinct unconformity in the Bowen Basin and coinciding with the Aldebaran Event as seen in the Denison Trough to the west of the study area.

7. The Moonie Fault is interpreted as a short cut thrust with major displacement, with the Leichhardt Fault to the west possibly being the leading thrust fault of the overall north-south trending fault system along the western side of the Tamworth Belt.

8. The succession in the western part of the Tamworth Belt is truncated by the Moonie Fault, but continues farther to the west beneath the Bowen Basin. The western extent of the fore-arc basin in the footwall is likely to be bounded by the Leichhardt Fault. The strata in the Moonie thrust sheet have a classic fault-bend fold geometry, with a hanging-wall anticline-syncline pair occurring immediately to the east of the thrust. Farther to the east, the sedimentary package dips moderately to the west.

9. To the east, on the western side of the Texas Orocline, the boundary between the Tamworth Belt and the Tablelands Complex is defined by a major westward-dipping structure, with a series of eastward-dipping backthrusts located farther to the west.

10. In the hanging-wall, immediately to the east of the Moonie Fault and within the upper Tamworth Belt succession, a second thrust surface (referred to as *FA*) can be identified above the Moonie thrust sheet.

11. The aeromagnetic traverses along the seismic lines A82-LT-24, H82-T-109 and BMR86.M01 correlate, at least in part with the corresponding seismic profiles. Some of the magnetic responses, especially those of broad wavelength, can be explained by the geometry of the subsurface Bowen Basin and the underlying Tamworth Belt, although the Mesozoic sedimentary cover is up to 2000 m thick.

12. The Moonie Fault to the west coincides with an elongated magnetic high that continues for at least 200 km to the south. The cause of this positive anomaly is speculative.

13. The eastern boundary of the Tamworth Belt coincides with a gravity and magnetic ridge, mimicking the gravity and magnetic pattern of the Lower Devonian serpentinites and iron-rich rocks that occur along the Peel Fault to the south.

REFERENCES

- ADAMSON, M. & DORSCH, C. (1988): Final Well Report Deep Crossing 1. Sydney Oil Company (Canning) Pty. Ltd., Sydney, New South Wales, Australia.
- AITCHISON, J. C. & FLOOD, P. G. (1995): Gamilaroi terrane: a Devonian rifted intra-oceanic island-arc assemblage, NSW, Australia. In: SMELLIE, J. L. (ed) *Volcanism associated with extension at consuming plate margins*. Geological Society of London, Special Publications, **81**, 155 - 168.
- ALMOND, C. S. (1985): GSQ Chinchilla 4 - Preliminary Lithologic Log and composite Log, Record Series, **34**, GSQ.
- BMR (1976): Magnetic Map of Australia, residuals of total intensity, scale 1 : 2 500 000, Bureau of Mineral Resources, Geology and Geophysics, Canberra.
- BOYER, S. E.; ELLIOTT, D. (1982): Thrust Systems. In: *The American Association of Petroleum Geologists Bulletin*, Volume 66, No. **9** (September 1982), pp. 1196 - 1230, 34 figures, 2 tables.
- BRAKEL, A. T.; WELLS, A. T.; TOTTERDELL, J. M.; HOFFMANN, K. L.; SIMPSON, G.; DIXON, O. and NICOLL, M. G. (in press): Sequence stratigraphy and fill history of the Bowen Basin, Queensland, Geoscience Australia, Canberra.
- CAWOOD, P. A. (1983): Modal composition and detrital Clinopyroxene geochemistry of lithic sandstones from the New England Fold Belt (east Australia): a Paleozoic forearc terrane. *Geological Society of America Bulletin*, **94**, 1199 - 1214.
- CATUNEANU, O.; BEAUMONT, C. & WASCHBUSCH, P. (1997): Interplay of static loads and subduction dynamics in foreland basins: reciprocal stratigraphies and the 'missing' peripheral bulge. *Geology*, **25**, 1087 - 1090.
- CLOOS, H. (1936): Einführung in die Geologie. Gebrüder Borntraeger Verlag, 503 pp., 357 figures, 3 tables, Berlin.
- DAY, R. W.; WHITAKER, W. G. & MURRAY, C. G. (1978): The eastern part of the Tasman Orogenic Zone. *Tectonophysics*, **48**, 327 - 364.
- DAY, R. W.; WHITAKER, W. G.; MURRAY, C. G.; WILSON, I. H. and GRIMES, K. G. (1983): Queensland Geology, GSQ, Publication, **383**, 194 pp, Brisbane.
- DEPARTMENT OF MINERAL RESOURCES NSW (1986): unpublished WCR No. 225, detailed core log DM Bellata 1, Sydney.
- DEPARTMENT OF NATIONAL DEVELOPMENT, BUREAU OF MINERAL RESOURCES, GEOLOGY AND GEOPHYSICS (1964): U-K-A. Cabawin No. 1, Queensland, Union Oil Development Corporation, Kern County Land Company and Australian Oil and Gas Corporation Limited, *Petroleum Search Subsidy Acts*, **43**, Commonwealth of Australia.
- DEPARTMENT OF NATIONAL DEVELOPMENT, BUREAU OF MINERAL RESOURCES, GEOLOGY AND GEOPHYSICS (1964): Summary of Data and Results Surat Basin, Queensland, U-K-A. Burunga No. 1, Union Oil Development Corporation, Kern County Land Company and Australian Oil and Gas Corporation Limited, *Petroleum- Search Subsidy Acts*, **53**, C. of A..
- DERRINGTON, S. S.; GLOVER, J. J. E. & MORGAN, K. H. (1959): The names in Queensland stratigraphy. Permian of the southeastern part of the Bowen Syncline. *Australian Oil and Gas Journal*, **5** (8), 27 - 35.
- DICKINSON, W. R. (1995): Forearc basins. In: BUSBY, C. J. & INGERSOLL, R. V. (eds): *Tectonics of Sedimentary basins*. Blackwell Science, Oxford, 221 - 261.
- DICKINSON, W. R. & SUSZEK, C. A. (1979): Plate tectonics and sandstone compositions. *The American Association of Petroleum Geologists Bulletin*, **63**, 2164 - 2182.
- DICKINSON, W. R. ; BEARD, L. S. ; BRAKENRIDGE, G. R. ; ERJAVEC, J. L. ; FERGUSON, R. C. ; INMAN, K. F.; KNEPP, R. A.; LINDBERG, F.A. & RYBERG, P. T. (1983): Provenance of North American Phanerozoic sandstones in relation to tectonic setting. *Geological Society of America Bulletin*, **94**, 222 - 235.
- DIESSEL, C. F. K. (1992): Coal-bearing depositional systems, 721 pp., Springer, Berlin - Heidelberg - New York.
- DURNEY, D. W. & KISCH, H. J. (1994): A field classification and intensity scale for first-generation cleavages, AGSO Journal of Australian Geology and Geophysics, **15**, 257 - 295, Canberra.
- EINSELE, G. (2000): Sedimentary Basins - Evolution, facies and sediment budget. 792 pp., 354 figures, Springer, Berlin - Heidelberg - New York.
- ELLIOTT, L. G. (1993): Post-Carboniferous tectonic evolution of eastern Australia. *The APEA Journal*, **33**(1), 215 - 236.
- EMERY, D. & MYERS, K. J. (1996): Sequence Stratigraphy. 297 pp., (Blackwell), Oxford.

- ESSO EXPLORATION AUSTRALIA, INC. (1966): Well Completion Report, Mt. Pleasant No. 1., New South Wales.
- FIELDING, C. R.; GRAY, A. R. G.; HARRIS, G. I. & SALOMON, J. A. (1990): The Bowen Basin and overlying Surat Basin. *In: FINLAYSON, D. M. (ed.): The Eromanga – Brisbane Geoscience Transect: a Guide to Basin Development across Phanerozoic Australia in Southern Queensland*. Bureau of Mineral Resources, Geology and Geophysics, Canberra.
- FIELDING, C. R.; STEPHENS, C. J. & HOLCOMBE, R. J. (1997a): Permian stratigraphy and palaeogeography of the eastern Bowen Basin, Gogango Overfolded Zone and Strathmuir Synclinorium in the Rockhampton-Mackay region, central Queensland. *In: ASHLEY, P. M. and FLOOD, P. G. (eds): Tectonics and Metallogenesis of the New England Orogen*, Geological Society of Australia, Special Publication, **19**, 80 – 95.
- FIELDING, C. R.; STEPHENS, C. J. & HOLCOMBE, R. J. (1997b): Submarine mass-wasting deposits as an indicator of the onset of foreland thrust loading: Late Permian Bowen Basin, Queensland, Australia. *Terra Nova* **9**, 14 – 18.
- FINLAYSON, D. M. (ed.) (1990): *The Eromanga – Brisbane Geoscience Transect: a Guide to Basin Development across Phanerozoic Australia in Southern Queensland*. Bureau of Mineral Resources, Geology and Geophysics, Canberra, 10 – 116.
- FLOOD, P. G.; JELL, J. S. & WATERHOUSE, J. B. (1981): Two new Early Permian stratigraphic units in the southeastern Bowen Basin, Central Queensland. *Queensland Government Mining Journal*, **82**, 179 – 184.
- FOSTER, C. B. (1979): Permian Plant Microfossils of the Blair Athol coal Measures, Baralaba coal Measures, and basal Rewan formation of Queensland, GSQ, Publication 372, Palaeontological Paper **45**, Brisbane.
- FÜCHTBAUER, H. (1988): *Sedimente und Sedimentgesteine*. 1141 pp., 4. Auflage, (Schweizerbart) Stuttgart.
- GALLOWAY, W. E. & HOBDAI, D. K. (1983): *Terrigenous Clastic Depositional Systems, application to Petroleum, Coal, and Uranium Exploration*, 423 pp., Springer, Berlin – Heidelberg – New York.
- GIBBS, A. D. (1983): Balanced cross-sections in areas of extensional tectonics, *Journal of Struct. Geol.*, **5**, 153 – 160.
- GLEN, R. A. & BROWN, R. E. (1993): A transect through a forearc basin: preliminary results from a transect across the Tamworth Trough at Manilla, N.S.W. *In: FLOOD, P. G. and AITCHISON, J. C. (eds): New England Orogen, eastern Australia*, Department of Geology and Geophysics, University of New England, Armidale, 105 – 111.
- GLEN, R. A.; KORSCH, R. J. and WAKE-DYSTER, K. D. (1993): A deep seismic cross section through the Tamworth Belt: preliminary interpretation of 4 seconds two-way time data. *In: FLOOD, P. G. and AITCHISON, J. C. (eds): New England Orogen, eastern Australia*, Department of Geology and Geophysics, University of New England, Armidale, 101 – 104.
- GONZALEZ-MIERES, R. & SUPPE, J. (2004): Analysis of shortening in an active detachment fold, Nankai Trough – an introduction to “thickness-relief analysis”. GSA Conference, Denver.
- GRAY, A. R. G. (1975): Bundamba Group stratigraphy relationships and petroleum prospects, Queensland Government Mining Journal, **76**, 311 – 324.
- HARRINGTON, H. J. & KORSCH, R. J. (1985): Tectonic model for the Devonian to mid Permian of the New England Orogen. *Australian Journal of Earth Sciences* **32**, 163 – 179.
- HATCHER jr., R. D. (1995): *Structural Geology* (2nd ed.) – Principles, Concepts and Problems. Department of Geological Sciences, University of Tennessee-Knoxville and Environmental Sciences Division, Prentice Hall, Englewood Cliffs New Jersey 07632.
- HAYWARD, A. B. & GRAHAM, R. H. (1989): Some geometrical characteristics of inversion. *In: COOPER, M. A. & WILLIAMS, G. D. (eds.): Inversion tectonics: Geological Society of London, Special Publication* **44**, p. 17 – 39.
- HERLIHY, J. W. (1993): Summary of coal exploration by the Department of Mineral Resources in the Gunnedah Basin over the period 1974 - 1991, Dept. of Min. Res., Coal & Petr. Geol. Branch, Geol. Surv. of NSW.
- HERRMANN, F. A. (1964): Geology. *In: Union Oil Development Corporation (1964): Well Completion Report No. 30.*, Union-Kern-A.O.G. - Goondiwindi No. 1., Authority to Prospect P.E.L. 8, New South Wales.
- HOLCOMBE, R. J. & JELL, J. S. (1983): Geology of Cracow Station area. *In: Waterhouse, J. B. (ed): Field conference Permian of the Biloela-Moura-Cracow area (1983)*, Geol. Soc. of Australia, Queensland Div., Brisbane, 69 – 74.

- HOLCOMBE, R. J.; STEPHENS, C. J.; FIELDING, C. R.; GUST, D.; LITTLE, T. A.; SLIWA, R.; KASSAN, J.; MCPHIE, J. and EWART, A. (1997): Tectonic evolution of the northern New England Fold Belt: the Permian-Triassic Hunter-Bowen event. *In: ASHLEY, P. M. and FLOOD, P. G. (eds): Tectonics and metallogenesis of the New England Orogen*, Geological Society of Australia, Special Publication, **19**, 52 – 65.
- HOLMES, P. R. (1983): Preliminary Interpretation of stratigraphic bores GSQ Mundubbera 9, 10 and 11, Cracow Homestead Area, Record Series, **70**, GSQ.
- HOLMES, P. R. (1984): GSQ Taroom 16 - Preliminary Lithologic Log and composite Log, Record Series, **14**, GSQ.
- HUTTON, L. J.; WITHNALL, I. W.; BULTITUDE, R. J.; VON GNIELINSKI, F. E. & LAM, J. S. (1999): South Connors-Auburn-Gogango Project: Progress report on investigations during 1998. *Queensland Geological Record*, 1999/7.
- JENYON, M. M. & FITCH, A. A. (1985): Seismic Reflection Interpretation, second, revised edition, 172 fig., 4 coloured plates, Gebrüder Borntraeger, Berlin, Stuttgart. *In: AUSTEY, N. A. & O'BRIEN, P. N. S., Geoexploration Monographs*, series 1, No **8**, London.
- KASSAN, J. (1993): Basin Analysis of the Triassic Succession, Bowen Basin, Queensland, Department of Earth Sciences, unpublished PhD Thesis, University of Queensland.
- KIRKEGAARD, A. G. (1974): Structural elements of the northern part of the Tasman Geosyncline. *In: DENMEAD, A. K.; TWEEDALE, G. W. & WILSON, A. F. (Editors): The Tasman Geosyncline: A Symposium*. Geol. Soc. of Austr., Queensland Div., **47-62**, Brisbane.
- KORSCH, R. J. (1977): A framework for the Paleozoic geology of the southern part of the New England geosyncline. *Journal of the Geological Society of Australia*, **23**, 339 – 355.
- KORSCH, R. J. (1984): Sandstone compositions from the New England orogen, eastern Australia: Implications for tectonic setting. *Journal of Sedimentary Petrology*, **54**, 192 – 211.
- KORSCH, R. J. (2004): A Permian-Triassic retroforeland thrust system – The New England Orogen and adjacent sedimentary basins, Eastern Australia. *In: K. R. MCCLAY (ed.): Thrust tectonics and Hydrocarbon systems. AAPG Memoir* **82**, p. 515-537.
- KORSCH, R. J. & HARRINGTON, H. J. (1987): Oroclinal bending, fragmentation and deformation of terranes in the New England Orogen, eastern Australia. *In: LEITCH, E. C. & Scheibner, E. (eds.): Terrane accretion and orogenic belts*. Am. Geophys. Union Geodyn. Series, **19**, 129 – 139.
- KORSCH, R. J. & SCHÄFER, A. (1991): Geological interpretation of DEKORP deep seismic reflection profiles 1C and 9N across the Variscan Saar-Nahe Basin, southwest Germany.- *Tectonophysics*, **191**, 127 – 146, Amsterdam.
- KORSCH, R. J. & SCHÄFER, A. (1995): The Permo-Carboniferous Saar-Nahe Basin, SW Germany and NE France: basin formation and deformation in a strike slip regime.- *Geol. Rundschau*, **84**, 2, 293 - 318, Heidelberg.
- KORSCH, R. J. & TOTTERDELL, J. M. (1995a): Eastern margin of the Bowen- Gunnedah-Sydney Basin: Geometry of the Burunga-Leichhardt-Moonie-Goondiwindi-Mooki-Hunter fault system. *In: Geological Society of Australia, Specialist Group in Tectonics and Structural Geology, Field conference*, Clare Valley, Geological Society of Australia, Abstracts, **40**, 85 – 86.
- KORSCH, R. J. & TOTTERDELL, J. M. (1995b): Structural events and deformational styles in the Bowen Basin. *In: FOLLINGTON, I. L.; BEESTON, J. W. & HAMILTON, L. H. (eds): Bowen Basin Symposium 1995... 150 years on ... Proceedings*, Geol. Soc. of Australia, Coal Geology Group, Brisbane, 27 – 35, Mackay, Queensland.
- KORSCH, R. J. & TOTTERDELL, J. M. (1995c): Permian and Mesozoic tectonic and structural events in the Bowen and Surat basins and New England Orogen, Southwest Pacific Rim. *In: MAUK, J. L. & ST GEORGE, J. D. (eds): Proceedings of the 1995 PACRIM Congress*, Australasian Institute of Mining and Metallurgy, Publication **9/95**, 305 – 310.
- KORSCH, R. J. & TOTTERDELL, J. M. (1996): Mesozoic deformational events in Eastern Australia and their impact on onshore sedimentary basins. *Proceedings of the Mesozoic geology of the Eastern Australia Plate Conference*, Geological Society of Australia Extended Abstracts, **43**, 308 – 318.
- KORSCH, R. J.; HARRINGTON, H. J.; MURRAY, C. J.; FERGUSSON, C. L. & FLOOD, P. G. (1990): Tectonics of the New England Orogen. Bureau of Mineral Resources, Australia, Bulletin **232**, 35 – 52.

- KORSCH, R. J.; WAKE-DYSTER, K. D. & JOHNSTONE, D. W. (1992a): Seismic imaging of Late Palaeozoic - Early Mesozoic extensional and contractional structures in the Bowen and Surat basins, Eastern Australia.- *Tectonophysics*, **215**, 273 - 294, Amsterdam.
- KORSCH, R. J.; WAKE-DYSTER, K. D.; O'BRIAN, P. E.; FINLAYSON, D. M. & JOHNSTONE, D. W. (1992b): Geometry of Permian to Mesozoic sedimentary basins in Eastern Australia and their relationship to the New England Orogen. *In*: RICKARD, M. J. et al. (eds): *Basement Tectonics*, **9**, 85 - 108, Kluwer, Amsterdam.
- KORSCH, R. J.; WAKE-DYSTER, K. D. & JOHNSTONE, D. W. (1993): The Gunnedah Basin - New England Orogen deep seismic reflection profile: implications for New England tectonics. *In*: FLOOD, P. G. & AITCHISON, J. C. (eds): *New England Orogen, Eastern Australia*, Department of Geology and Geophysics, University of New England, NEO '93, conference proceedings, 85 - 100, Armidale, NSW.
- KORSCH, R. J.; JOHNSTONE, D. W. and WAKE-DYSTER, K. D. (1997): Crustal architecture of the New England Orogen based on deep seismic reflection profiling. *In*: ASHLEY, P. M. and FLOOD, P. G. (eds): *Tectonics and Metallogenesis of the New England Orogen*, Geological Society of Australia, Special Publication, **19**, 29 - 51.
- KORSCH, R. J.; BOREHAM, C. J.; TOTTERDELL, J. M.; SHAW, R. D. and NICOLL, M. G. (1998): Development and Petroleum resource evaluation of the Bowen, Gunnedah and Surat Basins, Eastern Australia, APPEA Journal, **38**, 199 - 237.
- LEITCH, P. C. & RYCE, C. L. (eds) (1975): Plate tectonic interpretation of the Palaeozoic history of the New England Fold Belt. *Geological Society of America Bulletin*, **86**, 141-144.
- Li, Z. X. & Powell, C. McA. (2000): Earth-Science Reviews. Tectonics Special Research Centre, Department of Geology and Geophysics, University of Western Australia, Nedlands WA 6907, Australia.
- LIANG, T. C. K. (1991): Fault-related folding, Tulumba Ridge, western New England, Australian Journal of Earth Sciences, **38**, 349 - 355.
- LYONS, P. C. & RICE, C. L. (eds) (1987): Palaeoenvironmental and tectonic controls in coal-forming basins of the United States, Geological Society of America Special Paper **210**, 208 pp., Boulder.
- MACKENZIE, W. S.; ADAMS, A. E. (1993): A Colour Atlas of Rocks and Minerals in Thin Section, 192 pp., Manson publishing, London.
- MACKENZIE, W. S.; GUILFORD, C. (1994): Atlas of rock-forming minerals in thin section, 98 pp., Longman Scientific & Technical, Essex.
- MACK JNR., J. E. & CAREY, A. (1962): Geology. *In*: Union Oil Development Corporation, Authority to Prospect 57P (1962): Well Completion Report No.6, Union-Kern-A.O.G. Burunga No. 1, Queensland.
- MCKELVEY, B. C. and MCPHIE, J. (1995): Tamworth Belt. *In*: DIAZ, C. M. (ed): *The Carboniferous of the World II: Australia, Indian Subcontinent, South Africa, South America and North Africa*. International Union of Geological Sciences Publication, **20**, 15 - 23.
- MCPHIE, J. (1987): Andean analogue for Late Carboniferous volcanic arc and arc flank environments of the western New England Orogen, New South Wales, Australia. *Tectonophysics*, **138**, 269 - 288.
- MCQUILLIN, R.; BACON, M.; BARCLAY, W. (1984): An Introduction to Seismic Interpretation (Reflection Seismics in Petroleum Exploration), Graham & Trotman, 2nd ed., London.
- MIALL, A. D. (1984): Principles of Sedimentary Basin Analysis, 490 pp., Springer, Berlin - Heidelberg - New York.
- MILLER, J. MCL. & GRAY, D. R. (1996): Structural signature of sediment accretion in a Palaeozoic accretionary complex, southeastern Australia. *Journal of Structural Geology*, Volume 18, No. **10**, 1245-1258.
- MITCHUM JR, R. M.; VAIL, P.R. & THOMPSON, S. (1977): The depositional sequence as a basic unit for stratigraphic analysis. *In*: PAYTON, C. E. (ed.): Seismic stratigraphy - applications to hydrocarbon exploration. *AAPG Memoir* **26**, 53 - 62.
- MINES ADMINISTRATION PTY. LTD (1963): Well Completion Report, Report No. Q/55 - 56 p 131, A. A. O. Arbroath No. 1 Well, Queensland.
- MURRAY, A. S.; MORSE, M. P.; MILLIGAN, P. R. & MACKAY, T. E. (1997): Gravity Anomaly Map of the Australian Region (Second Ed.), scale 1 : 5 000 000, Australian Geological Survey Organisation, Canberra.
- MURRAY, C. G.; FERGUSON, C. L.; FLOOD, P.G.; WHITAKER, W. G. and KORSCH, R. J. (1987): Plate tectonic model for the Carboniferous

- evolution of the New England Fold Belt. *Australian Journal of Earth Sciences*, **34**, 213 – 236.
- MURRAY, C. G.; SCHEIBNER, E. & WALKER, R. N. (1989): Regional geological interpretation of a digital coloured residual Bouguer gravity image of eastern Australia with a wave length cut-off of 250 km. *Australian Journal of Earth Sciences* **36**, 423 – 429.
- MURRAY, C. G. (1994): Basement cores from the Tasman Fold Belt System beneath the Great Artesian Basin in Queensland. Queensland Department of Minerals and Energy, Geological Record 1994/10, 96 pp.
- MURRAY, C. G. and the Yarrol Project Team (1997a): The Yarrol Project – increasing the prospectivity of the New England Orogen in the Rockhampton-Monto region, central coastal Queensland. In: BEESTON, J. W. (compiler), *Proceedings of the Queensland Development 1997 Conference*, Queensland Department of Mines and Energy, Brisbane, 39 – 56.
- MURRAY, C. G. (1997b): From geosyncline to fold belt: a personal perspective on the development of ideas regarding the tectonic evolution of the New England Orogen. In: ASHLEY, P. M. & FLOOD, P. G. (eds): *Tectonics and Metallogenesis of the New England Orogen: Alan H. Voisey Memorial Volume*. Geological Society of Australia, Special Publication **19**, 1 – 28.
- MURRAY, C. G. (1997c): Basement terranes beneath the Bowen and Surat basins, Queensland. In: GREEN, P. (ed), *The Surat and Bowen basins, South-East Queensland*, Queensland Department of Mines and Energy, Brisbane, 13 – 40.
- MUSSETT, A. E. & KHAN, M. A. (2000): Looking into the earth – an introduction to geological geophysics. 470 pp., Cambridge University Press.
- O'BRIEN, P. E.; KORSCH, R. J.; WELLS, A. T.; SEXTON, M. J. & WAKE-DYSTER, K. D. (1990): Mesozoic basins at the eastern end of the Eromanga – Brisbane Geoscience Transect: strike-slip faulting and basin development. In: FINLAYSON, D. M. (ed.): *The Eromanga – Brisbane Geoscience Transect: a Guide to Basin Development across Phanerozoic Australia in Southern Queensland*. Bureau of Mineral Resources, Geology and Geophysics, Canberra, 117 – 132.
- PALFREYMAN, W. D. (1994): Guide to the Geology of Australia.- BMR Bulletin, **181**, 111 pp., Canberra.
- PRICE, P. L. (1997): Permian to Jurassic palynostratigraphic nomenclature of the Bowen and Surat basins. In: GREEN, P. M. (ed.), *The Surat and Bowen Basins, Southeast Queensland*. Queensland Minerals and Energy Review Series, Queensland Department of Mines and Energy, 137 – 178.
- Ramsay, W. R. H. & Stanley, J. M. (1976): Magnetic anomalies over the western margin of the New England foldbelt, northeast NSW. *Geological Society of America Bulletin*, **87**, pp. 1421 – 1428.
- REINECK, H.-E. & SINGH, I. B. (1980): *Depositional Sedimentary Environments*, 549 pp., 2nd ed., Springer, Berlin – Heidelberg – New York.
- RIDER, M. (1996): The geological interpretation of well logs, 280 pp., 2nd ed., Whittles Publishing, Caithness.
- SANDWELL, D. T. & SMITH, W. H. F. (1997): Marine gravity anomaly from Geosat and ERS-1 satellite altimetry, *Journal of Geophysical Research*, B, 102; **5**, pp. 10.039-10.054.
- SCHÄFER, A. & KORSCH, R. J. (1998): Formation and fill of the Saar-Nahe Basin (Permo-Carboniferous, Germany), *Zeitschrift der deutschen geologischen Gesellschaft*, **149**, **2**, pp. 233-269, Stuttgart.
- SCHEIBNER, E. & BASDEN, H. (eds) (1996): *Geology of New South Wales - Synthesis, Volume 1, Structural Framework*, Dept. of Min. Res., Geological Survey of NSW, *Memoir Geology* **13** (1), pp. 1-295.
- SCHEIBNER, E. (1998): *Geology of New South Wales – Synthesis, Volume 2, Geological Evolution*. Geological Survey of New South Wales, *Memoir Geology* **13** (2), 666 pp..
- SELLEY, R. C. (1980): *Ancient Sedimentary Environments*, 287 pp., 2nd ed., Chapman & Hall, London.
- SERRA, O. (1986): *Fundamentals of Well-Log Interpretation*, (2: the interpretation of logging data), *Developments in Petroleum Science*, **15 b**, 684 pp., Elsevier, Amsterdam.
- SUPPE, J. (1983): *Geometry and Kinematics of Fault-Bend Folding*. In: *American Journal of Science*, Vol. **283**, pp. 684 - 721, Kline Geol. Lab. Yale University, New Haven, Connecticut.
- SUPPE, J. (1985): *Principals of Structural Geology*, Dept. of Geol. and Geophys. Sciences, Princeton University, Prentice-Hall, New Jersey.
- TADROS, N. Z. (ed) (1993): *The Gunnedah Basin* New South Wales, Dept. of Min. Res., Coal &

- Petr. Geol. Branch, Geol. Surv. of NSW, *Memoir Geology* **12**, pp. 1-649.
- TARLOWSKI, C.; MILLIGAN, P. R. & MACKAY, T. E. (1996): Magnetic Anomaly Map of Australia, scale 1 : 5 000 000, Australian Geological Survey Organisation, Canberra.
- TOTTERDELL, J. M.; WELLS, A. T.; BRAKEL, A. T.; KORSCH, R. J. & NICOLL, M. G. (1992): Sequence stratigraphic interpretation of seismic data in the Taroom region, Bowen and Surat basins, Queensland.- Bureau of Mineral Resources, 1991/**102**, 61 pp., Canberra, Australia.
- TOTTERDELL, J. M.; BRAKEL, A. T.; WELLS, A. T. & HOFFMANN, K. L. (1995): Basin phases and sequence stratigraphy of the Bowen Basin. *In*: FOLLINGTON, I. L.; BEESTON, J. W. & HAMILTON, L. H. (eds): *Bowen Basin Symposium 1995*, 247 - 256, Mackay, Queensland.
- WAKE-DYSTER, K. D.; SEXTON, M. J.; JOHNSTONE, D. W.; WRIGHT, C. & FINLAYSON, D. M. (1987): A deep seismic profile of 800 km length recorded in southern Queensland, Australia. *Geophysical Journal of the Royal Astronomical Society* **89**, 423 - 430.
- WALKER, R. G. & JAMES, N. P. (1992): Facies Models. Response to sea level changes (2nd ed). Geol. Assoc. Canada, 409 pp, St. Johns.
- WARTENBERG, W.; KORSCH, R. J. & SCHÄFER, A. (1998): Geometry of the Tamworth Belt (New England Orogen) and its relationship to the Bowen Basin in the subsurface beneath the Surat Basin in southern Queensland, p 456. *In*: GSA, *14th Australian Geological Convention*, Abstracts No **49**, 506 pp., Townsville, Australia.
- WARTENBERG, W.; KORSCH, R. J. & SCHÄFER, A. (1999): Geometry of the Tamworth Belt in the New England Orogen beneath the Surat Basin, southern Queensland, pp 211-220. *In*: P. G. FLOOD (ed.): *Regional Geology; Tectonics and Metallogensis; New England Orogen Symposium*, Earth Sciences, UNE, 465 pp., Armidale, Australia.
- WARTENBERG, W.; KORSCH, R. J. & SCHÄFER, A. (2003): The Tamworth Belt in southern Queensland, Australia: thrust-characterised geometry concealed by Surat Basin sediments. *In*: MCCANN, T. (ed.): *Tracing tectonic deformation using the sedimentary record; Geological Society, Special Publications*, **208**, 185 - 203, London.
- WASS, R. E. (1965): The marine Permian formations of the Cracow district, Queensland, *Journal of Proceedings of the Royal Society of New South Wales*, **98**, 159 - 167.
- WATERHOUSE, J. B. (1983): Back Creek Group. *In*: Waterhouse, J. B. (ed): *Field conference Permian of the Biloela-Moura-Cracow area (1983)*, Geol. Soc. of Australia, Queensland Div., Brisbane, 26 - 50.
- WELLMANN, P. (1990): A tectonic interpretation of the gravity and magnetic anomalies in southern Queensland. *In*: Finlayson, D. M. (ed): *The Eromanga-Brisbane Geoscience Transect: a guide to basin development across Phanerozoic Australia in southern Queensland. Bureau of Mineral Resources, Geology and Geophysics, Australia, Bulletin* **232**, 21 - 34.
- WILES, L. (1996): Coal Resource Audit of the Gunnedah Basin, Coal Audit No **1**, Dept. of Min. Res., Coal & Petrol. Geol. Branch, Singleton NSW.
- WOODWARD, N. B. (1995): Thrust systems in the Tamworth Zone, southern New England Orogen, New South Wales. *Australian Journal of Earth Sciences*, **42**, 107 - 117.

LIST OF FIGURES AND TABLES

CHAPTER	DESCRIPTION	PAGE
1.	Fig. 1 Map of Eastern Australia, showing the relationship of the New England Orogen to the adjacent sedimentary basins.	2
2.1.	Tab. 2.1 Chart showing the stratigraphy, seismic reflectors and basin phases of the Bowen Basin and Tamworth Belt successions.	7
2.2.2.	Fig. 2.1 QFL plot of sandstones from the Tamworth Belt in relation to provenance fields of DICKINSON <i>et al.</i> (1983) after MURRAY (1997c).	9
2.2.2.	Fig. 2.2 Cartoon of the Late Devonian-Early Carboniferous palaeogeography (after MURRAY <i>et al.</i> , 1987).	10
2.3.	Fig. 2.3 Unmigrated deep seismic profile BMR91.G01 across the Tamworth Belt (from KORSCH <i>et al.</i> , 1997).	13
3.1.	Fig. 3.1 Map of Eastern Australia, showing the locations of the seismic profiles within the study area.	18
3.1.2.	Fig. 3.2 Structure Contour Map of the B30 seismic reflector.	20
3.1.2.	Fig. 3.3 Map identifying the shotpoints of the seismic reflection profiles of key interest within the study area.	20
3.1.2.	Fig. 3.4 Interpretation of the seismic reflection profile A82-LT-24 (final stack).	22
3.1.2.	Fig. 3.5 Interpretation of the migrated seismic reflection profile H82-T-109.	23
3.1.2.	Fig. 3.6 Interpretation of the migrated seismic reflection profile BMR86.MO1 ("Millmerran" profile).	24
3.1.3.	Fig. 3.7 Interpretation of the seismic reflection profile A82-WR-21 (final stack).	26 - 27
3.1.3.	Fig. 3.8 Structure Contour Map showing the distribution of the seismic horizon HA within the study area.	28
3.1.3.	Fig. 3.9 Structure Contour Map showing the distribution of the seismic horizon HB within the study area.	28
3.1.3.	Fig. 3.10 Structure Contour Map showing the distribution of the seismic horizon HC within the study area.	29
3.1.3.	Fig. 3.11 Structure Contour Map showing the distribution of the seismic	29

CHAPTER	DESCRIPTION	PAGE
	horizon HD within the study area.	
3.2.2. Fig. 3.12	Borehole data from the well Deep Crossing (Lat.: 27.468971S; Long.: 150.486693E) drilled by the petroleum exploration industry.	32
3.2.2. Fig. 3.13	Seismic profile A82-LT-19 (final stack) showing the position of the well Deep Crossing jump-tied on top of the seismic image.	33
4.2.1. Fig. 4.1	Aeromagnetic anomaly image (gradient-enhanced residuals of Total Magnetic Intensity) overlain by a terrane map of the NEO.	38
4.2.2.1. Fig. 4.2	Simplified terrane map of the NEO overlain on top of the shades of grey-aeromagnetic anomaly image. <i>Fig. 4.2a</i> identifies the magmatic arc-, fore-arc- and accretionary complex rocks of the NEO. <i>Fig. 4.2b</i> shows the 3D terrane map of the NEO.	40
4.2.2.1. Fig. 4.3	Magnetic traverse along the seismic reflection profile A82-LT-24. <i>Fig. 4.3a</i> : Magnetic anomaly graph of a dipole at medium latitudes (from MUSSETT & KHAN, 2000).	44
4.2.2.1. Fig. 4.4	Magnetic anomaly traverse along the seismic profile H82-T-109.	45
4.2.2.1. Fig. 4.5	Magnetic anomaly traverse along the seismic profile BMR86.MO1.	45
4.2.2.2. Fig. 4.6	Three dimensional aeromagnetic image of the study area.	46
4.2.2.2. Fig. 4.7	Aeromagnetic anomaly traverse across the Tamworth Belt, located to the south of the study area.	46
4.2.2.2. Fig. 4.8	3D aeromagnetic image of the NEO showing the Texas Orocline.	47
4.3.1. Fig. 4.9	Gravity anomaly image of the NEO overlain by a terrane map.	48
4.3.2. Fig. 4.10	Gravity image of the NEO (shades of grey) overlain by a simplified terrane map.	50
4.4. Fig. 4.11	Magnetic traverse across the exposed part of the Tamworth Belt in northern New South Wales (from RAMSAY & STANLEY, 1976).	52
4.4. Fig. 4.12	Three dimensional perspective of the NEO showing the boundaries of the subsurface fore-arc basin as interpreted from the aeromagnetic data. <i>Fig. 4.3a</i> : Three-dimensional perspective of the NEO, showing the aeromagnetic image, the gravity image and the gravity data overlain by the aeromagnetic data.	53
5.1.1. Fig. 5.1	Cartoon of the crustal architecture in the vicinity of the deep seismic survey BMR84.14 (from KORSCH <i>et al.</i> , 1997).	58
5.1.1. Fig. 5.2	Cartoon of the crustal architecture in the vicinity of the deep	58

CHAPTER	DESCRIPTION	PAGE
	seismic survey BMR91.G01 (from KORSCH <i>et al.</i> , 1997).	
5.1.2.	Fig. 5.3 Schematic progressive development of fault-bend folds as a thrust sheet rides over a step in décollement (from SUPPE, 1985).	60
5.1.2.	Fig. 5.4 Interpretation of the seismic reflection profile A82-LT-24 (final stack), illustrated beneath the aeromagnetic anomaly traverse.	60
5.1.2.	Fig. 5.5 Interpretation of the migrated seismic reflection profile H82-T-109, illustrated beneath the aeromagnetic anomaly traverse.	61
5.1.2.	Fig. 5.6 Interpretation of the migrated seismic reflection profile BMR86.MO1 (“Millmerran” profile), illustrated beneath the aeromagnetic anomaly traverse.	62
5.1.2.	Fig. 5.7 Interpretation of seismic reflection profiles (final stack) A82-LT-20 (NW) and A82-WR-22 (SE).	65
5.1.2.	Fig. 5.8 Interpretation of seismic reflection profiles (final stack) A82-LT-29 (NW) and H82-T-106 (SE).	65
5.1.2.	Fig. 5.9 Interpretation of seismic reflection profiles (final stack) 84-10 (NW) and H82-T-101 (SE).	65
5.2.1.	Fig. 5.10 Structure Contour Map of the Moonie thrust plane <i>FB</i> .	66
5.2.1.	Fig. 5.11 Schematic foot-wall morphology of the Moonie Fault.	66
5.2.2.	Fig. 5.12 Structure Contour Map of the thrust plane <i>FA</i> in the hanging-wall sequence of the subsurface Tamworth Belt.	68
5.3.	Fig. 5.13 Map of the seismic study area showing thrust faults and Tamworth Belt horizons at the location of the base of the Surat Basin.	68
5.3.3.	Fig. 5.14 Interpretation of the seismic reflection profile A82-LT-21 (final stack).	70
5.3.3.	Fig. 5.15 Interpretation of the seismic reflection profile M7803 (final stack) oblique to strike of the subsurface Tamworth Belt.	70
5.3.3.	Fig. 5.16 Interpretation of the seismic reflection profile A82-LT-25 (migrated). . <i>Fig. 5.16a</i> : Cartoon showing a simple-step fault-bend fold with two imbrications (from SUPPE, 1983).	71
5.3.4.	Fig. 5.17 Asymmetrical pop-up structure as seen on the NE-part of the seismic profile H82-T-110, offsetting the <i>B30</i> base of the Bowen Basin. <i>Fig. 5.17a</i> : Image comparing the seismic reflection record of the profile H82-T-110 with the Sonic and the Gamma Ray logs of the well Gilgai.	74
5.3.4.	Fig. 5.18 Detail of the SW-part of the seismic reflection profile A82-WR-21.	75
5.4.1.	Fig. 5.19 Interpretation of the migrated seismic reflection profile BMR86.MO1	76

CHAPTER	DESCRIPTION	PAGE
	with reprocessed data illustrated on boxes (down to 6 s TWT).	
5.4.2.	Fig. 5.20 Interpretation of the upper (5 s TWT), reprocessed part of the migrated deep seismic survey BMR84.14.	78 - 79
5.4.2.	Fig. 5.20a Cartoon of a snakehead duplex (from HATCHER, 1995).	79
5.5.	Fig. 5.21 Balanced cross-sections across the northernmost exposed part of the Tamworth Belt in northern NSW (from WOODWARD, 1995).	84
5.5.	Fig. 5.22 Cartoon showing the configuration of a fore-arc basin related to its evolution, depicting a ridged basin type (from EINSELE, 2000).	85
6.	Fig. 6.1 Aeromagnetic anomaly map of a part of the NEO to the NW of the Texas Orocline. Overlain on the aeromagnetic data is the distribution of structures at the level of the S10 disconformity.	93
6.	Fig. 6.2 Cartoon of the composite cross-section across the subsurface Tamworth Belt in southern Queensland.	96

ABBREVIATIONS and ACRONYMS

ACT	Australian Capital Territory
AGCRC	Australian Geodynamic Cooperative Research Centre
AGD	Australian Grid Data
AGSO	Australian Geological Survey Organisation (now Geoscience Australia)
APJ	Palynological Zone Jurassic
APP	Palynological Zone Permian
APT	Palynological Zone Triassic
BMR	Bureau of Mineral Resources (now Geoscience Australia)
Carb.	Carboniferous
cf.	compare to
Cgl	Conglomerate
COR	Core sample
c.	approximately
DFG	Deutsche Forschungsgemeinschaft
e.g.	for example
F	Feldspar
Fig.	Figure
Fm	formation
GA	Geoscience Australia
GIS	Geo Information System
Gp	group
GSNSW	Geological Survey of New South Wales
GSQ	Geological Survey of Queensland
Jur.	Jurassic
KISS	Keep it Simple Stupid
L	Lithic
Lat.	Latitude
Long.	Longitude
Lw	Lower
Moho	Mohorovicic discontinuity
NGMA	National Geoscience Mapping Accord
No	Number

NSW	New South Wales
NT	Northern Territory
Q	Quartz
QLD	Queensland
SA	South Australia
Sst	Sandstone
SP	Shotpoint
TAS	Tasmania
T.D.	Total Depth [m]
TMI	Total Magnetic Intensity [nT]
Tr.	Triassic
TWT	Two-way-travel-time
VIC	Victoria

INTERPRETATION INDEX

The following are some of the interpretations of structures and processes seen on seismic reflection profiles within the study area.

Baselap	Baselap is lapout at the lower boundary of a depositional sequence. Two important types are recognised. Later structural movement may necessitate the reconstruction of depositional surfaces. The study area proved to be an area of great structural complication. Therefore, the discrimination between onlap and downlap may be practically impossible and the author may be able to determine only that the strata are in a baselap relation. Onlap and downlap are indicators of nondepositional hiatuses rather than erosional hiatuses (MITCHUM <i>et al.</i> 1977). Because of the later structural movement, baselap is the more inclusive term to be used for two-dimensional seismic data.
Branch line	May be used to indicate the direction of major thrust movement.
Downlap	Downlap is baselap in which initially inclined stratum terminates downdip against an initially horizontal or inclined surface.
Flat	That part of a staircase thrust plane trajectory which has a horizontal or subhorizontal orientation.
Horizon	Surface separating two beds and hence having no thickness.
Horse	A lenticular or sigmoidal pod of rock which is completely bounded by two or more fault surfaces that may diverge after branching and then converge along strike and up-dip to meet again.
Imbricate	(<i>Latin: imbricare</i> = to cover with tiles) The structure resulting from the piling upon one another of wedges or sheets of rock, like the partly-overlapping tiles of a roof. It is a series of thrust slices, hence an "imbrication". Without incipient folding, the strata are repeated by a series of minor thrusts or reversed faults, which lie at an oblique angle to more important dislocations, termed thrust planes.
Onlap	Onlap is baselap in which initially horizontal stratum laps out against an initially inclined surface, or in which an initially inclined stratum laps out updip against a surface of greater initial inclination.

Ramp	That part of a staircase thrust trajectory which forms the steeply dipping sections between the <i>flats</i> . Where thrusting occurs in horizontally bedded strata the ramps dip up-section, obliquely to the bedding. A thrust belt may contain several types of a ramp, classified as <i>frontal</i> , <i>oblique</i> and <i>lateral</i> according to their respective perpendicular, oblique, and parallel strike orientations in relation to the main direction of transport.
Reflection	What is seen on the seismic profiles, that is, what is recorded by the equipment.
Reflector	Geological feature in the subsurface that the seismic waves bounce off.
Splay	Implies the existence of a main fault with higher displacement.
Thrust	A low-angle (commonly less than 45°) reverse fault with a significant dip-slip component, in which the hanging-wall overhangs the foot-wall. Synthetic thrust sets form <i>imbricate</i> fan structures which may be thrust-bound, when they form a <i>duplex</i> . Single thrusts typically show a staircase trajectory composed of <i>ramps</i> and <i>flats</i> . An individual thrust sheet may have a distinctive stratigraphy and may therefore be correlated long distances.

PERSONAL THANKS AND THOUGHTS

Throughout my time in Australia, I was given the opportunity not only to meet scientists of outstanding merit, moreover I met exceptionally friendly and open minded people wherever I've been – in the office and in the field, at sports and at barbecues, whilst cueing and whilst bushwalking – even in front of a club's entrance or on a passenger's seat in a towing truck in the middle of the Nullabor.

To me, it seems that there are only two exceptions dealing with earnest Aussies: (1) when you put your feet on farmer's ground without having asked the owner for permission – and – (2) when you dare to discuss the (non)sense of being “real Celtic” but Australian during later hours of BYO-parties – it doesn't get you any further.

Australia to me has been an outstandingly rewarding experience. I am very grateful to have had so many discussions, talks, chats and laughs whilst growing into the art of the Australian way of life. Cruising throughout Australia, I learnt that a van is still a “good van” even though it has 420.000 km on its clock. I very much enjoyed the continent's beauty and its wildlife (again and again, nature took me by surprise, whether skiing in the Snowy Mountains with Crimson Rosellas crossing my way or being visited by a group of Sting Rays whilst paddling in ACT coastal waters).

A warm thank goes to Andreas Schäfer, whose idea of initiating an Australian – German joint venture project set the cornerstone for all the impressions I've got and the experiences I was able to make Down Under.

I very much thank Russell for my lessons learned and for his support and advices. I thank the Korsch family for their great hospitality and for their warm welcoming and for providing the basic needs of an overseas visitor – my supervisor's pushbike and his daughters' bedding (it was the world beater in the Backpackers' dorms).

Thanks to Kate, Paddy, Cam and Joe for their clarifying words on indigenous culture, heritage and rights (including expositions on schizophrenic puddings); and - once more - thanks to Kate, who gave me the opportunity to help out dragging the order forms for an election. Together with my flatmates, I went through different inventive phases, such as melting beer bottles in a BBQ-fire (an inverted vacuum cleaner may help out speeding up the melting process). We worked out, how to guarantee the beer brewing process under near-Antarctic indoor conditions, keeping the brewing kit warm by applying an oven-blanket-radiator construction (so, thanks to the people who invented the beer brewing kit anyhow). Thanks to Andrew for the superb tree-and-mud tours, for long nights in our freezing living room in front of the Tele watching 62 matches of the Football World

Cup and for “lending his mum to me”. Thanks to Keith, Holger and Andrea for a place to stay and for unforgotten barbeques and “bonfires”.

Thanks to Sam, Edgar, Niculin, Alexander, Debby, Chris, Chris, Daniel, Alistair, Toni, Sue, John, Monica, Ben, Ken, Therese, Dan, Oliver, Matt and Peter.

Thanks to the girls of Unit 2/10, Commonwealth Parade – especially to Becky, Charl, Nic and Neroli – for the great time we’ve had across the street from the Manly singing sea lions, and thanks to Stephen making me a Millionaire at Melbourne Carnival.

Thanks to my unknown neighbour on Busselton Pier one summer night, whose advice finally stopped the fish from laughing at me – I was practicing trial fishing for over one year before I started my fisherman’s career using my neighbour’s so called “wonderbait” – freshly caught Mackerel. Thanks to Stephen, Paolo, Andrew and Malcolm for joining fun fishing forces with me.

Thanks to my stop-over-hosts Arne and Jonathan – splitting my flights to see how you are going was a good thing to do and will be unforgotten.

Finally, I thank the folks at the ANU Aikido Club, the Indoor Fußball team, the AGSO Socceros (and Aussie Rules players) and the Wednesday Volleyball Club for charging my battery and the Security people for the common nightly tea meetings that kept me going.

A very warm-hearted and special thank goes to Nina and to Ali.

Most of all, I thank Rike for her love and faith in my doing.

Ganz besonderen Dank möchte ich meinen Eltern für ihre Unterstützung und Geduld aussprechen. Meinem Bruder, Holger, Mark und Georg möchte ich herzlich danken für ihre Unterstützung. Dank an Marco für die fast täglich verfassten Nachrichten von Zuhause und an Ingo für seine Informationen, die das BTR-Procedere bei Weitem überstiegen. Dank an Stefan, der meine Z bei sich aufbewahrte und, als es nötig war, diese verkaufte und Dank an Andreas, der meine wichtigsten Besitztümer – meine Platten – während meiner Abwesenheit in Deutschland verwaltete. Dank auch an meine deutschen WG-Mitbewohner, Guido und Sébastien, die gerade die letzte, bei Zeiten „anspruchsvolle“ Phase des Zusammenschreibens tapfer ertragen haben. Zuletzt danke ich Stefan für seine „entzerrenden Maßnahmen“.

Am Ende möchte ich ganz besonders meinen Freunden danken, die einen ehrlichen Anteil an meinem Projekt Australien mittragen.